

Pricing and Hedging Fixed Income Derivatives under Negative Interest Rates: An SABR approach

Elizabet Tsvetanova Atanasova

Trabajo de investigación 003/017

Master en Banca y Finanzas Cuantitativas

Tutores: Dr. Manuel Moreno Fuentes
Gregorio Vargas Martínez

Universidad Complutense de Madrid

Universidad del País Vasco

Universidad de Valencia

Universidad de Castilla-La Mancha

Pricing and Hedging Fixed Income Derivatives under Negative Interest Rates: An SABR approach

MSc Thesis

for the degree

MSc in Banking and Quantitative Finance

Complutense University of Madrid

July, 2017

Elizabet Tsvetanova Atanasova

Supervisors: Manuel Moreno Fuentes [‡]
Gregorio Vargas Martínez [§]

[‡] Associate professor at *University of Castilla-La Mancha*

[§] Market Risk Manager at *EY*

Abstract

This MSc Thesis focuses on pricing and hedging fixed income derivatives under the current negative interest rates environment. The most commonly used models in practice are analysed and compared in order to select the most accurate one for pricing and hedging interest-rate derivatives. Since shifted SABR model has become the “market standard” tool for modelling negative interest rates, the main aim of this research is to examine and test its performance, providing an empirical evidence that corroborates its general acceptance.

Keywords: *negative interest rates, fixed income derivatives, pricing, hedging, volatility smile/skew, sensitivity, Greeks, shift, SABR, Black (lognormal), Bachelier (normal).*

Contents

Introduction	1
I Theoretical background	3
1 Preliminaries	4
1.1 Basic definitions	4
1.2 Interest rates	5
1.3 Interest-rate derivatives	6
1.4 Mathematical framework	8
2 Interest-rate Models	9
2.1 Bachelier (Normal) Model (1900)	9
2.2 Black (Lognormal) Model (1976)	10
2.3 Shifted Black Model (2012)	11
2.4 One-factor Short-rate Models	12
2.4.1 Vasicek Model (1977)	13
2.4.2 Hull-White Model (1990)	13
2.4.3 Differences between short-rate and forward-rate models	14
3 The SABR Model	16
3.1 Classic SABR Model (2002)	17
3.1.1 Implied volatilities within the SABR model	18
3.1.2 Behaviour of the SABR parameters	19
3.1.3 Calibration of the SABR parameters	20
3.2 Normal SABR Model (2002)	21
3.3 Shifted SABR Model (2014)	21
3.4 Free-Boundary SABR Model (2015)	22
3.5 Comparison of models able to cope with negative rates	23
4 Hedging under the SABR Model	24
4.1 SABR <i>Greeks</i>	25
4.1.1 <i>Delta</i> and <i>Vega</i> hedging. Bartlett's corrections	25
4.1.2 Other <i>Greeks</i>	28
4.2 SABR parameters sensitivities	29

II	Empirical analysis	31
5	Data	32
5.1	Data conventions	32
5.2	Data description	34
6	Methodology	36
6.1	Stripping caplet volatilities	36
6.2	Calibration of the models	38
6.3	Comparison of the models' pricing accuracy	40
6.4	Computation of the shifted SABR sensitivities	41
7	Empirical results	43
7.1	Comparison of the models	43
7.1.1	Volatility term structures	43
7.1.2	Calibration of the models	44
7.1.3	In-sample analysis	48
7.1.4	Strike out-of-sample analysis	52
7.1.5	Maturity out-of-sample analysis	54
7.2	<i>Greeks</i> and parameters sensitivities	57
7.2.1	<i>Delta</i> and <i>Vega</i>	57
7.2.2	<i>Gamma</i> , <i>Dual-delta</i> , <i>Vanna</i> and <i>Volga</i>	60
7.2.3	Parameters sensitivities	62
	Conclusion	65
	Bibliography	67
A	Constant Elasticity of Variance Model (1975)	70
B	Local Volatility Models (1994)	71
C	Vasicek and Hull-White calibrations. Numerical issues	72
D	Numerical differentiation	74
E	Market data	75

Introduction

“Essentially, all models are wrong, but some are useful.”

George E. P. Box (1919 – 2013)

In the height of the recent financial crisis large financial institutions collapsed, while the interdependence between them led to a financial contagion that happened at both international and domestic level. That became thereafter a potential risk for many countries, especially those in the hard core of the Eurozone.

The crash battered both banks and borrowers so that banks did not want to lend and consumers did not want to borrow due to the poor credit quality of the counterparty and the widespread propagation of the default risk. In this way, for many, especially small institutions, trading became either *too risky* or *too expensive*.

In order to avoid this new environment dominated by concern and economic inactivity, the use of negative interest rates, although it is an unconventional tool of economic policy, has become a standard practice in recent times. Indeed, European Central Bank, but also Central Banks of Sweden, Denmark, Switzerland, and Japan have set negative interest rates on reserves. The rationale behind these exceptional measures is to encourage investors to borrow money and invest into the economy in order to stimulate and improve the economic growth. A negative rate implies that investing money in a bank (deposits) would result in a loss, and borrowing money (loans) in a profit. Therefore, setting low and negative interest rates, the Central Banks would, in fact, punish investors for holding their cash and reward the borrowers, who are paid for taking out loans.

This new situation has led to great economic effects, but beside this it has caused many technical problems to the financial institutions, since most of the existing interest rate derivatives pricing models typically assume positive interest rates. In fact, in these models positiveness of interest rates has *always* seemed a reasonable and attractive property. Clearly, this assumption has become unacceptable under the current situation of very low or even negative rates, making valuation spreadsheets break down or not value properly, leading to incorrect prices and causing arbitrage possibilities. Therefore, in order to provide solutions to overcome these problems, adapting pricing models to deal with negative interest rates has emerged as a key concern at an international level.

This MSc Thesis provides an extensive theoretical and practical research that compares diverse commonly used pricing models able to cope with negative interest rates and that, therefore, might be very helpful and useful in this challenging environment. The model that outstands for its accuracy in pricing and hedging fixed income derivatives is the shifted SABR model. This model is a natural extension of the classic stochastic volatility SABR model introduced by (Hagan et al., 2002) [22], that handles negative interest rates and shows great capacity to fit adequately the implied volatility curves that are typically observed within markets. Due to these reasons, the shifted SABR model has become the benchmark of many financial institutions for pricing and hedging fixed income derivatives under the new context of negative rates.

This research is organized in two parts. The first one, named *Theoretical background*, is devoted to the theoretical topics covered through the research. Chapter 1 provides both brief interest-rate and mathematical frameworks necessary to understand subsequent arguments and developments. Chapter 2 reviews traditional interest-rate derivatives pricing models. Chapter 3 introduces the SABR model and its extensions able to cope with negative interest rates. Finally, Chapter 4 focuses on the shifted SABR hedging tools, including theoretical developments on Greeks and parameters sensitivities.

The second one, entitled *Empirical analysis*, includes the practical application to the topics analysed in the first part. Chapter 5 characterizes the market data used through the research. Chapter 6 provides a methodological scheme that gradually describes the steps followed along the empirical analysis. The attained results are presented and explained in Chapter 7.

Part I

Theoretical background

Chapter 1

Preliminaries

This Chapter includes some preliminary and relevant concepts, mainly based on (Brigo and Mercurio, 2006) [8] and (Rouah, 2007) [37], that will be necessary for the arguments and developments along the research.¹

1.1 Basic definitions

- **Bank account** ($B(t)$). The continuously compounded, at the rate $r(t)$, bank account (or also money-market account) represents a zero-risk investment. It is defined at time $t \geq 0$ by

$$B(t) = B(0) \exp \left(\int_0^t r(u) du \right), \quad (1.1)$$

according to the differential equation $dB(t) = r(t)B(t)dt$, and where $B(0)$ is the amount invested at time $t = 0$.

- **Stochastic discount factor** ($D(t, T)$). The continuously compounded (stochastic) discount factor between the time instants t and T is the amount at time t that is “equivalent” to one unit of currency payable at time T , with $t < T$. It is defined by

$$D(t, T) = \frac{B(t)}{B(T)} = \exp \left(- \int_t^T r(u) du \right). \quad (1.2)$$

- **Zero-coupon bond price** ($P(t, T)$). A T -maturity zero-coupon bond guarantees the payment of one unit of currency at time T , with no intermediate payments. Indeed, a zero-coupon bond for the maturity T is a contract that establishes the present value of one unit of currency to be paid at time T . Its value at time $t < T$ is defined by

$$P(t, T) = \mathbb{E}^{\mathbb{Q}} \left[\exp \left(- \int_t^T r(u) du \right) \middle| \mathcal{F}_t \right], \quad (1.3)$$

where \mathbb{Q} is an equivalent martingale measure, *risk-neutral measure*, that will be defined later. Clearly, $P(T, T) = 1$. Also, notice that if interest rates r are deterministic, then the discount factor $D(t, T)$ is deterministic as well, and $P(t, T) = D(t, T)$.

¹Experienced readers can ignore this Chapter if it is immediate for them.

- **Day-count convention** ($\delta(t, T)$). The day-count convention $\delta(t, T)$ is defined as the ratio of length of time interval $[t, T]$ over the length of a year. It reflects the particular choice that is made to measure the amount of time (in years) between two dates, i.e., the *time to maturity* defined as $\tau = T - t$.²
- **Tenor**. The tenor of a fixed income derivative is the time to maturity of the underlying. Therefore, the “maturity” is usually understood as the time to maturity of the derivative, and the “tenor” as the time to maturity of the underlying fixed income product.

1.2 Interest rates

- **Simply-compounded forward interest rate**. The simply-compounded forward interest rate prevailing *today*, at time t , for the future investment period $[T_1, T_2]$ is defined by

$$F(t, T_1, T_2) := \frac{1}{\delta(T_1, T_2)} \left(\frac{P(t, T_1)}{P(t, T_2)} - 1 \right). \quad (1.4)$$

- **Instantaneous forward interest rate**. The instantaneous forward interest rate prevailing *today*, at time t , is defined as

$$F_t := \lim_{T_1 \rightarrow T_2^-} F(t, T_1, T_2) = -\frac{\partial \log P(t, T_1)}{\partial T_1}. \quad (1.5)$$

Therefore, the instantaneous forward interest rate F_t is defined as the simply-compounded forward interest rate when the future investment period becomes infinitesimal, say $F_t \approx F(t, T_1, T_1 + \Delta T_1)$. It is important to remark that the instantaneous rates are theoretical constructions widely used in the literature for accomplishing analytical formulae, although they do not exist in the markets.

- **Forward swap rate**. The forward swap rate observed *today*, at time t , for the specified interval $[T_1, T_2]$ ³ is given by

$$S(t, T_1, T_2) := \frac{P(t, T_1) - P(t, T_2)}{L(t, T_1, T_2)}, \quad (1.6a)$$

where $L(t, T_1, T_2)$ is usually called *forward level function* and it is defined as the present value at t of an annuity paying one unit of currency on the n fixed payment dates T_1, \dots, T_2 :

$$L(t, T_1, T_2) := \sum_{j=T_1+1}^{T_2} \delta_j \cdot P(t, T_j), \quad (1.6b)$$

where δ_j is the day-count convention applying to the period starting at T_{j-1} and ending at T_j .

²This definition is a simplification, since there are different ways to compute the day-count convention. In the page <http://www.deltaquants.com/day-count-conventions> are described some of the most commonly followed conventions.

³The length of the interval $[T_1, T_2]$ accounts for the tenor of the corresponding swap.

Important *interbank* interest rates for the European financial markets are LIBOR and EURIBOR.

- **LIBOR.** The *London Interbank Offered Rate* (LIBOR) is the average of interest rates estimated by each of the leading banks in the *London interbank market* that would be charged were it to borrow from other banks.
- **EURIBOR.** The *Euro Interbank Offered Rate* (EURIBOR) is a daily reference rate based on the averaged interest rates at which Eurozone banks offer to lend unsecured funds to other banks in the *European interbank market*.

Another important interest rate that actually will be used in this research as a proxy for the *risk-free rate*⁴ for both computing the forward rates and the discount factors is the OIS rate.

- **OIS.** The *Overnight Index Swap* (OIS) is an interest rate swap in which a fixed rate of interest is exchanged for a floating rate of interest that is the geometric mean of a specific daily overnight rate. The overnight rates for the EUR, USD and GBP market are the *Euro Overnight Index Average* (EONIA), the effective *Federal Funds Rate* and the *Sterling Overnight Index Average* (SONIA) respectively.

The election of a market rate as a proxy for the risk-free rate is not obvious. In fact, this issue is currently under discussion, since the recent financial crisis changed progressively the tendency of the market practice. Before the credit crunch the standard election for discounting used to be the LIBOR rate. However, it has turned out to be a poor proxy for the risk-free rate under stressed market conditions during recent years, and therefore has been gradually substituted by the OIS rate. (Hull and White, 2012) [26] examines this practice and concludes that OIS curve is currently the most suitable proxy for the risk-free discount curve.⁵

1.3 Interest-rate derivatives

- **Swap.** Usually an interest rate swap (IRS) is used to transform a fixed-rate loan into a floating-rate loan or vice versa.⁶ It is a financial product in which two parties exchange interest rate cash flows during a fixed period of time. One of the cash flows has a fixed rate and the other has a floating rate indexed to a reference (market) interest rate. The cash flow with the fixed rate is called the *fixed leg* and the cash flow based on the floating rate is called the *floating leg*. Identification of the payer and the receiver of the swap is based on the fixed leg. The one that pays the fixed

⁴The *risk-free interest rate* is a theoretical rate of return of an investment with zero risk, and its term structure is a key input to the pricing of financial products.

⁵Actually, the use of single discount curve for both computing the forward rates and the discount factors is a simplification of today's standard market practice, where *multi-curve framework* is used, i.e., the process of implying forward rates is separated from the process of computing discounting factors. This topic is extensively analysed in (Bianchetti, 2004) [5], however it lies beyond the objectives of the research and consequently its discussion will not be included here.

⁶These types of IRS receive the name *fixed-floating swaps*. However, there also exist *floating-floating swaps*, based on two different floating rates or on the same floating rate but with different tenors; and *fixed-fixed swaps*, in which both counterparties pay a (different) fixed interest rate.

rate and receives the floating rate is called the *payer swap*. On the other hand, the *receiver swap* pays the floating rate and receives the fixed rate. An IRS is usually structured so that one side transfers the difference between the two payments to the other side. Interest rate swaps allow financial managers to effectively hedge their interest rate exposure.⁷

- **Caplet/Floorlet.** A European call/put option is a financial contract between two parties, the buyer and the seller of this option, agreed at time t . The buyer of the call/put option has the right, but not the obligation, to buy/sell the underlying asset from the seller of the option at a certain time, the *maturity date* T , for a certain price, the *strike price* K . The seller is obligated to sell the underlying asset to the buyer if the buyer so decides (*exercises* their option). The buyer pays a fee, called *premium*, for this right. When the underlying asset is an interest rate, particularly a forward interest rate, the call and put option are known as **caplet** and **floorlet**, respectively. The payoffs of a caplet and floorlet at the maturity date are

$$P_{caplet} = N \cdot \delta(t, T) \cdot (F_T - K)^+, \text{ and} \quad (1.7a)$$

$$P_{floorlet} = N \cdot \delta(t, T) \cdot (K - F_T)^+, \quad (1.7b)$$

where F_T is the value of the underlying forward interest rate at the option-maturity date T , $\delta(t, T)$ is the day-count convention, and N accounts for the notional outstanding the caplet/floorlet.

- **Cap/Floor.** An interest rate cap/floor is a contract on an interest rate whereby the seller pays the buyer, at periodic payment dates, the positive/negative difference between a reference (market) interest rate (floating rate) and the agreed floor-rate (fixed rate, like a strike), i.e., when the reference interest rate exceeds/is below the agreed floor-rate. The interest rate cap/floor is actually equivalent to a series of call/put options (caplets/floorlets) each written on an individual forward interest rate. Interest rate caps are used often as a hedging tool: by a cap, a borrower with a floating rate loan can hedge against interest rate increases. Otherwise, an interest rate floor reduces the risk to lenders receiving the interest payments and guarantees a minimum rate for their loaned money (the floor-rate). Therefore, the payoff of a cap/floor is simply the sum of the payoffs of its caplets/floorlets as shown in the next equations.

$$P_{cap} = N \sum_{j=T_1+1}^{T_2} \delta(T_{j-1}, T_j) \cdot (F(T_{j-1}, T_j) - K)^+, \text{ and} \quad (1.8a)$$

$$P_{floor} = N \sum_{i=T_1+1}^{T_2} \delta(T_{j-1}, T_j) \cdot (K - F(T_{j-1}, T_j))^+. \quad (1.8b)$$

⁷Recall that for an IRS, the tenor of the floating leg does not have to match the tenor of the fixed leg, and, contrary, both legs have the same notional. The *notional* in this context is the pre-specified amount on which interest payments are based on.

Caps and floors are usually understood as the “positive parts” of a payer/receiver swap respectively, since their payoffs can be computed as the sum of those exchange payments which are above zero for every date of the interval $[T_1, T_2]$. Therefore, a cap/floor can be characterised as a portfolio of n caplets/floorlets, referred to the floating rate of an IRS for each one of the n dates among the interval $[T_1, T_2]$.

1.4 Mathematical framework

In the *no-arbitrage* approach to pricing derivatives, the t -time value $V(t)$ of a contingent claim (derivative) is obtained by choosing a numeraire $N(t)$ ⁸ and taking an expectation with respect to an equivalent martingale measure \mathbb{N} under which the discounted value of the derivative is a martingale. Accordingly, $V(t)$ is defined from the expression

$$V(t) = N(t) \mathbb{E}^{\mathbb{N}} \left[\frac{V(T)}{N(T)} \mid \mathcal{F}_t \right]. \quad (1.9)$$

- **Risk-neutral measure (\mathbb{Q}).** The risk-neutral measure \mathbb{Q} has the bank account $B(t)$ as a numeraire. Under \mathbb{Q} , and in the absence of arbitrage, a contingent claim is valued as

$$V(t) = B(t) \mathbb{E}^{\mathbb{Q}} \left[\frac{V(T)}{B(T)} \mid \mathcal{F}_t \right]. \quad (1.10)$$

- **T-forward measure (\mathbb{F}^T).** The T-forward measure \mathbb{F}^T has the T -maturity zero-coupon bond $P(t, T)$, with $P(T, T) = 1$, as a numeraire. Under \mathbb{F}^T , and in the absence of arbitrage, a contingent claim is valued as

$$V(t) = P(t, T) \mathbb{E}^{\mathbb{F}^T} \left[\frac{V(T)}{P(T, T)} \mid \mathcal{F}_t \right] = P(t, T) \mathbb{E}^{\mathbb{F}^T} [V(T) \mid \mathcal{F}_t]. \quad (1.11)$$

(Rouah, 2007) [37] proves that **the forward rate $F(t, T)$ is a martingale under the T-forward measure.**

- **Radon-Nikodym Derivative. Change of numeraire.** The Radon-Nikodym derivative $\frac{d\mathbb{F}^T}{d\mathbb{Q}}$ to change the measure \mathbb{Q} to \mathbb{F}^T can be obtained by considering the expectations

$$\mathbb{E}^{\mathbb{F}^T} \left[\frac{P(t, T)}{P(T, T)} V(T) \mid \mathcal{F}_t \right] = \mathbb{E}^{\mathbb{Q}} \left[\frac{P(t, T)}{P(T, T)} V(T) \frac{d\mathbb{F}^T}{d\mathbb{Q}} \mid \mathcal{F}_t \right] = \mathbb{E}^{\mathbb{Q}} \left[\frac{B(t)}{B(T)} V(T) \mid \mathcal{F}_t \right], \quad (1.12)$$

where the first equality comes from applying the Radon-Nikodym derivative so that $\mathbb{E}^{\mathbb{F}^T}[X] = \mathbb{E}^{\mathbb{Q}}[X \cdot \frac{d\mathbb{F}^T}{d\mathbb{Q}}]$, and the second one comes from matching both definitions (1.10) and (1.11), and bringing the corresponding elements inside the expectations. Therefore,

$$\frac{d\mathbb{F}^T}{d\mathbb{Q}} = \frac{B(t)/B(T)}{P(t, T)/P(T, T)} = \frac{e^{-\int_t^T r(u) du}}{P(t, T)}. \quad (1.13)$$

⁸A numeraire $N(t)$ normalizes the value of any asset in the market $V(t)$ by referring it to the numeraire units, i.e., $V(t)/N(t)$. The only necessary conditions to be imposed to the numeraire is to be positive and to pay no dividends.

Chapter 2

Interest-rate Models

This Chapter presents some of the most popular interest-rate models jointly with a brief description and discussion for each of them.⁹

2.1 Bachelier (Normal) Model (1900)

The Bachelier (or normal) model introduced by (Bachelier,1900) [3] is the most simple model for modelling negative interest rates. It is given by the following stochastic differential equation for the instantaneous forward rate F_t :

$$dF_t = \sigma_N \cdot dW_t, \quad (2.1)$$

where σ_N is the constant *normal volatility* and W_t is a Brownian Motion under the T -forward measure \mathbb{F}^T . The solution to the SDE (2.1) is

$$F_t = f + \sigma_N \cdot W_t, \quad \text{where } f = F_0, \quad (2.2)$$

so the process F_t is normally distributed.

The Bachelier model allows working with negative interest rates in a natural way because of its normal distribution. However, this advantage also results in one of the main drawbacks of the model. Indeed, the solution (2.2) evidences that with nonzero probability, F_t may become arbitrarily negative. Under typical circumstances, however, this is a relatively unlikely event, since rates are not assumed to go far away from the zero-barrier into the negative domain.

Furthermore, the basic premise of this model is that σ_N is constant, however this assumption is not supported by the interest volatility markets. In particular, for a given maturity, option implied volatilities exhibit a pronounced dependence on their strikes. This phenomenon is called the *volatility smile* or *skew*. The volatility smile/skew is different for each maturity as well, and the implied volatility as a function of both strike and maturity is called the *implied volatility surface*.

⁹The next Chapter focuses on the SABR model and several of its versions.

Under the Bachelier model the prices for a caplet/floorlet on a forward rate $F(t, T_1, T_2)$ with strike K and notional N are given by

$$V_{caplet}^{Bachelier}(T, K, f, \sigma_N) = N \cdot \delta(T_1, T_2) \cdot P(t, T_2) \cdot B_{call}^{Bachelier}(T_1, K, f, \sigma_N), \quad (2.3a)$$

$$V_{floorlet}^{Bachelier}(T, K, f, \sigma_N) = N \cdot \delta(T_1, T_2) \cdot P(t, T_2) \cdot B_{put}^{Bachelier}(T_1, K, f, \sigma_N), \quad (2.3b)$$

where

$$B_{call}^{Bachelier}(T_1, K, f, \sigma_N) = (f - K)\Phi(d) + \sigma_N \sqrt{T_1} \phi(d), \quad (2.4a)$$

$$B_{put}^{Bachelier}(T_1, K, f, \sigma_N) = (K - f)\Phi(-d) + \sigma_N \sqrt{T_1} \phi(d), \quad (2.4b)$$

where $\Phi(\cdot)$ and $\phi(\cdot)$ are the normal distribution function and the probability density, respectively, and

$$d = \frac{f - K}{\sigma_N \sqrt{T_1}}. \quad (2.4c)$$

The quantity $\delta(T_1, T_2)$ is the day-count convention and f denotes here *today's* value of $F(t, T_1, T_2)$.

Then, the prices for a cap and floor are

$$V_{cap}^{Bachelier} = N \sum_{j=T_1+1}^{T_2} \delta_j \cdot P(t, T_j) \cdot B_{call}^{Bachelier}(T_{j-1}, K, F_j, \sigma_N), \quad (2.5a)$$

$$V_{floor}^{Bachelier} = N \sum_{j=T_1+1}^{T_2} \delta_j \cdot P(t, T_j) \cdot B_{call}^{Bachelier}(T_{j-1}, K, F_j, \sigma_N), \quad (2.5b)$$

where δ_j is the day-count convention applying to the accrual period starting at T_{j-1} and ending at T_j , and F_j is the *today's* forward rate for that period.

2.2 Black (Lognormal) Model (1976)

The Black model is a variant of the original Black-Scholes model adapted to deal with forward underlying assets. It was introduced by (Black, 1976) [6], and it is given by the following stochastic differential equation for a instantaneous forward rate F_t :

$$dF_t = \sigma_B \cdot F_t \cdot dW_t, \quad (2.6)$$

where σ_B is the constant *lognormal volatility* and W_t is a Brownian Motion under the T -forward measure \mathbb{F}^T . The solution to the SDE (2.6) is

$$F_t = f e^{\sigma_B W_t - \frac{1}{2} \sigma_B^2 t}, \quad \text{where } f = F_0, \quad (2.7)$$

so the process F_t is lognormally distributed.

Using the T -maturity zero-coupon bond $P(t, T)$ as the numeraire asset for the T -forward measure \mathbb{F}^T with the property that, in the units of that numeraire, $F(t, T_1, T_2)$

is a tradable asset, then the Black formula states the *today's* prices, at time t , for a caplet/floorlet on a forward rate $F(t, T_1, T_2)$ with strike K and notional N are given by

$$V_{caplet}^{Black}(T, K, f, \sigma_B) = N \cdot \delta(T_1, T_2) \cdot P(t, T_2) \cdot B_{call}^{Black}(T_1, K, f, \sigma_B), \quad (2.8a)$$

$$V_{floorlet}^{Black}(T, K, f, \sigma_B) = N \cdot \delta(T_1, T_2) \cdot P(t, T_2) \cdot B_{put}^{Black}(T_1, K, f, \sigma_B), \quad (2.8b)$$

where

$$B_{call}^{Black}(T_1, K, f, \sigma_B) = f\Phi(d_+) - K\Phi(d_-), \quad (2.9a)$$

$$B_{put}^{Black}(T_1, K, f, \sigma_B) = K\Phi(-d_-) - f\Phi(-d_+), \quad (2.9b)$$

where $\Phi(\cdot)$ is the normal distribution function, and

$$d_{\pm} = \frac{\log\left(\frac{f}{K}\right) \pm \frac{1}{2}\sigma_B^2 T_1}{\sigma_B \sqrt{T_1}}. \quad (2.9c)$$

The quantity $\delta(T_1, T_2)$ is the day-count convention and f denotes here the present value of $F(t, T_1, T_2)$.

Then, the prices for a cap and floor are

$$V_{cap}^{Black} = N \sum_{j=T_1+1}^{T_2} \delta_j \cdot P(t, T_j) \cdot B_{call}^{Black}(T_{j-1}, K, F_j, \sigma_B), \quad (2.10a)$$

$$V_{floor}^{Black} = N \sum_{j=T_1+1}^{T_2} \delta_j \cdot P(t, T_j) \cdot B_{call}^{Black}(T_{j-1}, K, F_j, \sigma_B), \quad (2.10b)$$

where δ_j is the day-count convention applying to the accrual period starting at T_{j-1} and ending at T_j , and F_j is the *today's* forward rate for that period.

The Black model has two important drawbacks. Firstly, it cannot be used with negative interest rates. Note that the option prices just obtained depend, among other variables, on the logarithm of the forward rate and if the market-quoted forward rate is negative then the logarithm is undefined. On the other hand, if the strike were negative too, in which case the logarithm would be well defined, the model still could not be used since, theoretically, it is not defined for negative rates.

Furthermore, as occurs in the Bachelier model (2.1), the basic premise of this model, that σ_B is independent of K and f , is clearly rejected by the markets, where the volatility smile/skew is observed. Therefore, in order to accurately value and risk manage financial products, refinements to the Black model are necessary.

2.3 Shifted Black Model (2012)

Shifted Black model tries to solve the first drawback of the Black model (2.6) in order to deal with negative forward rates. Black model has some highly desired features that make institutions explore ways to remedy its breakdown for negative rates. One such remedy

is the inclusion of a constant displacement parameter s to the forward rate F_t , resulting the SDE

$$dF_t = \sigma_B \cdot (F_t + s) \cdot dW_t, \quad (2.11)$$

where $\sigma_B > 0$ and W_t is a Brownian Motion under the T -forward measure \mathbb{F}^T .

The Black model only allows rates to be nonnegative, however a shifted model with shift $s > 0$ allows rates larger than $-s$ to be modelled. In practice, this shift is chosen *a priori* by the analyst and this fact is the main drawback of the shifted model. The process of fixing s should be done meticulous and accurately. Its value should be *high enough* to avoid the magnitudes $F_t + s$ and $K + s$ going below zero for any given time, but should not be *extremely high* because in this case there can be obtained arbitrarily negative values for the forward interest rate.

Furthermore, note that by defining $\tilde{F}_t := F_t + s$ and $\tilde{K} := K + s$ as well, shifted Black model's formulation is equivalent to the Black's one. Consequently, pricing formulae obtained through Black model, equations (2.8) and (2.10), are valid for the shifted Black model. However, it is important to note that for any given cap/floor price, the implied volatilities of the shifted model and the lognormal model are not identical for $s > 0$, i.e., the model would require a specific calibration for given option prices.

2.4 One-factor Short-rate Models

One-factor short-rate models (short-rate models from now on) are defined through the dynamics for the instantaneous short-rate process r_t . These models differ significantly to the ones exposed in the previous sections, and also to the SABR model and its extensions, which will be explained in the Chapter 3, and therefore should be treated in a different way. Since Bachelier, (Shifted) Black, Normal SABR, Shifted SABR and Free-Boundary SABR models assume dynamics for the forward rate F_t , they could be called *forward-rate models*.¹⁰ Due to their nature, forward-rate models are devoted to deal with commonly-traded instruments of the market, such as caps/floors or swaptions, on the easiest possible way. Conversely, the short-rate models provide a complete scheme for the evolution of the instantaneous short rate from where prices for the mentioned instruments are consequently deducted. Analytical formulation, if possible, usually becomes far more complicated under this new scheme, since these models are not focused on pricing this kind of interest-rate derivatives. In spite of this, they have been included in the research in order to expand its framework through short-rate models context.

This Section is focused on two *basic* short-rate models able to cope with negative interest rates: Vasicek model and Hull-White model (also known as Extended Vasicek model).¹¹

¹⁰Notice that this notation is adopted for an easy differentiation between both types of models, but it is not generally used.

¹¹There exist other short-rate models able to cope with negative rates, as, for instance, Ho-Lee (1986), Cox (1975) or Heath-Jarrow-Morton (1992), which is not strictly considered a short-rate model, since it models the instantaneous forward rate (see (Heath et al., 1992) [24] for further details). However, the study will be limited to the Hull-White model, and its particularization the Vasicek model, due to its wide use among the industry, which is owed to the availability of analytical formulae for pricing caps/floors.

2.4.1 Vasicek Model (1977)

The Vasicek model, firstly introduced in (Vasicek, 1977) [41], assume that the instantaneous short rate r_t follows an *Ornstein-Uhlenbeck process* with constant coefficients under the risk-neutral measure. Its formulation is given by the following stochastic differential equation

$$dr_t = k(\theta - r_t) dt + \sigma dW_t, \quad (2.12)$$

where k, θ, σ are positive constants, and W_t is a Brownian Motion under the risk-neutral measure \mathbb{Q} .

The Ornstein-Uhlenbeck process is *mean-reverting*, in the sense that the instantaneous short rate r_t tends to return to the *long-term value* θ on a rate specified by the *mean reversion speed* k . The coefficient σ is the instantaneous short-rate volatility.

As shown in (Brigo and Mercurio, 2006) [8], under Vasicek model, the prices for a cap and floor at time t with notional N , strike rate K and set of times $T = [T_1, T_2]$ are

$$V_{cap}^{Vasicek} = N \sum_{j=T_1+1}^{T_2} \left(P(t, T_{j-1}) \Phi(\sigma_j - h_j) - (1 - \delta_j K) P(t, T_j) \Phi(-h_j) \right), \quad (2.13a)$$

$$V_{floor}^{Vasicek} = N \sum_{j=T_1+1}^{T_2} \left(-P(t, T_{j-1}) \Phi(h_j - \sigma_j) + (1 + \delta_j K) P(t, T_j) \Phi(h_j) \right), \quad (2.13b)$$

where $\Phi(\cdot)$ denotes the normal distribution function, and

$$P(t, T) = A(t, T) e^{-r_t B(t, T)}, \quad (2.14a)$$

$$A(t, T) = \exp \left\{ \left(\theta - \frac{\sigma^2}{2k^2} \right) (B(t, T) - T + t) - \frac{\sigma^2}{4k} B^2(t, T) \right\}, \quad (2.14b)$$

$$B(t, T) = \frac{1}{k} \cdot (1 - e^{-k(T-t)}), \quad (2.14c)$$

$$\sigma_j = \sigma \cdot \sqrt{\frac{1 - e^{-2k(T_{j-1}-t)}}{2k}} \cdot B(T_{j-1}, T_j), \quad (2.14d)$$

$$h_j = \frac{1}{\sigma_j} \log \left(\frac{(1 + \delta_j K) P(t, T_j)}{P(t, T_{j-1})} \right) + \frac{\sigma_j}{2}. \quad (2.14e)$$

2.4.2 Hull-White Model (1990)

The model that present Hull and White in (Hull and White, 1990) [28] extends the Vasicek model (2.12) by allowing its parameters to depend deterministically on time. As it has been frequently done along previous literature (see (Brigo and Mercurio, 2006) [8], for instance), here is analysed a restricted version of the Hull-White model which only allows the long-term value θ to change with time. Therefore, this *restricted* model states that the instantaneous short rate r_t satisfies the following stochastic differential equation

$$dr_t = k(\theta_t - r_t) dt + \sigma dW_t, \quad (2.15)$$

where k and σ are positive constants, θ_t is a deterministic function of time chosen so as to exactly fit the currently observed market term structure of interest rates,¹² and W_t is a Brownian Motion under the risk-neutral measure \mathbb{Q} .

The formulae for the *today's* values of a cap and floor under the Hull-White model are deduced by incorporating the currently observed term structure of interest rates in the form of both *market instantaneous forward rates* (at time 0 for maturity t) $F^m(0, t)$ and *market discount factors* $P^m(0, t)$, which are actually equivalent to the theoretical market zero-coupon bond price. Therefore, as shows (Brigo and Mercurio, 2006) [8], once Hull-White model is calibrated to market data, the prices for a cap and floor with notional N , strike rate K and set of times $T = [T_1, T_2]$ are

$$V_{cap}^{HullWhite} = N \sum_{j=T_1+1}^{T_2} \left(P(t, T_{j-1}) \Phi(\sigma_j - h_j) - (1 - \delta_j K) P(t, T_j) \Phi(-h_j) \right), \quad (2.16a)$$

$$V_{floor}^{HullWhite} = N \sum_{j=T_1+1}^{T_2} \left(-P(t, T_{j-1}) \Phi(h_j - \sigma_j) + (1 + \delta_j K) P(t, T_j) \Phi(h_j) \right), \quad (2.16b)$$

where $\Phi(\cdot)$ denotes the normal distribution function, and

$$P(t, T) = A^m(t, T) e^{-r_t B(t, T)}, \quad (2.17a)$$

$$A^m(t, T) = \frac{P^m(0, T)}{P^m(0, t)} \exp \left\{ B(t, T) F^m(0, t) - \frac{\sigma^2}{4k} B^2(t, T) (1 - e^{-2kt}) \right\}, \quad (2.17b)$$

$$B(t, T) = \frac{1}{k} \cdot (1 - e^{-k(T-t)}), \quad (2.17c)$$

$$\sigma_j = \sigma \cdot \sqrt{\frac{1 - e^{-2k(T_{j-1}-t)}}{2k}} \cdot B(T_{j-1}, T_j), \quad (2.17d)$$

$$h_j = \frac{1}{\sigma_j} \log \left(\frac{(1 + \delta_j K) P(t, T_j)}{P(t, T_{j-1})} \right) + \frac{\sigma_j}{2}. \quad (2.17e)$$

2.4.3 Differences between short-rate and forward-rate models

Once the previous models have been introduced, the differences between the short-rate models and the so-called forward-rate models can be clearly noticed. These differences are described below.

- The stochastic differential equations that describe the forward-rate models use the T -forward measure, while the short-rate models are defined under the risk-neutral measure.
- The parameter σ that describes the volatility of the instantaneous forward rate F_t is related to one particular maturity date, the one given by the maturity of the instantaneous forward rate which is specifically modelled under the T -forward measure, and therefore depends on the maturity under consideration. Conversely, the parameter σ that describes the volatility of the instantaneous short rate r_t is not related to any other specific date.

¹²In (Brigo and Mercurio, 2006) [8] there is an explicit expression of the calibration formula of θ_t in terms of market instantaneous forward rates, which can be bootstrapped from the risk-free discount curve observed at time t .

- Since both class of models have distinct nature, its calibration procedure, that will be fully explained later, is completely different. The calibration of the forward-rate models is performed by comparing market implied volatilities with theoretical implied volatilities, since these ones depend on the maturity under consideration. Conversely, short-rate models are calibrated by directly comparing market prices of caps/floors with theoretical prices.

Since there is no strict dependence on the maturity for the parameters of both Vasicek and Hull-White models, these can be calibrated by a non-linear least-squares comparison between theoretical cap/floor prices given by equations (2.13) and (2.16), and market cap/floor prices obtained by inserting the cap/floor implied volatility in the Black/Bachelier pricing formula (2.10)/(2.5).¹³

Finally, an important issue shall be commented. Notice that, within previous formulation, since the Hull-White parameter θ_t is estimated previously the calibration of the model, so as to exactly fit the currently observed market term structure of interest rates (TSIR), this model actually presents only two parameters (k, σ), less than its particularization the Vasicek model, which has three (k, θ, σ). Conversely, if the parameter θ_t is let to be a free time-dependent parameter, the calibration would be done by trinomial trees¹⁴, and therefore Vasicek model would be a particular case of the Hull-White model. However, doing this would imply an unfair pricing accuracy comparison between short-rate and forward-rate models. Indeed, since the original aim of the short-rate models that allow their parameters evolve with time is to fit today's TSIR, if θ_t is included in the caps calibration process, cap prices would be fitted within the model, but observed market TSIR probably would not be fitted at all. Furthermore, all forward-rate models studied in this research account for time-independent parameters. Then, introducing time-dependent parameters in the caps' calibration process is equivalent to introduce an independent-time model with infinite parameters. The model is therefore guaranteed to fit cap prices exactly, and the comparison lacks of sense. Then, since in comparability terms every model should have a finite number of parameters, numerical calibrations are not considered through the research.

¹³Notice that the market price of a cap/floor depends on the nature of the quoted volatility (whether if it is Black's or Bachelier's). Therefore, to obtain the cap/floor price, the nature of this quote should be considered.

¹⁴See (Kooiman, 2015) [29], for instance, about more details on the Hull-White model's calibration via trinomial trees.

Chapter 3

The SABR Model

Fixed income derivatives have been often priced and hedged among the industry by using the models exposed in Chapter 2 because of their simplicity. However, their major drawback is assuming the volatility parameter to be constant, since nowadays is well known that options with different strikes require different implied volatilities to match their market prices. Therefore, those models result unable to manage the phenomenon of volatility smile/skew observed within markets.

Local Volatility models, introduced by (Dupire, Derman, Kani, 1994) [16] [14] [13], are able to handle this problem, but they predict the behaviour of smiles and skews opposite to the behaviour observed in the marketplace, specifically when the underlying forward rate decreases, local volatility models predict that the smile/skew shifts to higher strike prices, and when the forward increases, these models predict that the curve shifts to lower strikes.¹⁵ That results in other problem, since due to this contradiction between model and market, delta and vega hedges derived from the model can be unstable and may perform worse than simple Black's hedges.

To solve it (Hagan et al., 2002) [22] derive the *Stochastic Alpha Beta Rho (SABR) model*, a stochastic-volatility version of the *Constant Elasticity of Variance (CEV) model*¹⁶ in which the forward rate and its volatility are correlated. This model provides an approximate closed-form formula for the implied volatility that fits *really* accurately the implied volatility curves observed in the markets and, more essentially, it captures the correct dynamics of the smile/skew, what yields stable hedges.

As it can be deduced from the paragraph above, the SABR model appears in response to the contradiction between the prediction for the dynamics of the volatility curve by the local volatility models and the observed market smile/skew, and therefore it is important

¹⁵Local volatility models are the first proposal for dealing with volatility smiles/skews within markets. These models consist on an improvement over the Black model (2.6) by using the market prices of options to find an effective specification of the underlying process, so that the implied volatilities match the market implied volatilities. However, a major problem with these models is that they predict the wrong dynamics of the volatility curve, and this fact leads to unstable and incorrect hedges. Their discussion is not included during the text, although interested readers can consult its main features in Appendix B.

¹⁶Since the CEV is not able to cope with negative rates (unless $\beta = 0$, in which case the Bachelier model (2.1) is obtained), it is not explained during the text. However, interested readers can consult the main features of the model in Appendix A.

to note that the value in the SABR model and its superiority over the local volatility models is an empirical issue, not an *a priori* theoretical one.

3.1 Classic SABR Model (2002)

The classic SABR model introduced by (Hagan et al., 2002) [22] is a two-factor stochastic volatility model whose dynamics is given by a system of two stochastic differential equations. The state variables F_t and σ_t can be thought of as the forward interest rate of maturity T and its volatility parameter. In more detail, there state the following equations.

$$dF_t = \sigma_t \cdot F_t^\beta \cdot dW_t^{(1)}, \quad F_0 = f, \quad (3.1a)$$

$$d\sigma_t = \nu \cdot \sigma_t \cdot dW_t^{(2)}, \quad \sigma_0 = \alpha, \quad (3.1b)$$

$$\mathbb{E}^{\mathbb{F}^T} [dW_t^{(1)} \cdot dW_t^{(2)}] = \rho dt, \quad (3.1c)$$

where $\nu \geq 0$, $0 \leq \beta \leq 1$, $-1 < \rho < 1$.

The parameter ν is the volatility of σ_t , so it is the *volatility-of-volatility* of the forward rate. The parameter β is called the *power parameter* of the model. Furthermore, note that all the parameters of the model, α , β , ρ and ν , are just constants, not functions of time, and all they are specific to a particular forward rate, the one of maturity T . $W_t^{(1)}$ and $W_t^{(2)}$ are two ρ -correlated Brownian Motions under the T -forward measure \mathbb{F}^T . Under this measure both the forward rate and its volatility are martingale (*driftless*) always if you work with one forward rate in isolation at a time. Under this same measure, however, the process for another forward rate and for its volatility would not be *driftless*.

It is crucial to notice that the model is specified for a particular forward rate, in this case, the one of maturity T (the superscript T is omitted in the equations for a shorthand notation). Therefore, within the SABR model there is no way for the various forward rates to interact with each other. The SABR model as it stands cannot describe the dynamics of a yield curve (TSIR), but it can be used to accurately fit the implied volatility curves observed in the marketplace for any single exercise date. More importantly, it predicts the correct dynamics of the implied volatility curves. This makes the SABR model an effective tool to manage the smile risk in markets where each asset only has a single exercise date.

Furthermore, the model is an stochastic volatility model, but unlike other stochastic volatility models such as the Heston's one¹⁷, for example, the SABR model does not produce option prices directly. Rather, it produces an estimate of the implied volatility curve, which is subsequently used as an input in the Black or Bachelier model to price interest rate derivatives.

¹⁷For more details about this model see (Heston, 1993) [25].

3.1.1 Implied volatilities within the SABR model

One of the reasons of the popularity of the SABR model is the availability of an approximated analytical solution for the implied (Black) volatility, called **Hagan's formula**.¹⁸ This implied volatility, which should be introduced in the Black formulae (2.10) in order to price a cap/floor for future investment period $T = [T_1, T_2]$, strike K and present value of the forward rate f , is given by

$$\sigma_B(T_1, K, f) = a_B(K, f) \cdot b_B(T_1, K, f) \cdot \frac{c(K, f)}{g(c(K, f))}, \quad (3.2a)$$

where

$$a_B(K, f) = \alpha \left[(Kf)^{\frac{1-\beta}{2}} \left(1 + \frac{(1-\beta)^2}{24} \log^2 \frac{f}{K} + \frac{(1-\beta)^4}{1920} \log^4 \frac{f}{K} + \dots \right) \right]^{-1}, \quad (3.2b)$$

$$b_B(T_1, K, f) = 1 + \left(\frac{\alpha^2(1-\beta)^2}{24 \cdot (Kf)^{1-\beta}} + \frac{\alpha \cdot \beta \cdot \rho \cdot \nu}{4 \cdot (Kf)^{\frac{1-\beta}{2}}} + \frac{2-3\rho^2}{24} \nu^2 \right) T_1 + \dots, \quad (3.2c)$$

$$c(K, f) = \frac{\nu}{\alpha} (Kf)^{(1-\beta)/2} \cdot \log \frac{f}{K}, \text{ and} \quad (3.2d)$$

$$g(x) = \log \left(\frac{\sqrt{x^2 - 2\rho x + 1} + x - \rho}{1 - \rho} \right). \quad (3.2e)$$

For at-the-money options ($f = K$), Hagan's formula reduces to

$$\sigma_B^{ATM}(T_1, K = f) = \frac{\alpha}{f^{1-\beta}} \left[1 + \left(\frac{\alpha^2(1-\beta)^2}{24 \cdot f^{2-2\beta}} + \frac{\alpha \cdot \beta \cdot \rho \cdot \nu}{4 \cdot f^{1-\beta}} + \frac{2-3\rho^2}{24} \nu^2 \right) T_1 \right]. \quad (3.3)$$

Hagan's formula (3.2) is typically used by analysts to calibrate an *implied Black volatility smile*. Similarly, there exists a formula for the Bachelier model to calibrate an *implied Bachelier volatility smile*. As shown in (Hagan et al., 2002) [22], the implied volatility that should be introduced in the Bachelier formula (2.5) in order to price a cap/floor for future investment period $T = [T_1, T_2]$, strike K and present value of the forward rate f is given by

$$\sigma_N(T_1, K, f) = a_N(K, f) \cdot b_N(T_1, K, f) \cdot \frac{c(K, f)}{g(c(K, f))}, \quad (3.4a)$$

where

$$a_N(K, f) = \alpha \cdot (Kf)^{\beta/2} \cdot \frac{1 + \frac{1}{24} \log^2 \frac{f}{K} + \frac{1}{1920} \log^4 \frac{f}{K} + \dots}{1 + \frac{(1-\beta)^2}{24} \log^2 \frac{f}{K} + \frac{(1-\beta)^4}{1920} \log^4 \frac{f}{K} + \dots}, \quad (3.4b)$$

$$b_N(T_1, K, f) = 1 + \left(\frac{-\alpha^2 \cdot \beta \cdot (2-\beta)^2}{24 \cdot (Kf)^{1-\beta}} + \frac{\alpha \cdot \beta \cdot \rho \cdot \nu}{4 \cdot (Kf)^{\frac{1-\beta}{2}}} + \frac{2-3\rho^2}{24} \nu^2 \right) T_1 + \dots, \quad (3.4c)$$

$$c(K, f) = \frac{\nu}{\alpha} (Kf)^{(1-\beta)/2} \cdot \log \frac{f}{K}, \text{ and} \quad (3.4d)$$

$$g(x) = \log \left(\frac{\sqrt{x^2 - 2\rho x + 1} + x - \rho}{1 - \rho} \right). \quad (3.4e)$$

¹⁸(Hagan et al., 2002) [22] made a small error when deriving the formula for the implied volatility, which was fixed by (Oblój, 2008) [34]. From here on, the corrected formula of Oblój is referred to as Hagan's formula.

The asymptotic solutions (3.2) and (3.4) are very easy to implement but they can lead to arbitrage opportunities. The formula of Hagan is known to become increasingly inaccurate as the strike approaches zero, producing wrong prices in region of small strikes for large maturities, since it is derived under the condition that $\nu^2 T_1 \ll 1$. So, it is not suitable for calibration of products with large maturity, in a market where volatility changes rapidly. It implies a negative probability density for the forward rate process in some region, although probability densities clearly should not be negative.

In addition, when the SABR model was introduced, positivity of the rates seemed a reasonable and attractive property. However, in the current market conditions, when rates are extremely low and even negative, in its current form the SABR (3.1) has the drawback that it cannot be used. In spite of this, because the SABR model is widely used within the industry, it would be practically preferable to adapt that model in a consistent way to deal with negative rates. Sections 3.2, 3.3 and 3.4 present three possible solutions, all of which have their pros and cons.

3.1.2 Behaviour of the SABR parameters

When fitting the SABR model, there are four parameters, α , β , ρ and ν , to calibrate¹⁹ for each forward rate with maturity T . Each parameter has a different interpretation and a different impact on the volatility curve (smile/skew). Table (3.1) summarizes these relevant features of the SABR parameters. Notice that each parameter has a main effect (in bold in the table), but also some of them have a smaller second and even third effect on the volatility curve.²⁰

Parameter	Curve property	Impact on the volatility curve
α : initial volatility	Level Slope	An increase in α shifts the curve upwards. As α increases, the steepness of the curve increases.
β : power parameter	Slope Level Curvature	A decrease in β decreases the steepness of the curve. An increase in β lowers the level of the curve. A decrease in β decreases the curvature of the curve.
ρ : correlation	Slope Curvature	As ρ decreases, the steepness of the curve increases. As ρ decreases, the curvature of the curve decreases.
ν : volatility-of-volatility	Curvature Slope	An increase in ν increases the curvature of the curve. An decrease in ν increases the steepness of the curve.

Table 3.1: *Impact of the SABR parameters on the volatility curve (smile/skew).*

¹⁹The next Subsection explains why, in general, the parameter β is not actually estimated but fixed before starting the estimation of the parameters.

²⁰(Rebonato et al., 2009) [35] explains in detail the qualitative behaviour of the SABR model. Furthermore, Figure (7.4), plotted in Chapter 7, shows the effects on the volatility curve exposed in Table (3.1).

3.1.3 Calibration of the SABR parameters

Now are described two methods for estimating the SABR parameters. Both methods start *estimating* the parameter β . Its value is predetermined either by fitting historical market volatility data or by choosing a value deemed appropriate for that market as stated in (Hagan et al., 2002) [22]. (Rebonato et al., 2009) [35] explains in detail why the market seems to endorse the choice of $\beta = 0.5$ for the SABR model. It is important to remark that, in practice, the choice of the parameter β has little effect on the resulting shape of the volatility curve produced by the SABR model, so the choice of this parameter is not crucial. Its choice, however, can affect the risk sensitivities. This issue will be treated later.

Method 1: Calibrate α , ρ , and ν directly

In this first calibration method, after fixing $\hat{\beta}$, the parameters α , ρ , and ν are all fitted directly. This can be accomplished by minimizing the sum of quadratic errors between the implied volatilities (either Black's or Bachelier's) computed by the model and the market volatilities σ_i^{mkt} , obtained from interest rate derivatives (caplets) with identical maturity and different strikes. Hence, the minimization algorithm used is

$$(\hat{\alpha}, \hat{\rho}, \hat{\nu}) = \arg \min_{\alpha, \rho, \nu} \sum_i (\sigma_i^{mkt} - \sigma(T_1, f^i, K^i; \alpha, \rho, \nu))^2. \quad (3.5)$$

Different weights $w_i \in [0, 1]$ can be allocated to the set of market volatilities according to the analyst criteria.

Method 2: Calibrate ρ and ν by implying α from at-the-money volatility

In this second calibration method the value of β is again predetermined as in Method 1. However, in this case, after fixing $\hat{\beta}$, the parameters ρ and ν are fitted directly while α is implied from the market at-the-money volatility. Therefore, the number of parameters to be estimated now is reduced by using the market σ^{ATM} to obtain $\hat{\alpha}$ by equation (3.3), rather than estimating it directly. This means that ρ and ν are estimated as in the previous method, while α is obtained by inverting equation (3.3) and taking into account that this parameter is the root of the following cubic polynomial that must be numerically solved

$$\left(\frac{(1 - \beta)^2}{24 \cdot f^{2-2\beta}} T_1 \right) \alpha^3 + \left(\frac{\beta \cdot \rho \cdot \nu}{4 \cdot f^{1-\beta}} T_1 \right) \alpha^2 + \left(1 + \frac{2 - 3\rho^2}{24} \nu^2 T_1 \right) \alpha - \sigma^{ATM} f^{1-\beta} = 0. \quad (3.6)$$

(West, 2004) [42] explains that this cubic polynomial can have more than one real root and the author suggests selecting the smallest positive root in this case. In the minimization algorithm, at every iteration α is found in terms of ρ and ν by solving (3.6) for $\alpha = \alpha(\rho, \nu)$. Then, the equation (3.5) becomes

$$(\hat{\alpha}, \hat{\rho}, \hat{\nu}) = \arg \min_{\alpha, \rho, \nu} \sum_i (\sigma_i^{mkt} - \sigma(T_1, f^i, K^i; \alpha(\rho, \nu), \rho, \nu))^2. \quad (3.7)$$

Although the number of parameters to be calibrated simultaneously is reduced, this estimation method might take more time to converge, since a root-finding algorithm must be used in every-step to obtain α from equation (3.6).²¹

3.2 Normal SABR Model (2002)

The normal SABR model is an extension of the Bachelier model (2.1) and it is the only version of the classic SABR model, obtained by fixing $\beta = 0$ in equation (3.1), that can model negative forward rates. It is defined as

$$dF_t = \sigma_t \cdot dW_t^{(1)}, \quad F_0 = f, \quad (3.8a)$$

$$d\sigma_t = \nu \cdot \sigma_t \cdot dW_t^{(2)}, \quad \sigma_0 = \alpha, \quad (3.8b)$$

$$\mathbb{E}^{\mathbb{F}^T} [dW_t^{(1)} \cdot dW_t^{(2)}] = \rho dt. \quad (3.8c)$$

In this case, as it stated in (Rebonato et al., 2009) [35], the expression for the implied Bachelier volatility becomes

$$\sigma_N(T_1, K, f) = \frac{\alpha}{f - K} \cdot \log \frac{f}{K} \cdot \frac{d(K, f)}{g(d(K, f))} \cdot \left[1 + \left(\frac{\alpha^2}{24 \cdot K f} + \frac{2 - 3\rho^2}{24} \nu^2 \right) T_1 + \dots \right], \quad (3.9a)$$

where

$$d(K, f) = \frac{\nu}{\alpha} \cdot \sqrt{Kf} \cdot \log \frac{f}{K}, \text{ and} \quad (3.9b)$$

$$g(x) = \log \left(\frac{\sqrt{x^2 - 2\rho x + 1} + x - \rho}{1 - \rho} \right). \quad (3.9c)$$

3.3 Shifted SABR Model (2014)

Shifted SABR model, originally proposed in (Sebastian, 2014) [39], is an extension of the shifted Black model (2.11) and it belongs to the class of shifted or displaced models. In these models, forward rate F_t is replaced with shifted forward rate $F_t + s$, where s is a positive constant, the shift parameter, and it moves the lower bound on F_t from 0 to $-s$. Therefore, the shifted SABR model under the T -forward measure \mathbb{F}^T is defined as

$$dF_t = \sigma_t \cdot (F_t + s)^\beta \cdot dW_t^{(1)}, \quad F_0 = f, \quad (3.10a)$$

$$d\sigma_t = \nu \cdot \sigma_t \cdot dW_t^{(2)}, \quad \sigma_0 = \alpha, \quad (3.10b)$$

$$\mathbb{E}^{\mathbb{F}^T} [dW_t^{(1)} \cdot dW_t^{(2)}] = \rho dt. \quad (3.10c)$$

The classic SABR model only allows rates to be nonnegative, however the shifted SABR model with shift $s > 0$ allows rates larger than s to be modelled. Furthermore, notice that with $\tilde{F}_t := F_t + s$ the classic SABR model (3.1) is obtained. So with \tilde{F}_t and $\tilde{K} := K + s$ as well, all expressions for the classic SABR apply.

²¹See, for instance, (Rouah, 2007) [36].

A drawback of the shifted SABR model is that the shift parameter needs to be selected *a priori*, since it is not known how low the interest rates can go. Although there is no clear consensus as to the exact value of the shift, it should however be such that the logarithm of the forward rate plus the shift is well-defined (Deloitte, 2016) [11]. Selecting the shift value manually and calibrating only the classic SABR parameters might require readjustment of the shift if rates went lower than anticipated and afterwards the present value and risk of the entire portfolio need to be recomputed.²²

3.4 Free-Boundary SABR Model (2015)

The free-boundary SABR (FB-SABR) model can be seen as a natural extension of the classic SABR model (3.1). The main strength of this model is that it is designed to handle with negative forward rates. This is done by introducing the absolute value in the stochastic differential equation of the forward rate F_t . As it can be seen in (Deloitte, 2016) [10], for instance, the dynamics of the FB-SABR model is given by

$$dF_t = \sigma_t \cdot |F_t|^\beta \cdot dW_t^{(1)}, \quad F_0 = f, \quad (3.11a)$$

$$d\sigma_t = \nu \cdot \sigma_t \cdot dW_t^{(2)}, \quad \sigma_0 = \alpha, \quad (3.11b)$$

$$\mathbb{E}^{\mathbb{F}^T} [dW_t^{(1)} \cdot dW_t^{(2)}] = \rho dt, \quad (3.11c)$$

where $0 \leq \beta < \frac{1}{2}$ guarantees the stability of the solution, as shown in (Frankena, 2016) [18].

Analytical solutions for the forward rate under the FB-SABR model are available just for the cases $\nu = 0$ and $\rho = 0$. Despite of this fact, a close formula for the implied volatility of this model can be computed. As is known, Hagan's formula is used to calibrate an implied Black and Bachelier volatility smile (3.2), (3.4). Since FB-SABR can model rates from the whole real line, it is natural to use implied Bachelier volatilities. Then, as shown in (Frankena, 2016) [18], the implied Bachelier volatility for the FB-SABR is given by

$$\sigma_N(T_1, K, f) = \alpha \cdot \frac{(f - K)(1 - \beta)}{f/|f|^\beta - K/|K|^\beta} \cdot \frac{e(K, f)}{g(e(K, f))} \cdot i(T_1, K, f), \quad (3.12a)$$

where

$$e(K, f) = \frac{\nu}{\alpha} \cdot \frac{(f - K)}{|F_{GM}|^\beta}, \quad (3.12b)$$

$$i(T_1, K, f) = 1 + \left(\frac{-\alpha^2 \cdot \beta \cdot (2 - \beta)}{24 \cdot |F_{GM}|^{2-2\beta}} + \frac{\alpha \cdot \beta \cdot \rho \cdot \nu \cdot \text{sign}(F_{GM})}{4 \cdot |F_{GM}|^{1-\beta}} \right) T_1 + \dots, \quad (3.12c)$$

$$g(x) = \log \left(\frac{\sqrt{x^2 - 2\rho x + 1} + x - \rho}{1 - \rho} \right), \text{ and} \quad (3.12d)$$

$$F_{GM} = \text{sign}(Kf) \sqrt{|Kf|}, \quad (3.12e)$$

that is chosen as the generalized geometric mean.

As stated in (Frankena, 2016) [18], the main drawback of the FB-SABR model is that its implied probability density is negative for a large area around zero, which in fact

²²See (Antonov et al., 2015) [2] for further details.

is the most relevant area in a low rate environment. Therefore, although the FB-SABR is able to model negative interest rates, its breakdown around zero makes it unreliable and unrealistic. For this reason, the model has been generally unused in practice, while the shifted SABR has become the natural candidate to replace the classic SABR model in a context of negative interest rates.

3.5 Comparison of models able to cope with negative rates

Table (3.2) presents a summarized *theoretical* comparison among all the models able to cope with negative interest rates explained up to now.

Model	Range F_t	Analytical solution	Model the smile/skew	Advantages	Disadvantages
Shifted Black	$(-s, +\infty)$	Yes	No	Analytical simplicity. Negative values below the shift (s) are not allowed.	Requires as input an appropriate volatility that may not be quoted in the market (s).
Bachelier	$(-\infty, +\infty)$	Yes	No	Analytical simplicity.	Extreme negative values are possible.
Shifted SABR	$(-s, +\infty)$	Yes	Yes	Negative values below the shift (s) are not allowed.	Requires as input an appropriate volatility that may not be quoted in the market (s).
Normal SABR	$(-\infty, +\infty)$	Yes	Yes	Able to deal with negative interest rates without the need of additional input (s).	Extreme negative values are possible.
FB-SABR	$(-\infty, +\infty)$	No, in general	Yes	Able to deal with negative interest rates without the need of additional input (s).	Extreme negative values are possible.
Vasicek	$(-\infty, +\infty)$	Yes	No	Able to deal with negative interest rates.	Complicated analytical formulation, since it is not focused on pricing market instruments.
Hull-White	$(-\infty, +\infty)$	Yes	No	Able to deal with negative interest rates. Fits the TSIR.	Complicated analytical formulation, since it is not focused on pricing market instruments.

Table 3.2: Comparison of the models able to cope with negative interest rates.

Chapter 4

Hedging under the SABR Model

The main goal of the previous models, jointly with the possible pricing applications, is the ability to produce reliable risk measures, and this fact is of significant practical importance. Since this research focuses on the performance of the (shifted) SABR model (under the current context of negative interest rates), this Chapter will be devoted to the hedging properties of this model.²³ The *Greeks* *delta*, *vega*, *dual-delta*, *gamma*, *vanna* and *volga* will be computed in the (shifted) SABR framework. Additionally, the sensitivities with respect to the parameters of the model (β , ρ and ν)²⁴ will be analysed, as well as the sensitivity with respect to the shift parameter s .²⁵

During the hedging analysis through this Chapter the (shifted) Black model is considered as the basis for option pricing. Furthermore, since the (shifted) SABR model provides the value of a caplet, the treatment will focus on a caplet on a forward rate $F(0, T_1, T_2)$ with strike rate K and notional N . Let f denote the current value of the underlying forward rate and let α be the currently observed value of the instantaneous volatility σ_t .²⁶ Then, it should be recalled that the caplet price obtained by the model under consideration is given by $V_{caplet}^{Black}(T, K, f, \sigma_B) = N \cdot \delta(T_1, T_2) \cdot P(0, T_2) \cdot B_{call}^{Black}(T_1, K, f, \sigma_B)$, (see formulae (2.8a) and (2.9a)), where $\sigma_B \equiv \sigma_B(T_1, K, f)$ is the implied Black volatility for the SABR model (see formula (3.2a)).²⁷

Furthermore, as it was explained in previous sections, with $\tilde{F}_t = F_t + s$ and $\tilde{K} = K + s$, all expressions obtained for the SABR model also apply for the shifted SABR model. Therefore, as s is a constant, the formulae for the sensitivities of the SABR model are exactly the same as those for the shifted SABR, taking into account that in the shifted SABR the forward rate and the strike are shifted by s .

²³It would be highly interesting and useful to analyse and test the hedges under all already explained models that admit negative interest rate (Shifted Black, Bachelier, Normal SABR, Shifted SABR, Free-Boundary SABR, Vasicek and Hull-White models). However, this comparison states beyond the scope of the Thesis and, therefore, it will not be included in the research.

²⁴As it is well known the (shifted) SABR model has four parameters, α , β , ρ and ν . As it will be explained next, however, the sensitivity with respect to the parameter α is defined as the Greek vega.

²⁵Notice that both parameters β and s are assumed to be given constants. Despite of this fact, it seems interesting to include the derivatives with respect to them to the hedging part in order to contribute to a complete sensitivity analysis.

²⁶The analysis is similar for floorlets, and easily extends to caps, floors.

²⁷For simplicity and clarity in the notation, the specification by the superscript *SABR* will be omitted.

4.1 SABR Greeks

This Section develops the *original* delta and vega risks within the SABR model presented in (Hagan et al., 2002) [22]. However, (Bartlett, 2006) [4] argues that these risks can be hedged more precisely by adding new terms to the original formulae. This claim is also supported by empirical and numerical arguments in (Agarwal and McWilliams, 2010) [1], (Hagan et al., 2014) [21] and (Hull and White, 2017) [27]. Therefore, the *modified* formulae for the delta and vega risks that lead to more robust hedges than the original ones will be also presented.

A crucial issue that would be commented with respect to the new terms added to the original formulae is that their effect is minimized when both delta and vega risks are hedged, but are substantial when only delta is hedged. As it was explained before, in the SABR model usually the parameter β is fixed before the model's calibration, and its choice does not have a big effect on the resulting shape of the volatility curve produced by the model. However, the original delta risk then depends on the β chosen as explained in (Hagan and Lesniewski, 2017) [20]. With the new term, the delta risk (i.e., the modified delta risk) is much less sensitive to the particular value of the parameter β .

This Section will also present the Greeks gamma, dual-delta, vanna and volga.

4.1.1 Delta and Vega hedging. Bartlett's corrections

The delta risk is defined as the change in the caplet price caused by a unit change in the value of the underlying forward rate.

The SABR delta depends on the calibration method used: Method 1 - calibrating α , ρ , and ν directly (see formula (3.5)), or Method 2 - calibrating ρ and ν by implying α from the ATM volatility σ^{ATM} (see formula (3.7)).²⁸

With the first method, where $\sigma_B \equiv \sigma_B(T_1, K, f, \alpha, \beta, \rho, \nu)$, the original delta with respect to the present value of the underlying forward rate f , as presented in (Hagan et al., 2002) [22], is given by²⁹

$$\Delta_{Hagan}^{(1)} = \frac{\partial V_{caplet}^{Black(1)}}{\partial f} = N \cdot \delta(T_1, T_2) \cdot P(0, T_2) \cdot \left(\frac{\partial B_{call}^{Black}}{\partial f} + \frac{\partial B_{call}^{Black}}{\partial \sigma_B} \cdot \frac{\partial \sigma_B}{\partial f} \right). \quad (4.1)$$

With the second method, where $\sigma_B \equiv \sigma_B(T_1, K, f, \alpha(\sigma^{ATM}), \beta, \rho, \nu)$ with σ^{ATM} given in the formula (3.3)³⁰, the original delta with respect to the present value of the underlying forward rate f , as presented in (Hagan et al., 2002) [22], is given by

$$\Delta_{Hagan}^{(2)} = \frac{\partial V_{caplet}^{Black(2)}}{\partial f} = N \cdot \delta(T_1, T_2) \cdot P(0, T_2) \cdot \left(\frac{\partial B_{call}^{Black}}{\partial f} + \frac{\partial B_{call}^{Black}}{\partial \sigma_B} \cdot \left(\frac{\partial \sigma_B}{\partial f} + \frac{\partial \sigma_B}{\partial \alpha} \cdot \frac{\partial \alpha}{\partial f} \right) \right). \quad (4.2)$$

²⁸Although in the research the first calibration method is used, as it will be explained later, here are presented *both types* of delta for continuity of the analysis.

²⁹Notice that here, and also in all partial derivatives through the Chapter, it will be applied the *Chain Rule of Differentiation*, which can be refreshed, if was needed, in (Sydsæter, 2005) [40], for instance.

³⁰Note that σ_{ATM} depends on f , and therefore α depends on f implicitly.

Moving on to the vega risk, the focus is now the effect on the caplet price when the volatility of the underlying forward rate changes by a unit amount.

Before defining the expression of the vega it is important to discuss the nature of this Greek in the SABR model. In the (shifted) Black model the hedging is often expressed in terms of price sensitivities to quantities that are unambiguously defined. Particularly, the vega is unambiguously defined as the sensitivity of the caplet price to a change in the lognormal volatility. However, when dealing with the (shifted) SABR model, one has to be careful when taking derivatives with respect to the *the volatility*, since in this case there are the implied Black volatility $\sigma_B(T_1, K, f, \alpha, \beta, \rho, \nu)$ and the instantaneous volatility σ_t , whose currently observed value was denoted as α . Then, should the derivative be taken with respect to σ_B or with respect to α ? Through the revised literature the authors compute the vega by deriving the price of a caplet with respect to α . Despite of this fact, computing vega as the derivative with respect to the implied volatility $\sigma_B(\cdot)$ also makes sense, since the implied volatility is the volatility that is quoted in the markets, so when this volatility changes, the price of the cap is, obviously, also changing. Therefore, it would be convenient, for comparison purposes, to compute *both types* of vega.³¹ In what follows the vega will be defined as it can be found in the bibliography³², but in the part of *Empirical analysis both types* of vega will be computed numerically and compared.

The expression of the original vega is as follows.

$$\Lambda_{Hagan} = \frac{\partial V_{caplet}^{Black}}{\partial \alpha} = N \cdot \delta(T_1, T_2) \cdot P(0, T_2) \cdot \frac{\partial B_{call}^{Black}}{\partial \sigma_B} \cdot \frac{\partial \sigma_B}{\partial \alpha}. \quad (4.3)$$

As it was mentioned before, in general, the expressions of delta and vega just described do not provide the *best hedge*, understanding by best hedge the optimal position in the forward rate to minimize the variance of the hedged portfolio returns, as shown in (Rebonato et al., 2009) [35]. Therefore, the Bartlett's corrections to the delta and vega risks are presented now.

As it was seen, in the SABR model, the Brownian motions in the dynamics of the forward rate process F_t and the volatility process σ_t are ρ -correlated. However, this correlation is not accounted in the Δ_{Hagan} and Λ_{Hagan} derivations shown above. Roughly speaking, the risk measures are computed by shifting only one parameter. This means that the shift to f and α in both cases are as the following diagrams indicate.

$$\Delta_{Hagan} : \begin{array}{l} f \rightarrow f + \Delta f \\ \alpha \rightarrow \alpha \end{array} \quad (4.4)$$

$$\Lambda_{Hagan} : \begin{array}{l} f \rightarrow f \\ \alpha \rightarrow \alpha + \Delta \alpha \end{array} \quad (4.5)$$

³¹As explained in (Deloitte, 2016) [12], in practice the traditional vega, i.e., vega computed with respect $\sigma_B(\cdot)$, is not often a quantity used in Front-Office risk management. As the authors agree, banks using a (shifted) SABR would hedge the individual SABR parameters, particularly the vega computed with respect to α , rather than the traditional vega. Traditional vega, however, will still have to be computed for regulatory purposes, in particular for the Fundamental Review of the Trading Book.

³²During the Chapter, this argumentation will be applied to all the SABR Greeks that use a derivative with respect to the volatility, particularly to vanna and volga.

Taking into account the correlation in the dynamics of the SABR model, these diagrams are not fully correct, since when one factor (f or α) changes, the other factor (α or f) is also likely to change according to the correlation ρ .

Following the Bartlett's approach, when deriving delta it is necessary to introduce a shift for α that depends on the shift in f ($\Delta_f \alpha$), and when deriving vega a shift for f that depends on the shift in α ($\Delta_\alpha f$) should be added. Graphically this idea states as follows.

$$\Delta_{\text{Bartlett}} : \begin{array}{l} f \rightarrow f + \Delta f \\ \alpha \rightarrow \alpha + \Delta_f \alpha \end{array} \quad (4.6)$$

$$\Lambda_{\text{Bartlett}} : \begin{array}{l} f \rightarrow f + \Delta_\alpha f \\ \alpha \rightarrow \alpha + \Delta \alpha \end{array} \quad (4.7)$$

The corresponding mathematical approach for this correction proceeds as follows.³³

Firstly, the dynamics of the SABR model is expressed in terms of two *independent* Brownian motions by using the *Cholesky decomposition*³⁴

$$dF_t = \sigma_t \cdot F_t^\beta \cdot dW_t^{(1)}, \quad F_0 = f, \quad (4.8a)$$

$$d\sigma_t = \nu \cdot \sigma_t \cdot (\rho \cdot dW_t^{(1)} + \sqrt{1 - \rho^2} \cdot dZ_t), \quad \sigma_0 = \alpha, \quad (4.8b)$$

$$\mathbb{E}^{\mathbb{F}^T} [dW_t^{(1)} \cdot dZ_t] = 0 dt, \quad (4.8c)$$

where $dW_t^{(2)} = \rho \cdot dW_t^{(1)} + \sqrt{1 - \rho^2} \cdot dZ_t$.

When combining equations (4.8a) and (4.8b), and rearranging terms, the following expressions are obtained

$$d\sigma_t = \frac{\rho \nu}{F_t^\beta} \cdot dF_t + \nu \sigma_t \sqrt{1 - \rho^2} \cdot dZ_t, \quad \text{and} \quad (4.9a)$$

$$dF_t = \frac{\rho F_t^\beta}{\nu} \cdot d\sigma_t + \sigma_t F_t^\beta \sqrt{1 - \rho^2} \cdot dZ_t. \quad (4.9b)$$

It can be clearly seen that the changes to σ_t and the changes to F_t come from one of the two terms in each expression, respectively, originating two types of changes which are denoted as

$$\Delta_F \sigma_t := \frac{\rho \nu}{F_t^\beta} dF_t \quad \left(\Rightarrow \Delta_f \alpha := \frac{\rho \nu}{f^\beta} \right) \quad (4.10a)$$

for the “changes in σ_t caused by a change in F_t ”, and

$$\Delta_\sigma F_t := \frac{\rho F_t^\beta}{\nu} d\sigma_t \quad \left(\Rightarrow \Delta_\alpha f := \frac{\rho f^\beta}{\nu} \right) \quad (4.10b)$$

for the “changes in F_t caused by a change in σ_t ”.

³³For a thorough discussion, see (Hagan and Lesniewski, 2017) [20] and (Hansen, 2011) [23].

³⁴The Cholesky decomposition states that if $W_t^{(1)}$ and Z_t are two uncorrelated Brownian motions, then $W_t^{(1)}$ and $dW_t^{(2)} = \rho \cdot dW_t^{(1)} + \sqrt{1 - \rho^2} \cdot dZ_t$ are two ρ -correlated Brownian motions, with $\rho \neq 0$. See (McDonald, 2006) [33], for example, if a refreshment about the Cholesky decomposition was needed.

Therefore, with the corrections, the modified expressions for delta and vega are³⁵

$$\Delta_{Bartlett} = N \cdot \delta(T_1, T_2) \cdot P(0, T_2) \cdot \left(\underbrace{\frac{\partial B_{call}^{Black}}{\partial f} + \frac{\partial B_{call}^{Black}}{\partial \sigma_B} \cdot \frac{\partial \sigma_B}{\partial f}}_{\Delta_{Hagan}} + \underbrace{\frac{\partial B_{call}^{Black}}{\partial \sigma_B} \cdot \frac{\partial \sigma_B}{\partial \alpha} \cdot \frac{\rho \nu}{f^\beta}}_{\text{Bartlett's correction}} \right), \text{ and} \quad (4.11)$$

$$\Lambda_{Bartlett} = N \cdot \delta(T_1, T_2) \cdot P(0, T_2) \cdot \left(\underbrace{\frac{\partial B_{call}^{Black}}{\partial \sigma_B} \cdot \frac{\partial \sigma_B}{\partial \alpha}}_{\Lambda_{Hagan}} + \underbrace{\left(\frac{\partial B_{call}^{Black}}{\partial f} + \frac{\partial B_{call}^{Black}}{\partial \sigma_B} \cdot \frac{\partial \sigma_B}{\partial f} \right) \cdot \frac{\rho f^\beta}{\nu}}_{\text{Bartlett's correction}} \right). \quad (4.12)$$

Note that in both formulae (4.11) and (4.12), the Bartlett's correction involves the term f^β . Then, recall that when dealing with negative interest rates through the shifted SABR model this term should be \tilde{f}^β , where $\tilde{f} := f + s$. Otherwise, since $f < 0$ and $0 \leq \beta \leq 1$ (particularly, $\beta = 0.5$), this term would result in *complex number* and, therefore the Bartlett's delta and vega would not be correctly computed.

4.1.2 Other Greeks

Dual-delta is defined as the sensitivity of the caplet price with respect to infinitesimal changes in the strike rate, and it is given by

$$\text{Dual} - \Delta = \frac{\partial V_{caplet}^{Black}}{\partial K} = N \cdot \delta(T_1, T_2) \cdot P(0, T_2) \cdot \left(\frac{\partial B_{call}^{Black}}{\partial K} + \frac{\partial B_{call}^{Black}}{\partial \sigma_B} \cdot \frac{\partial \sigma_B}{\partial K} \right). \quad (4.13)$$

The Greek *gamma*, which accounts for the sensitivity of delta with respect to infinitesimal changes in the forward rate, is given by

$$\Gamma = \frac{\partial^2 V_{caplet}^{Black}}{\partial f^2} \equiv \frac{\partial \Delta}{\partial f} = N \cdot \delta(T_1, T_2) \cdot P(0, T_2) \cdot \left(\frac{\partial^2 B_{call}^{Black}}{\partial f^2} + \frac{\partial B_{call}^{Black}}{\partial \sigma_B} \cdot \frac{\partial^2 \sigma_B}{\partial f^2} \right). \quad (4.14)$$

The *vanna* and *volga* Greeks, which account for the sensitivity of delta and vega, respectively, to infinitesimal changes in the volatility of the underlying forward rate, are given by the following expressions.

$$\text{Vanna} = \frac{\partial^2 V_{caplet}^{Black}}{\partial f \partial \alpha} \equiv \frac{\partial \Delta}{\partial \alpha} = N \cdot \delta(T_1, T_2) \cdot P(0, T_2) \cdot \left(\frac{\partial^2 B_{call}^{Black}}{\partial f \partial \sigma_B} + \frac{\partial B_{call}^{Black}}{\partial \sigma_B} \cdot \frac{\partial^2 \sigma_B}{\partial f \partial \alpha} \right). \quad (4.15)$$

$$\text{Volga} = \frac{\partial^2 V_{caplet}^{Black}}{\partial \alpha^2} \equiv \frac{\partial \Lambda}{\partial \alpha} = N \cdot \delta(T_1, T_2) \cdot P(0, T_2) \cdot \left(\frac{\partial^2 B_{call}^{Black}}{\partial \sigma_B^2} + \frac{\partial B_{call}^{Black}}{\partial \sigma_B} \cdot \frac{\partial^2 \sigma_B}{\partial \alpha^2} \right). \quad (4.16)$$

Given the significant complexity of obtaining a closed-form solution for the SABR Greeks, it is a common practice to compute the partial derivatives numerically by using *finite difference methods*.³⁶

³⁵No information has been found about the modified delta for the second calibration method, therefore here is presented only the adjustment to the delta for the first calibration method. However, since in the research the *Method 1* is used, the absence of developments for the corrected delta under the *Method 2* is not concerning.

³⁶See Appendix D.

4.2 SABR parameters sensitivities

This Section analyses the dependence of the caplet price (2.8a) with respect to the SABR parameters β , ρ , ν (and s in the shifted SABR model).³⁷ Parameters sensitivities are an important aspect, in addition to the Greeks, since know how the price of an instrument changes when quantities that the model assumes to be constant are allowed to *vary*, improves the quality of the hedge providing robustness. This type of sensitivities are related to possible misspecifications of the model parameters, which can arise from an incorrect calibration of the model, i.e., from the use of an inappropriate model, and since SABR parameters are determined by fitting the implied volatility curve observed in the marketplace, risks to β , ρ and ν changing (especially, to ρ and ν , as it was commented before) clearly exist and they should be analysed.

Regarding the SABR parameters sensitivities analysis through the literature, not too much information has been found. The idea of the hedging against the parameters of the model is commented by (Rebonato et al., 2009) [35], although the authors do not perform an explicit analysis on the topic. The authors of (Hagan et al., 2002) [22] suggest that the parameters ρ and ν ³⁸ are very stable (need to be updated only every few weeks, contrary to α , which may need to be updated every few hours in fast-paced markets), because the SABR model reproduces the usual dynamics of smiles and skews, but they do not accomplish any study on the topic.

Let denote these sensitivities of the caplet price V_{caplet}^{Black} with respect to the parameters as $\mathcal{S}^{(\beta)}$, $\mathcal{S}^{(\rho)}$ and $\mathcal{S}^{(\nu)}$. Therefore, they are given by the expressions

$$\mathcal{S}^{(\beta)} = \frac{\partial V_{caplet}^{Black}}{\partial \beta} = N \cdot \delta(T_1, T_2) \cdot P(0, T_2) \cdot \frac{\partial B_{call}^{Black}}{\partial \sigma_B} \cdot \frac{\partial \sigma_B}{\partial \beta}, \quad (4.17a)$$

$$\mathcal{S}^{(\rho)} = \frac{\partial V_{caplet}^{Black}}{\partial \rho} = N \cdot \delta(T_1, T_2) \cdot P(0, T_2) \cdot \frac{\partial B_{call}^{Black}}{\partial \sigma_B} \cdot \frac{\partial \sigma_B}{\partial \rho}, \text{ and} \quad (4.17b)$$

$$\mathcal{S}^{(\nu)} = \frac{\partial V_{caplet}^{Black}}{\partial \nu} = N \cdot \delta(T_1, T_2) \cdot P(0, T_2) \cdot \frac{\partial B_{call}^{Black}}{\partial \sigma_B} \cdot \frac{\partial \sigma_B}{\partial \nu}. \quad (4.17c)$$

As in the case of the SABR Greeks, these sensitivities will be numerically computed, and the obtained results will be fully explained in Section 7.2.

Finally, a *new* shifted SABR sensitivity is defined. It accounts for the sensitivity of a caplet price with respect to the shift parameter s .³⁹

As it was explained, all sensitivities already computed are valid for both the SABR and shifted SABR models. Therefore, until now the dependence of the forward rate and the strike rate on the shift parameter s was implicitly considered, since the notation was not changed by $\tilde{F}_t = F_t + s$ and $\tilde{K} = K + s$ for clarity and simplicity in the text. However, since the sensitivity of a caplet price with respect to the shift parameter s will be derived

³⁷Recall that the sensitivity with respect to the parameter α was already computed, since this sensitivity is defined as the Greek vega.

³⁸The parameter β is assumed to be a given constant.

³⁹It is remarkable that this sensitivity analysis is an innovative contribution to the research, since no information about it has been found during the literature review.

now, an explicit expression that contains s is needed.

Let denote the caplet price obtained through the shifted SABR model by $\tilde{V}_{caplet}^{Black}(T_1, \tilde{K}, \tilde{f}, \tilde{\sigma}_B)$, where $\tilde{\sigma}_B(T_1, \tilde{K}, \tilde{f}, \alpha, \beta, \rho, \nu)$ is the implied shifted Black volatility, and $\tilde{f} = f + s$ and $\tilde{K} = K + s$. Then, the formula for this sensitivity, which is denoted by $\mathcal{S}^{(s)}$, is given by

$$\mathcal{S}^{(s)} = \frac{\partial \tilde{V}_{caplet}^{Black}}{\partial s} = N \cdot \delta(T_1, T_2) \cdot P(0, T_2) \cdot \frac{\partial \tilde{B}_{call}^{Black}}{\partial \tilde{\sigma}_B} \cdot \frac{\partial \tilde{\sigma}_B}{\partial s}. \quad (4.18)$$

This sensitivity will also be numerically computed and analysed in Section 7.2.

Part II
Empirical analysis

Chapter 5

Data

This Chapter is devoted to the description of the data used through this second part of the research. Firstly, some basic and relevant issues related to the market conventions for the datasets included in the study are explained, particularly for the implied volatilities used in the calibration procedure of the models. Secondly, the main features of these data are described and explained in detail.

5.1 Data conventions

The first issue that should be commented is that the interest rate markets use implied volatilities, instead of monetary units such as EUR or USD, for quoting interest rate derivatives such as caps/floors.⁴⁰ The main reason of this practice is that the implied volatility does not change as frequently as the derivative prices, since the implied volatility removes the effect of parameters not related to the volatility that affect the derivative price, such as the discount curve, the strike, the maturity and the tenor. When the price of the underlying interest rate changes, the derivative price might change while the volatility may not.

In markets where the interest rates have not yet reached negative values, the implied Black volatilities are fully defined and there are no technical problems (for instance, in the US market), i.e., in these markets the implied Black volatilities are quoted as usual. However, in markets where interest rates have gone negative (for instance, in the EUR market) the implied Black volatilities are not defined for negative values and this brings technical problems into the market quoting system. As a solution to this problem the affected markets have started to quote implied volatilities using the shifted Black or the Bachelier (normal) model. The corresponding quoted cap volatilities in these markets are then shifted Black implied volatilities and Bachelier (normal) implied volatilities respectively.

Another important issue, especially when calibrating models using caps (as it is done in this research, and as it will be fully explained later), is that caps contracts do not necessarily have the same definition across different markets. Since through the research EUR market implied cap volatilities are used, the convention of how caps are defined in

⁴⁰Recall that the implied volatility is the volatility that should be introduced in a benchmark pricing model (as the Black or the Bachelier models) in order to recover the market price of a derivative product.

this market is explained.

First, for cap maturities up to 2 years the corresponding underlying caplets are of 3 months, i.e., the EUR quoted caps with maturity up to 2 years (1Y, 18M and 2Y) have a tenor of 3 months, and the caplet corresponding to the first 3-month interval is excluded from the cap.⁴¹ However, the caps with maturities above 2 years (3Y, 4Y,..., 20Y) are based on 6-month underlying caplets, then these caps have a tenor of 6 months.⁴²

In Figure (5.1) and Figure (5.2) are illustrated the quoting features of the EUR quoted caps in order to clarify the differences just commented.

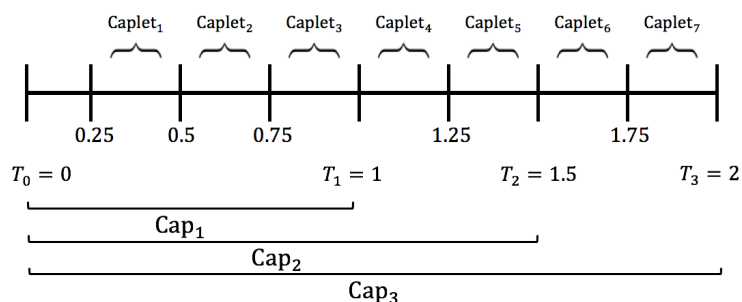


Figure 5.1: *Cap grid for cap maturities up to 2 years in the EUR market. The caps are composed of 3-month underlying caplets. Note that the first caplet is omitted.*

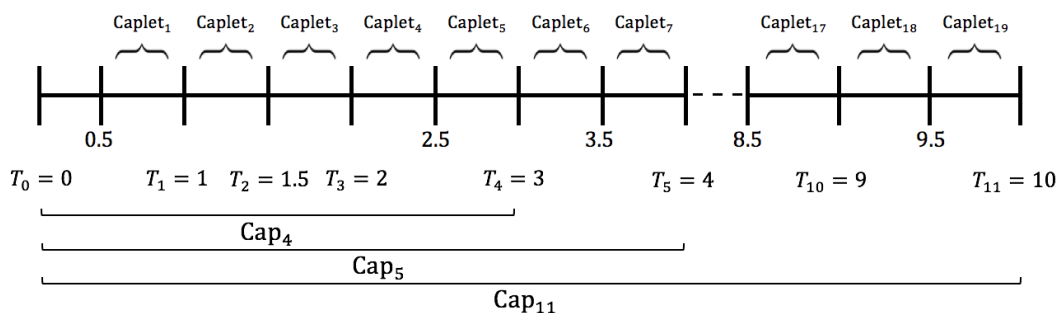


Figure 5.2: *Cap grid for cap maturities between 3 and 10 years in the EUR market. The caps are composed of 6-month underlying caplets.*

⁴¹The convention of omitting the very first period of the cap, i.e., its first caplet, is applied to all quoted *spot-starting* caps. In a cap as that the first caplet payment is done on the cap-start date. Therefore, since the first payment is already known, the optionality is left in the first 3-month period. Then, the first caplet is excluded when calibrating models in order to achieve a *synthetic forward-starting* cap, in which the randomness of all caplet payments is recovered. See (Lesniewski, 2008) [32] for further details.

⁴²In the EUR market the convention of how caps are defined are quite different from the US market, for instance, where caps are defined with 3-month underlying caplets for all maturities of the cap, i.e., the USD quoted caps have a tenor of 3 months for all maturities.

5.2 Data description

The implied cap volatilities, also known as *volatility surface*, since they depend on both the cap maturity and strike, and the discount curves used through the research are accessed through *Thomson Reuters Eikon*. It is important to know that the quoted implied cap volatilities are stated in the platform from different sources and on different markets, therefore they are changing depending on the source used, and also available strikes may be different. In this research, the volatilities are obtained from the source *ICAP*, which offers a wide range of strikes that are close to ATM-strikes.

The implied cap volatilities are the following.

- Implied SHIFTED BLACK EUR cap volatilities (Reuters identifier (RIC): VCAP3A) corresponding to the trading day 23-May-2017.
 - Range of strikes (%): {ATM, -0.75, -0.5, -0.25, -0.13, 0, 0.25, 0.5, 1, 1.5, 2, 3, 5, 10}.
 - Range of maturities (years): {1, 1.5, 2, 3, 4, 5, 6, 7, 8, 9, 10, 12, 15, 20}, the maturities {1Y, 18M, 2Y} have tenor 3 months and the rest 6 months.
 - Shift: 3.00%.
 - Use: To obtain the EUR caplet shifted Black volatility term structure, and consequently to calibrate the Shifted Black, Shifted SABR, Vasicek and Hull-White models.
- Implied BACHELIER (NORMAL) EUR cap volatilities (Reuters identifier (RIC): VCAP10) corresponding to the trading day 23-May-2017. Unfortunately, for these volatilities, several quoting inefficiencies were detected. The two more disturbing are:
 - *Gaps for several particular data.* The Bachelier volatility values corresponding to the shortest maturities and the highest strikes, which coincide with the lowest caplet prices (roughly zero), are not quoted in the market.
 - *Arbitrage exists.* It has been tested that introducing shifted Black and Bachelier quoted volatilities in their pricing formulae, (2.10a) and (2.5a), does not result in the recovery of identical prices for the considered caps. Then, an arbitrage is allowed if both datasets are used together.

Therefore, in order to avoid these quoting inefficiencies and to be able to accomplish the empirical analysis, data corresponding to the Bachelier volatilities are obtained from shifted Black quoted volatilities by an *unique-price hypothesis*. That means,

1. Firstly, for every strike and maturity outstanding, it is imposed that the recovered cap prices by Black's formula (2.10a) using implied market shifted Black volatilities, equals the ones which would have been obtained by Bachelier's formula (2.5a) using implied market Bachelier volatilities.

2. Secondly, the *transformed* implied Bachelier volatilities are extracted from the cap prices via formula (2.5a) by applying an one-dimensional root finder.⁴³

Applying this hypothesis, the arbitrage is forbidden, and no gaps quote in the *transformed* data. Resulting implied Bachelier volatilities share, obviously, their main features with the implied market shifted Black volatilities,

- Range of strikes (%): {ATM, -0.75, -0.5, -0.25, -0.13, 0, 0.25, 0.5, 1, 1.5, 2, 3, 5, 10}.
- Range of maturities (years): {1, 1.5, 2, 3, 4, 5, 6, 7, 8, 9, 10, 12, 15, 20}, the maturities {1Y, 18M, 2Y} have tenor 3 months and the rest 6 months.
- Use: To obtain the EUR caplet Bachelier volatility term structure, and consequently to calibrate the Bachelier, Normal SABR and Free-Boundary SABR models.

The zero-coupon curve used for both computing the discount factors and implying the forward rates⁴⁴ is the EUR OIS curve (EONIA)⁴⁵ (Source: OIS EONIA) corresponding to the trading day 23-May-2017 with a set of tenors from 1 day to 50 years. The curve is continuously-compounded and the day-count convention on which the EUR OIS is quoted, is the *Actual/Actual* basis.⁴⁶

In Appendix E are presented the data corresponding to the implied market shifted Black cap volatilities (Table (E.1)), and to the OIS discount curve (Figure (E.1)).

⁴³Here is used the standard *Newton-Raphson* algorithm. For more details about one-dimensional root finding methods see (Kopecky, 2007) [30].

⁴⁴The 1-week rate of the EUR OIS curve is also used as a proxy for the instantaneous short rate that appears as input in the Vasicek and Hull-White models. This issue is explained in detail later.

⁴⁵Euro Overnight Index Average

⁴⁶This convention accounts for the number of days in the period of one year based on the portion in a leap year and the portion in a non-leap year.

Chapter 6

Methodology

This Chapter is devoted to the methodology followed so as to analyse empirically the topics already discussed in the theoretical part.⁴⁷

Firstly, an empirical comparison of the models able to cope with negative interest rates will be performed. This part of the practical analysis is the most extended one, since a large number of models is tested: Shifted Black, Bachelier, Shifted SABR, Normal SABR, Free-Boundary SABR, Vasicek, and Hull-White models. The relative performance of each model when pricing caplets is analysed in terms of precision of both calibration procedure (*in-sample analysis*), and predictive capacity when pricing caplets not used within the calibration (*out-of-sample analysis*). As it will be seen, under both approaches, the shifted SABR model arises as the most accurate one among the range of models under consideration, what corroborates its general acceptance in the industry through an empirical evidence.

Secondly, since the shifted SABR model emerges as the best model among the considered ones, its ability to reproduce reliable risk metrics will be test empirically. The hedge analysis under the shifted SABR will be performed for caplets by computing numerically both the most relevant Greeks and the sensitivities with respect to the parameters of the model, including the shift parameter.

6.1 Stripping caplet volatilities

The SABR calibration methods given by formulae (3.5) and (3.7) require caplet implied volatilities, since by its approach the (shifted) SABR model provides the value of caplets. However, markets are not quoting caplets but caps. Indeed, as it was explained in Chapter 5, markets quote cap prices, ordered by strike and maturity, through their implied *flat* volatilities.⁴⁸ Therefore, a *conversion* is needed from the quoted cap flat volatilities to

⁴⁷The empirical analysis is fully performed using the software *MATLAB*, version R2017a.

⁴⁸The *implied flat volatility* quoted in the interest-rate markets for given strike K and maturity T is the volatility that should be introduced in the Black/Bachelier formula (2.8a)/(2.3a) for every cap-constituent caplet in order to obtain every caplet price and, therefore, to recover the price of the cap under consideration. In this sense, notice that the implied flat volatility is an averaged implied volatility extrapolated to every caplet constituting a given cap.

caplet volatilities.

The process that allows extract caplet volatilities from market quoted cap volatilities is known as *caplet stripping* and it is thoroughly explained in (Såmark and Jönsson, 2016) [38], (Deloitte, 2016) [11] and (Hagan and Konikov, 2004) [19], for example. There are several types of such stripping process and through this research it will be used the so-called *bootstrapping* technique.⁴⁹ The bootstrapping technique is based on assuming a specific functional dependence of the caplet implied volatilities, for both strike and tenor given, with the time to maturity of the cap under consideration. In this sense, different functional form can be used for modelling this dependence. In the sake of simplicity, here is selected a *piecewise constant functional form* for the caplet implied volatility between every cap maturity under consideration, for any strike and tenor given.

The caplet stripping process under the piecewise constant bootstrapping technique can be structured as follows.

1. Using the formula (2.8a) or (2.3a), depending on which quoted implied flat volatilities are used (shifted Black's or Bachelier's), every constituent caplet of each cap under consideration is priced with the same cap flat implied volatility. Therefore, the price of each cap is obtained by aggregating single caplet prices through the formula (2.10a) or (2.5a).
2. For a given strike K , the n cap prices obtained $V_{cap}(T_1, K), V_{cap}(T_2, K), \dots, V_{cap}(T_n, K)$, are settled in ascending order of maturity, starting from the shortest one.

3. For the strike K , the series of price differences for consecutive caps is computed as follows

$$V_{cap}(T_j, K) - V_{cap}(T_{j-1}, K), j = 1, \dots, n, \quad (6.1)$$

where $V_{cap}(T_0, K) := 0$.

4. Every price difference of the series is assigned to the corresponding number of caplets on that set. For instance, the first price difference corresponds to the first set of caplets (in this case the caplets in the first cap), the second price difference corresponds to the second set of caplets, and so on.
5. Every price difference is therefore allocated with a given number of caplets on specific start and maturity dates that lie in the considered set. Since a piecewise constant assumption on the caplet implied volatilities is stated, the implied caplet volatilities $\sigma_j(K)$, $j = 1, \dots, n$, are constant on each interval between two subsequent cap maturities, i.e., for a given interval $[T_{j-1}, T_j]$ all caplets have the same volatility, and therefore they can be obtained by applying an one-dimensional root finding method⁵⁰ to the equation

$$V_{cap}(T_j, K) - V_{cap}(T_{j-1}, K) = \sum_{i=j_1}^{n_j} V_{caplet}(T_i, K, \sigma_j(K)), j = 1, \dots, n, \quad (6.2)$$

⁴⁹In (Såmark and Jönsson, 2016) [38] three different types of such stripping caplet process are widely discussed: *Bootstrapping*, *Rebonato* and *Global SABR*. In this research the bootstrapping technique is selected because of its simplicity, fastness and efficiency, as the authors claim.

⁵⁰Here is used the standard *Newton-Raphson* algorithm. For more details about one-dimensional root finding methods see (Kopecky, 2007) [30].

where n_j is the number of caplets in that specific set.

It is important to notice that the stripping process with cap implied volatilities requires to be implemented separately for the maturities up to 2 years and the rest of maturities (from 3 to 20 years), since the tenor of the underlying forward rate changes from 3 months to 6 months, as explained in the previous Chapter 5, and consequently, the piecewise constant bootstrapping technique provides two implied volatility term structures.

For at-the-money caps the strikes are specific for each maturity, as it can be seen in Table (E.1). Therefore, the stripping process explained above is not valid anymore, since the difference $V_{cap}(T_j, K_j^{ATM}) - V_{cap}(T_{j-1}, K_{j-1}^{ATM})$, $j = 1, \dots, n$ do not provide the ATM caplets on the desired set. Then, in order to extract caplet volatilities from quoted ATM cap implied volatilities there would be used a strike-interpolating model, such as the (shifted) SABR model, since it allows to obtain prices for caps with strikes that are not quoted in markets. The process can be summarized as follows.⁵¹

1. Using the formula (2.8a) or (2.3a), depending on which quoted implied flat volatilities are used (shifted Black's or Bachelier's), every constituent caplet of each ATM cap under consideration is priced with the same ATM cap flat implied volatility. Therefore, the price of each ATM cap is obtained through the formula (2.10a) or (2.5a).
2. For each maturity T_j , $j = 1, \dots, n$, there is a different ATM cap. Therefore, the different fixed-strike ATM caps are stripped as described above.
3. The (shifted) SABR model is calibrated for each cap maturity.
4. A price difference series between the current cap market prices and the previous cap theoretical prices for the current ATM strike is built by using the interpolated implied volatility from the previous maturity at the current ATM strike

$$V_{cap}(T_j, K_j^{ATM}) - V_{cap}^{theoretical}(T_{j-1}, K_j^{ATM}), j = 1, \dots, n, \quad (6.3)$$

where $V_{cap}^{theoretical}(T_0, K) := 0$.

5. Steps 4 and 5 of the fixed-strikes stripping algorithm are replicated.

6.2 Calibration of the models

The calibration procedure used for the models under consideration is different in *each* case, since the nature of *each* model is different. Indeed, there are three different classes of models, whose calibration is completely different: Shifted Black and Bachelier models; Shifted SABR, Normal SABR and Free-Boundary SABR models; and, Vasicek and Hull-White models. The calibration procedures used during this empirical part of the research are as follows.⁵²

⁵¹The authors of (Deloitte,2016) [11] present an illustrative example that can be helpful in understanding the ATM-strikes stripping algorithm, which was firstly stated in (Zhang and Wu,2016) [43].

⁵²In each model calibration is used the *MATLAB* standard routine *fmincon* which optimizes with constrains.

- **Shifted Black and Bachelier models.**

In both shifted Black and Bachelier models, the unique parameter σ , which accounts for the volatility of the models (σ_B in shifted Black and σ_N in Bachelier), is calibrated using the expression (3.5) for any given maturity. In both models the imposed constraint when using *fmincon* is $\sigma \geq 0$.

- **Shifted SABR, Normal SABR and Free-Boundary SABR models.**

In Section 3.1 there were presented two methods for calibrating the (shifted) SABR model. However, when putting in practice both of them, the formula (3.5) provides more robust results than the formula (3.7) and needs less time to converge. Accordingly, the calibration of the shifted SABR, normal SABR and free-boundary SABR models is accomplished using the expression (3.5) for any given maturity. The imposed constraints when using *fmincon* are $\alpha \geq 0$, $-1 \leq \rho \leq 1$, and $\nu \geq 0$. Furthermore, each model uses the following specifications.

- **Shifted SABR.** The parameter β is fixed at 0.5 for every maturity to simplify the calibration process, as suggested by (Rebonato et al., 2009) [35], among others; and, since the model is calibrated with implied flat shifted Black volatilities, formulae (3.2) is used for computing the theoretical shifted SABR implied volatilities.
- **Normal SABR.** In this case $\beta = 0$ by definition, and the model is calibrated with implied flat Bachelier volatilities. For computing the theoretical normal SABR implied volatilities formula (3.9) is used.
- **Free-Boundary SABR.** In terms of fair comparison with the shifted SABR model, here the parameter β is fixed to a close value to 0.5 that allows stable solutions. The model is calibrated with implied flat Bachelier volatilities, and the formula (3.12) is used for computing the theoretical FB-SABR implied volatilities.

- **Vasicek and Hull-White models.**

Unlike the previous ones, the calibration process of these models can be accomplished with either cap or caplet prices, since the caplets are a particular case of caps with a single payment date. However, both procedures are different.

- Calibration using caps.
 1. Recover the cap market prices from the quoted implied shifted Black (or Bachelier)⁵³ volatilities for any maturity and strike given by using a shifted Black (or Bachelier) pricing formula, see (2.8a) (or (2.3a)).

⁵³Given the *unique-price hypothesis* explained in Chapter 5, the prices computed with the flat implied shifted Black volatilities should be equivalent to the ones computed with the flat implied Bachelier volatilities. Therefore, calibrating the Vasicek and Hull-White models with either one of both type of volatilities is equivalent.

2. Minimize the sum of squared differences for every strike and given maturity between the cap market price and the theoretical cap price given by (2.13a) in Vasicek or (2.16a) in Hull-White:

$$(\hat{\sigma}, \hat{k}, \hat{\theta}) = \arg \min_{\sigma, k, \theta} \sum_i (V_{cap}^{mkt}(T, K_i) - V_{cap}^{Vasicek}(T, K_i))^2, \quad (6.4a)$$

$$(\hat{\sigma}, \hat{k}) = \arg \min_{\sigma, k} \sum_i (V_{cap}^{mkt}(T, K_i) - V_{cap}^{HullWhite}(T, K_i))^2. \quad (6.4b)$$

– Calibration using caplets.

1. Strip caplet volatilities from flat cap quoted volatilities as explained in Section 6.1.
2. Steps 1 and 2 of the calibration using caps are replicated.

Despite of involving a data transformation, the calibration using caplets is chosen for being the Vasicek and Hull-White models calibrated under *equal conditions* with the rest of models. Indeed, the previously-calibrated models need to be calibrated by minimizing caplets' (and not caps') pricing error, therefore the *error* introduced in the stripping process, due to its dependence on the interpolation method used (piecewise constant), might prejudice the calibration results. Consequently, in order to remove the dependence of the instrument used (caps or caplets) for the calibration procedure, and to achieve a fair comparison between all models under consideration, the stripping process should be used in every model's calibration. Indeed, if Vasicek's and Hull-White's calibrations are performed without prior caplet stripping, there exists an advantage for those models, which is not due to the nature of the models itself, but to the way the data is quoted in the markets.

Additionally, as it can be noticed in formulae (2.14a) and (2.17a), Vasicek's and Hull-White's calibrations need a proxy for the instantaneous short rate r_t . The 1-week rate of the OIS curve is chosen as the optimal proxy in terms of avoiding excess of market noise, and representing the instantaneous short rate. This choice can be discussed, since it has been thoroughly done among previous literature and no agreement seems to have been reached.⁵⁴

6.3 Comparison of the models' pricing accuracy

As mentioned before, in order to test all models under consideration, their caplets pricing accuracy is compared by using both *in-sample* and *out-of-sample* analysis.

- **In-sample analysis.** After all models have been calibrated, the corresponding pricing formula is applied to each term structure of stripped caplet volatilities in order to recover each matrix of caplet prices.⁵⁵ Therefore, in order to analyse the models' performance in pricing in-sample, these matrices are compared with the one of the caplet market prices obtained by the quoted implied volatilities.

⁵⁴See, for instance, (Elton et al., 1990) [17].

⁵⁵An standard notional of $N = 100$ is used in every pricing algorithm.

- **Out-of-sample analysis.**

- Excluding an arbitrary **strike**. As each column of the matrix containing stripped caplet volatilities corresponds to a different strike⁵⁶, an arbitrary column⁵⁷ is removed from the array, and each model is recalibrated without these data. After that, the caplet price for each maturity and the omitted strike is forecasted by using the corresponding pricing formula.
- Excluding an arbitrary **maturity**. As each row of the matrix containing stripped caplet volatilities corresponds to a different maturity, an arbitrary row⁵⁸ is removed from the array, and each model is recalibrated without these data. After that, the caplet price for every strike and the omitted maturity is forecasted by using the corresponding pricing formula.

In both types of out-of-sampling, when recovering the caplet prices in the shifted Black, Bachelier, shifted SABR, normal SABR and free-boundary SABR models, the pricing shifted Black/Bachelier formula, (2.8a)/(2.3a), is used. Otherwise, in the short-rate models Vasicek and Hull-White, the caplet prices are directly forecasted through the pricing formulae (2.13a) and (2.16a) respectively.

Additionally, in the strike out-of-sampling under the shifted SABR, normal SABR and free-boundary SABR models, the implied volatility for the omitted strike is interpolated through the volatility smile/skew, which is an horizontal line in the shifted Black and Bachelier models. In the maturity out-of-sampling under these models, the previous interpolation is substituted by a constant interpolation, since by the piecewise constant hypothesis the implied volatility for the omitted maturity is the one of the previous maturity for any strike under consideration.⁵⁹ Therefore, in this case might be made bigger errors than in the strike out-of-sample analysis.

6.4 Computation of the shifted SABR sensitivities

The procedure used for the computation of the shifted SABR sensitivities (Greeks and parameters sensitivities) requires *only* the finite difference methods presented in Appendix D, since the sensitivities are defined by partial first and second order derivatives, which are computed numerically. Next the *modus operandi* for each case is explained.

- **Bartlett's Delta.** Since Bartlett's delta is Hagan's delta plus a correction term (see formula (4.11)), firstly Hagan's delta is computed, and then the correction term is added.

⁵⁶Recall that the matrices of caplet volatilities and caplet prices account for maturities in their rows and strikes in their columns.

⁵⁷This column shall not be neither the first nor the last one of the matrix, to avoid the problem of extrapolating in strike.

⁵⁸This row shall not be neither the first nor the last one of the matrix, to avoid the problem of extrapolating in maturity.

⁵⁹Notice that when applying shifted Black/Bachelier pricing formulae, (2.8a)/(2.3a), the maturity of the caplet should be the actual maturity of the caplet being priced, not the previous one, i.e., the piecewise constant hypothesis applies in implied volatilities, but not in prices.

1. The derivative $\Delta_{Hagan} = \partial V_{caplet}^{Black} / \partial f$ is computed by stressing the value of f by a small perturbation ($\Delta f = 1\text{b.p.}^{60}$), and then using the difference method (D.2) or (D.3).⁶¹
2. Bartlett's delta correction term is given by $\Lambda_{Hagan} + \frac{\rho\nu}{(f+s)^\beta}$, then once Λ_{Hagan} is computed (see the next step), the other term is added, and the Bartlett's delta is obtained.

- **Bartlett's Vega** (with respect to α and with respect to $\sigma_B(\cdot)$).

- Λ_α . Since Bartlett's vega is Hagan's vega plus a correction term (see formula (4.12)), firstly Hagan's vega is computed, and then the correction term is added.

1. The derivative $\Lambda_{Hagan} = \partial V_{caplet}^{Black} / \partial \alpha$ is computed by stressing the value of α by a small perturbation ($\Delta \alpha = 1\text{b.p.}$), and using the difference method (D.2) or (D.3).

2. Bartlett's vega correction term is given by $\Delta_{Hagan} + \frac{\rho(f+s)^\beta}{\nu}$, then once Δ_{Hagan} is computed (see the previous step), the other term is added, and the Bartlett's vega is obtained.

- Λ_{σ_B} . In this case the volatility surface (implied caplet volatilities for each strike and each maturity computed by shifted SABR model) is stressed by a small perturbation ($\Delta \sigma_B = 1\text{b.p.}$), and then the derivative $\Lambda_{\sigma_B} = \partial V_{caplet}^{Black} / \partial \sigma_B$ is computed using the difference method (D.2) or (D.3).

- **Dual-delta.** The strike K is perturbed by 1b.p. and the derivative $\text{Dual-}\Delta = \partial V_{caplet}^{Black} / \partial K$ is computed by (D.2).

- **Gamma.** The forward value f is stressed by 1b.p. and the derivative $\Gamma = \partial^2 V_{caplet}^{Black} / \partial f^2$ is approximated by the formula (D.4).

- **Vanna.** The values of f and α are both stressed by 1b.p. and the cross derivative $\text{Vanna} = \partial^2 V_{caplet}^{Black} / \partial f \partial \alpha$ is approximated by the formula (D.5).

- **Volga.** The value of α is stressed by 1b.p. and the derivative $\text{Volga} = \partial^2 V_{caplet}^{Black} / \partial \alpha^2$ is computed by using (D.4).

- **β, ρ, ν , and s sensitivities.** Each parameter is stressed by a small quantity (1b.p.) and the corresponding first order derivatives (see formulae (4.17) and (4.18)) are approximated by the difference method (D.3).

⁶⁰1 b.p. (basis point) = 0.01% = 0.0001.

⁶¹The finite difference methods (D.1), (D.2) and (D.3) for approximating the first order derivative provide similar or different results depending on the values of the function to be numerically computed. Although, the *Forward Difference Method* is the most immediate one, since it results directly from the definition of the first order derivative, usually, *Central Difference Method* and *Secant Method* provide more accurate results. Furthermore, *Secant Method* is usually the most precise one, however for null values it does not apply, so in this case the *Central Difference Method* is applied.

Chapter 7

Empirical results

7.1 Comparison of the models

7.1.1 Volatility term structures

Figure (7.1) presents both piecewise constant caplet volatility term structures recovered by the stripped European marked-quoted cap shifted Black and Bachelier volatilities.

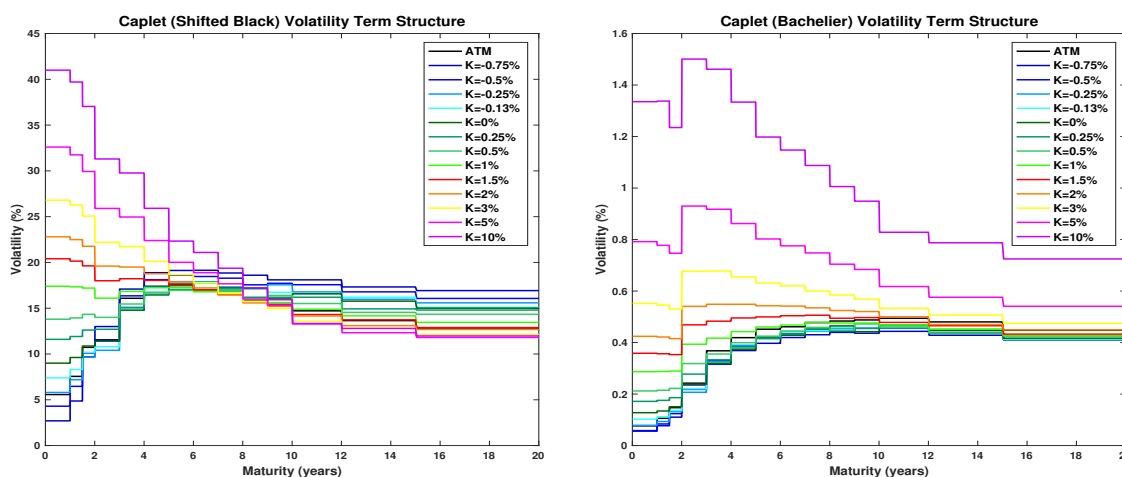


Figure 7.1: *Caplet volatility term structure recovered by stripped market-quoted cap shifted Black (left) and Bachelier (right) volatilities.*

As it can be seen, both volatility term structures converge to a given long-term value with the time to maturity of the caplets, being this convergence especially pronounced in the shifted Black volatilities. However, this convergence is different in both cases. The shifted Black dynamic evolution is characterized by the switch of the low strike and the high strike-volatilities when time to maturity increases (for short maturities the high-strike volatilities are bigger than the low-strike ones, and for large maturities this behaviour is switched). On the other hand, the Bachelier dynamic evolution is monotonous with time to maturity, i.e., the different strike volatilities never cross each other.

Regarding the caplet volatilities behaviour as time to maturity grows, in both cases

for short-maturity volatilities they increase with the strike.⁶² For large maturities this behaviour is maintained in the Bachelier volatilities, but it is fully reverted in the shifted Black volatilities.

Additionally, in both shifted Black and Bachelier volatility term structures, two different patterns are observed for the different strikes under consideration. In the low-strike range (negative, ATM and lowest positive strikes) volatilities increase with time to maturity, but in the high-strike range (highest positive strikes) this tendency is switched resulting in decreasing volatilities when increases time to maturity. These patterns can be clearly observed in Figure (7.2) where the volatility term structures are separated in strike.

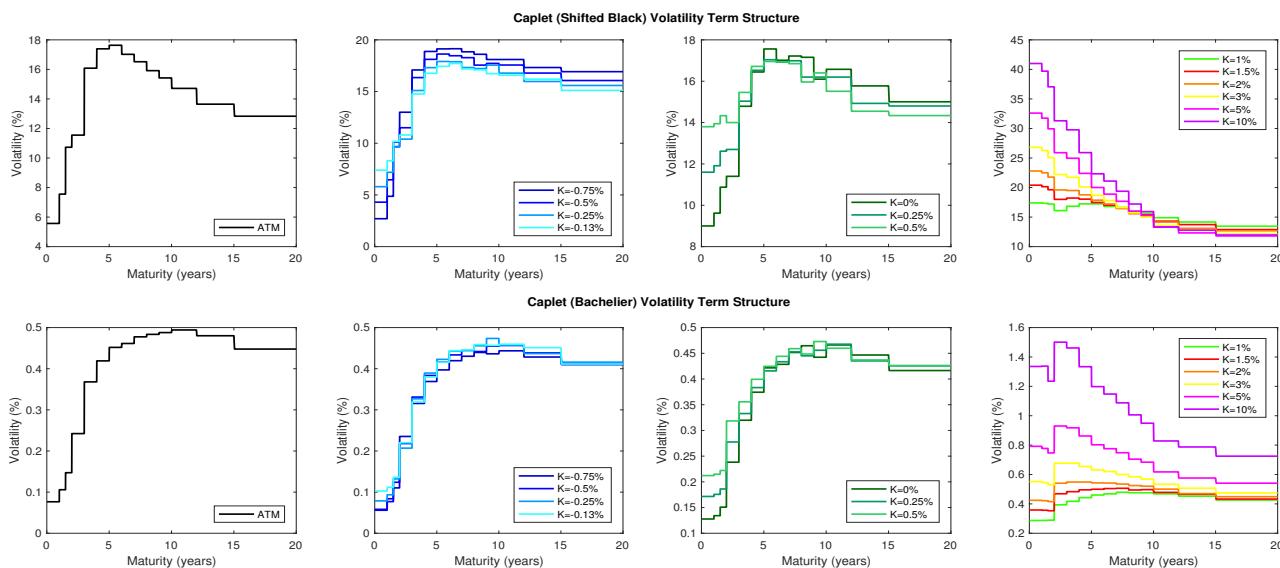


Figure 7.2: Strike dependence of the shifted Black (up) and Bachelier (down) volatility term structures.

7.1.2 Calibration of the models

Figure (7.3) presents the calibrated parameters of each model under consideration obtained by fitting each of them to the corresponding volatility term structure presented in Figure (7.1), for every maturity outstanding.

The resulting parameters in the shifted SABR, normal SABR, free-boundary SABR, shifted Black and Bachelier models seem to evolve quite smoothly, and this accounts for the *stability*⁶³ of these models. On the other hand, the Vasicek and Hull-White parameters

⁶²As regards caplet pricing, a trade-off between several magnitudes appears at this point. While increasing the strike results in a pricing descent (in order to guarantee that the price term structure is *arbitrage-free*), higher implied volatilities increase the price of the caplet. Therefore, the volatility term structures suggest a trade-off between higher strikes (lower prices) and higher volatilities (higher prices).

⁶³The concept of *stable model* accounts for a model whose parameters term structure evolves *smoothly*, i.e., in a continuous way, suggesting that the model is correctly specified avoiding the *overparameterization*. On the other hand, an *unstable model* accounts for a model whose parameters (at least one of

evolving accounts for the *instability* of both models. The reason of this fact is that during the Vasicek and Hull-White models calibration, several numerical difficulties have been found.⁶⁴

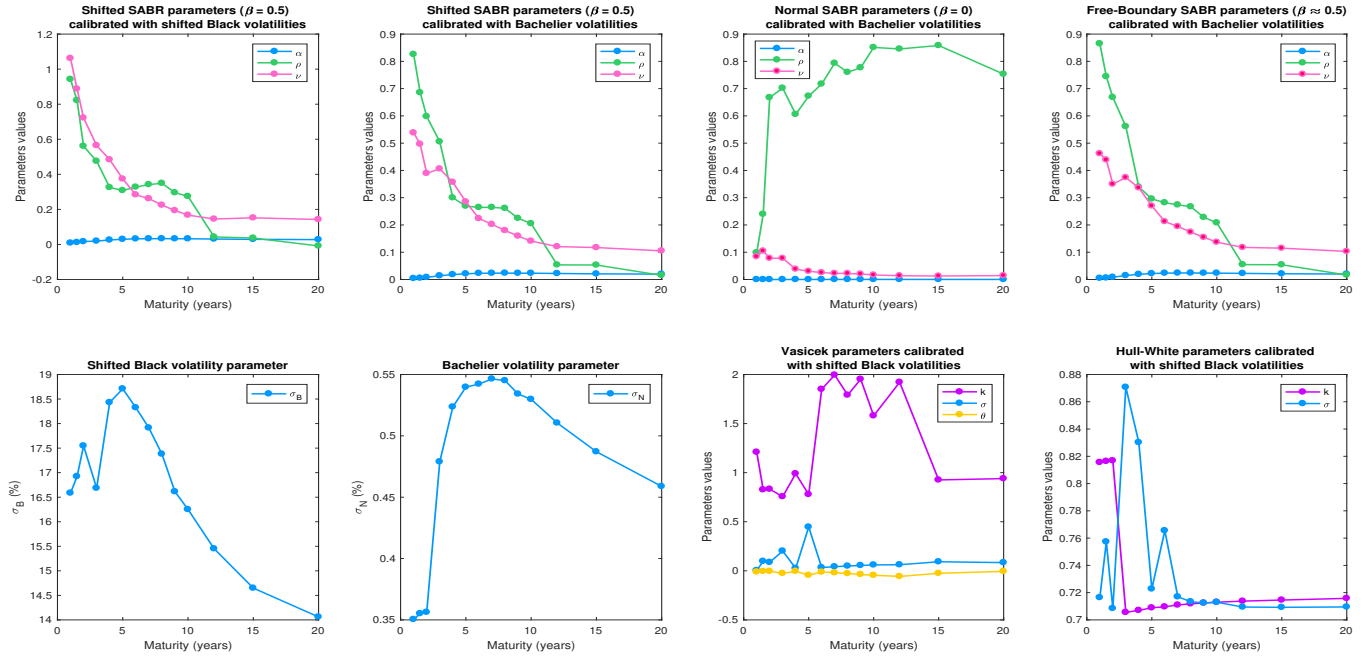


Figure 7.3: *Calibrated parameters of Shifted SABR, Normal SABR, Free-Boundary SABR, Shifted Black, Bachelier, Vasicek and Hull-White models.*

Regarding the estimated parameters of the SABR model extensions, their behaviour is very similar, except in the normal SABR model. For every SABR extension, the value of *today's* forward rate volatility, α , is almost zero, irrespective of the maturity being considered, and the value of the volatility-of-volatility, ν , tends to decrease smoothly with time to maturity. On the other hand, the dynamic evolution of the correlation between the Brownian Motions of F_t and σ_t , ρ , depends on the model being considered. For the shifted SABR model, with independence of the market-quoted volatility used in the calibration (shifted Black or Bachelier), and for the FB-SABR model, ρ decreases quite monotonically from close-to-one values in the short maturity range (from 1 to 4-5 years approximately) to almost null values in the long-maturity range (from 12 to 20 years). In the normal SABR model, however, its behaviour is fully opposite.

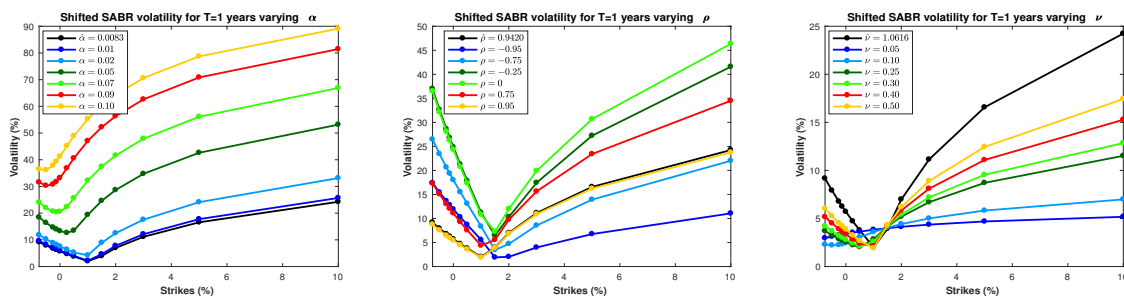
In both Vasicek and Hull-White models, the instantaneous volatility of the short rate, σ , fluctuates wildly in the short-maturity range, becoming stable in the middle-long-maturity range. In the Vasicek model, the mean reversion speed of the short rate towards its long term value, k , evolves in discontinuous peaks with time to maturity, while in the Hull-White model, its value is much more stable, except one pronounced *jump* (from the value for $T = 3$ to the one for $T = 4$), and also lower. Regarding the long term value of

them) evolve *widely*, with peaks, i.e., in a discontinuous way, suggesting that the model specification is not correct (*misspecification* of the parameters in the calibration process).

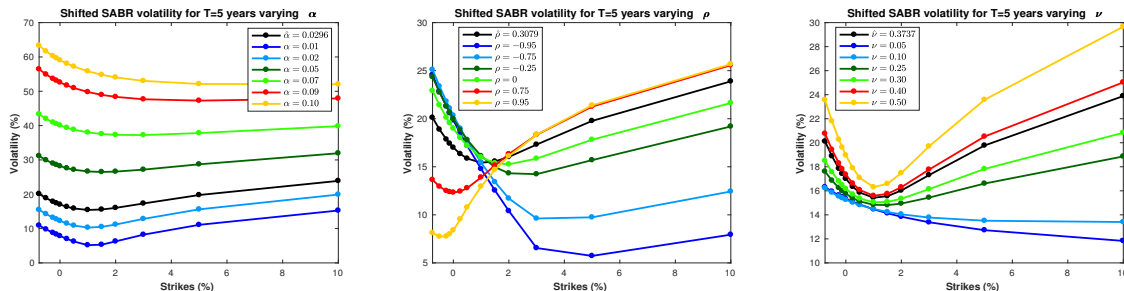
⁶⁴See Appendix E for further discussion about this issue.

the short rate, θ , in the Hull-White model, its value is very close to zero for any maturity under consideration, in consonance with the current situation of low and even negative interest rates.

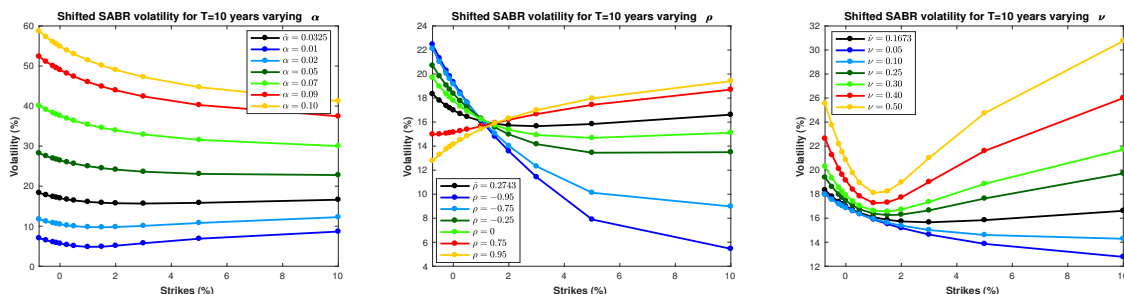
Figure (7.4) presents the fitted volatility smiles/skews for some representative maturities, particularly $T = 1$, $T = 5$ and $T = 10$, when modifying *ceteris paribus* each one of the shifted SABR parameters α, ρ, ν to several values close to the calibrated ones.⁶⁵



(a) Varying α ($\hat{\alpha} = 0.0083$), ρ ($\hat{\rho} = 0.9420$) and ν ($\hat{\nu} = 1.0616$) for $T = 1$ year.



(b) Varying α ($\hat{\alpha} = 0.0296$), ρ ($\hat{\rho} = 0.3079$) and ν ($\hat{\nu} = 0.3737$) for $T = 5$ years.



(c) Varying α ($\hat{\alpha} = 0.0325$), ρ ($\hat{\rho} = 0.2743$) and ν ($\hat{\nu} = 0.1673$) for $T = 10$ years.

Figure 7.4: Behaviour of the shifted SABR parameters α, ρ and ν (the parameter β is fixed at 0.5) for the maturities (a) $T = 1$, (b) $T = 5$ and (c) $T = 10$ years.

As it can be observed, for each maturity outstanding the main effect of an increase in the initial volatility α is to shift parallel the curve upwards. This behaviour has sense, since α is just the expectation at time 0 of the future volatility for any time $t \leq T$ and, therefore, a small perturbation of α upwards will result in higher average volatility. Looking at small effects, it can be also observed that an increase in the initial volatility

⁶⁵This figure illustrates the behaviour of the shifted SABR parameters, whose interpretation and impact on the volatility curve (smile/skew) was explained in Section 3.1. Recall that α accounts mainly for the curve level, ρ for the curve slope, and ν for the curvature of the curve.

brings about a modest steepening of the curve (low strikes increase more than high strikes). Additionally, when time to maturity grows, the curve becomes more stable in strike, since the volatilities of the high-strike range decrease considerably.

Regarding dependence on ρ , Figure (7.4) shows principally a pronounced change in the steepens of the curve, in fact, as ρ increases the steepness of the curve decreases. Furthermore, for negative and close-to-zero values of the parameter, the curve is negatively sloped, while for high correlation values the slope becomes positive. As well as, when time to maturity grows the curve becomes more stable, since the values of the implied volatilities are smaller and their evolving through the strikes under consideration is smoother.

Finally, it can be seen that increasing the parameter ν increases the curvature of the smile/skew. On the other hand, in general, the values of the volatilities-of-volatilities are higher when time to maturity grows.

Furthermore, notice that, the changes, with respect the parameters ρ and ν mainly, are not entirely symmetric across the volatility curve, since ρ has a secondary effect on curvature just as ν has secondary effect on steepness.⁶⁶ The interaction of these parameters (and also β , but not now, since its value is fixed to 0.5) on slope and curvature allows this model to capture subtle differences in the shape of the implied volatility curve. Indeed, Figure (7.5) shows clearly the capacity of the shifted SABR model to adjust many different smile/skew shapes to the ones observed in the markets, as well as the incapacity of the shifted Black model to adjust these curves due to its assumption on constant volatility.

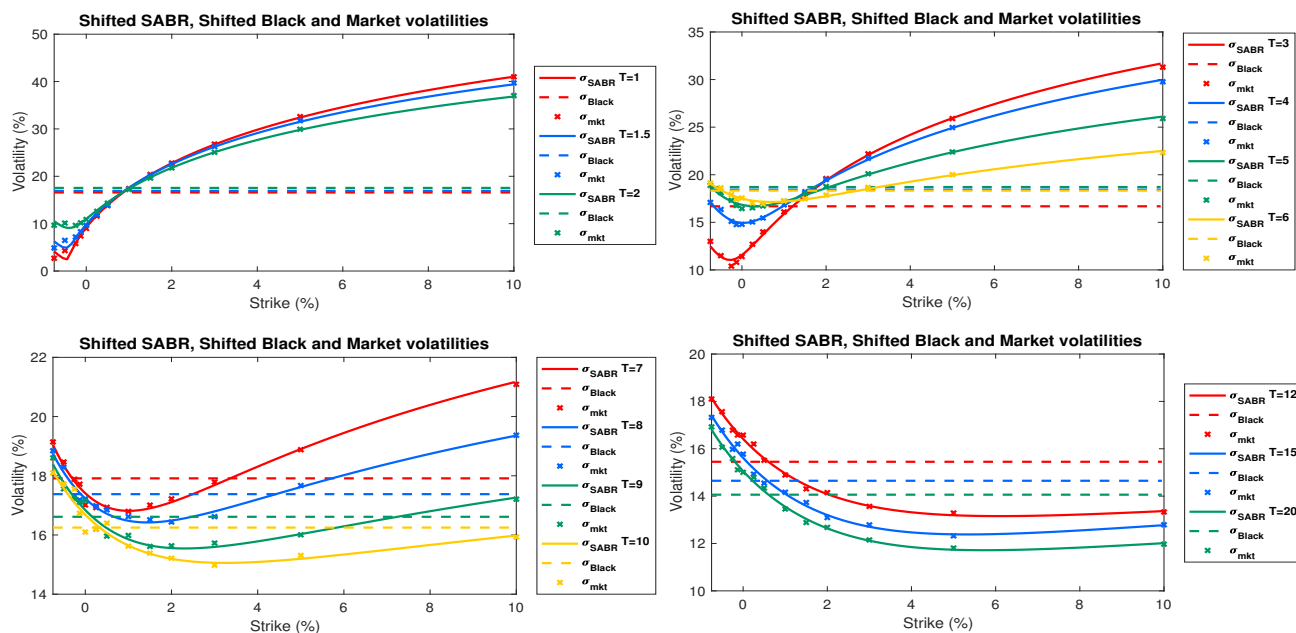


Figure 7.5: *Shifted SABR, shifted Black and market volatilities through all strikes and for every maturity under consideration. Evidence for smile/skew existence in the markets.*

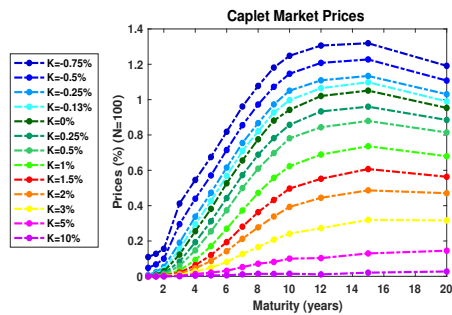
⁶⁶See Table 3.1.

As it can be seen, the existence of market smiles/skews for any given maturity is empirically evidenced in Figure (7.5) (notice σ_{mkt} behaviour through the strike, for each maturity under consideration), what fully refuses the constant volatility hypothesis assumed by shifted Black (and Bachelier) model (notice σ_{Black} behaviour through the strike, for each maturity under consideration). By itself, shifted SABR model shows its great flexibility for fitting market volatility curves (notice σ_{SABR} behaviour through the strike, for each maturity under consideration).

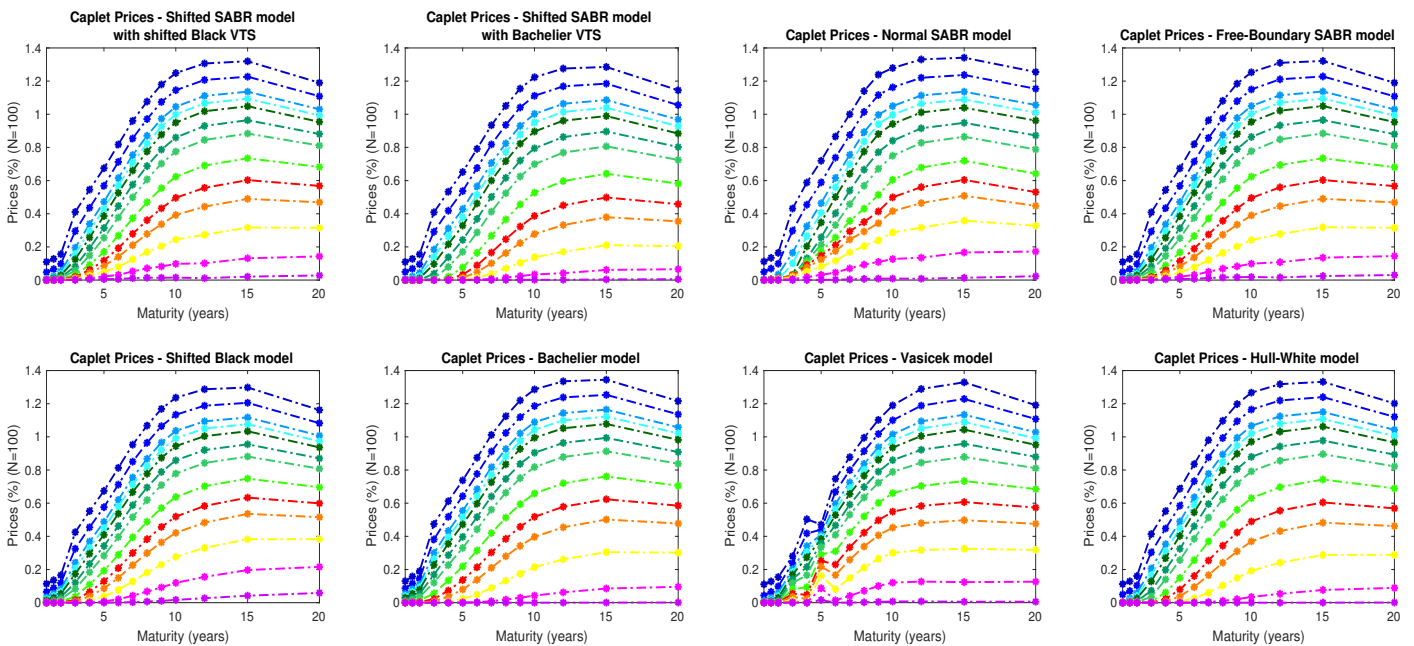
7.1.3 In-sample analysis

Now is tested the *in-sample* accuracy of each previously calibrated model when recovering caplet prices.

Figure (7.6) compares caplet market prices term structure with caplet prices term structures implied by every calibrated model for every strike under consideration.



(a) Caplet market prices term structure.



(b) Caplet prices term structures recovered by the calibrated models.

Figure 7.6: Caplet prices term structures.

This figure illustrates that every model fits the caplet market prices⁶⁷ *fairly well*. At a first sight, only Vasicek model tends to fail systematically, for every strike, for the maturity $T = 5$ regarding typical market behaviour. Market prices term structure as well as each model term structure are *arbitrage-free*, since caplet prices are sorted in descending order in strike for any given maturity, never crossing each other's curve. Furthermore, for any given strike, caplet prices tend to increase for longer maturities, although they stabilize, and even decay, for the last maturity ($T = 20$).

Figure (7.7) aggregates the caplets prices term structures for every model for several representative strikes in order to perform a more explicit comparison with the market prices term structure.

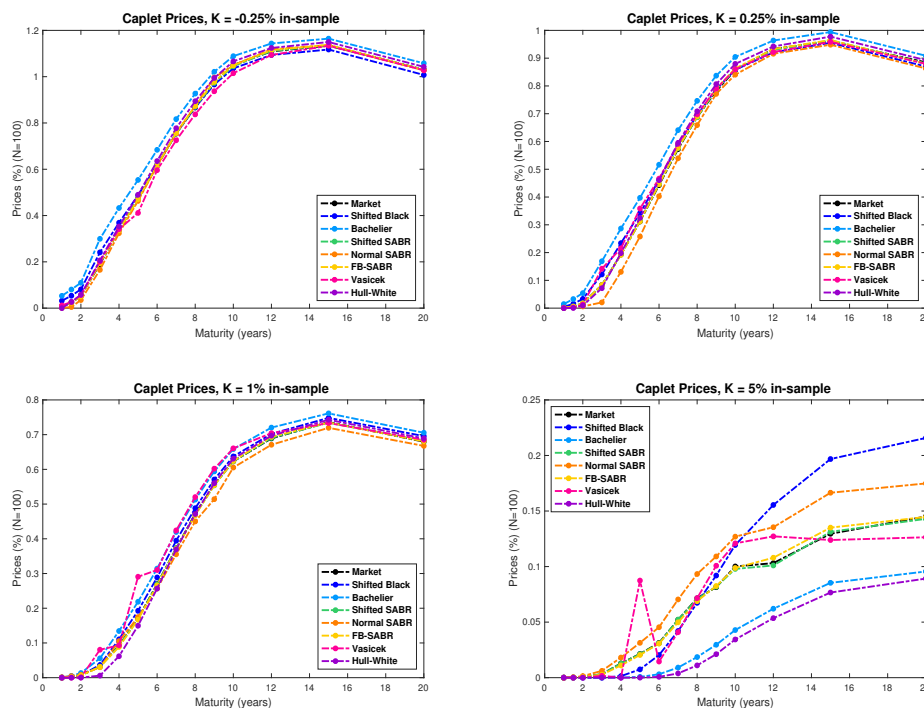


Figure 7.7: *Models' pricing in-sample accuracy within the market benchmark for some representative strikes.*

Indeed, in this figure can be clearly observed that pricing accuracy of the models is essentially challenged for the highest strikes under consideration, which correspond to the lower prices. While negative and low-positive strike prices curves are very similar, prices term structures for $K = 5\%$ differ significantly. In fact, only shifted SABR and FB-SABR prices curves reproduce market prices behaviour.

In Figure (7.8) is tested the pricing accuracy of each model outstanding in terms of absolute and relative errors. First and second columns of the figure present the absolute and relative pricing errors, respectively, of every model. Third column of the figure aggregates the models with, at a first sight, smallest relative pricing errors. Finally, since shifted SABR and FB-SABR are the models that best reproduce market prices behaviour,

⁶⁷Notice that the caplet market prices term structure is the same irrespective of the implied volatilities used (shifted Black or Bachelier), since the *unique price hypothesis* applies when recovering that prices.

the fourth column is devoted to their relative pricing errors. This analysis is performed for the previously considered strikes.

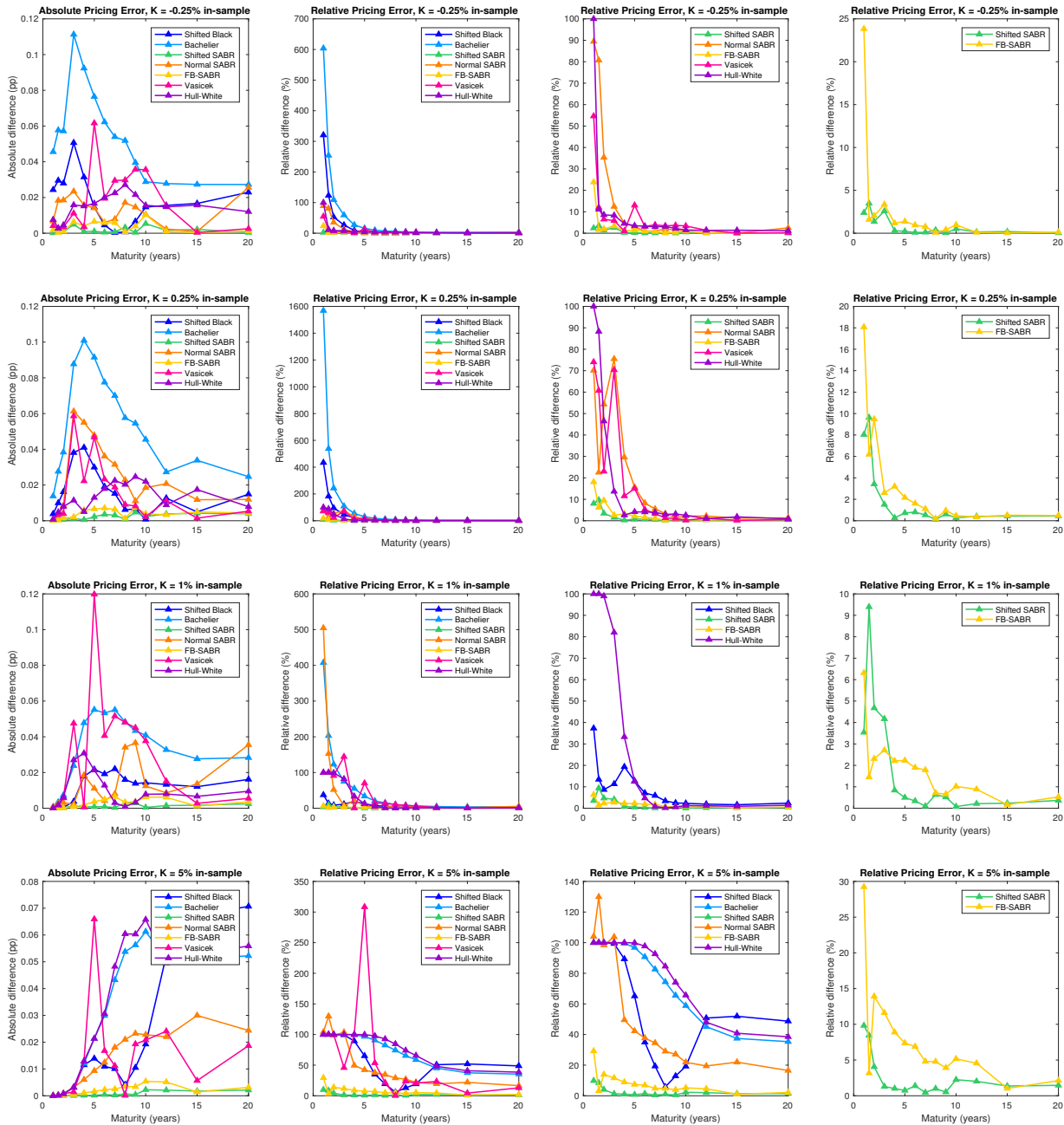


Figure 7.8: *In-sample comparison of the different models in terms of absolute and relative pricing errors for some representative strikes.*

Regarding the first column of Figure (7.8), no model commits a high absolute pricing error irrespective of the maturity under consideration, since it not surpasses the maximum value of 0.12% for a standard notional of $N = 100$ (except Vasicek model's absolute pricing error for $K = 1\%$ and $T = 6$). Term structures of absolute errors tend to decrease when the strike increases in every model. Shifted SABR and FB-SABR arise as the best models in terms of absolute pricing errors irrespective of the maturity or strike being

considered, with slight superiority of the first one, and, contrary, Bachelier and Vasicek are, in general, the worst models in absolute error terms. On the other hand, shifted Black, normal SABR and Hull-White models accomplish reasonably well for the negative and low-positive strikes, but tend to fail for higher strikes.

As it can be seen in the second and third columns of Figure (7.8), relative pricing errors grow hugely, particularly for shortest maturities (from $T = 1$ to $T = 3, 4, 5$ years, depending on the model), since caplet market prices are especially small in this range, and also for the highest strikes. Table (7.1) shows its values, which reach magnitudes $\sim 10^{-7}$ in the problematic area. This results in a great difficulty when fitting such small caplet prices and the relative errors show this fact. Indeed, except for the shifted SABR and FB-SABR models, every model outstanding fails for the shortest maturities in relative pricing errors terms, highlighting as the worst models shifted Black and Bachelier, followed by normal SABR, Vasicek and Hull-White models.

Then, shifted SABR and FB-SABR relative pricing errors should be compared apart from the others. This comparison is accomplished through the fourth column of the Figure (7.8). In the long-maturity range (from $T = 3, 4$ to $T = 20$), shifted SABR relative errors are smaller than the FB-SABR ones for all strikes under consideration, while along the shortest maturities shifted SABR tends to present smaller relative errors, but not always (for instance, for $K = 1\%$ and $T = 1.5$ the shifted SABR relative pricing error is bigger than the FB-SABR one for maturities $T = 1.5, 2, 3$ years).

T/K(%)	-0.75	-0.50	-0.25	-0.13	0.00	0.25	0.5	1.00	1.50	2.00	3.00	5.00	10.00
1Y	0.1092	0.0477	0.0076	0.0037	0.0021	0.0009	0.0005	0.0002	0.0001	4e-5	2e-5	5e-7	5e-7
18M	0.1275	0.0675	0.0240	0.0150	0.0100	0.0054	0.0035	0.0018	0.0011	0.0007	0.0004	0.0002	4e-5
2Y	0.1557	0.0998	0.0532	0.0390	0.0282	0.0171	0.0116	0.0063	0.0040	0.0028	0.0016	0.0007	0.0002
3Y	0.4119	0.2953	0.1904	0.1539	0.1231	0.0833	0.0595	0.0329	0.0209	0.0143	0.0077	0.0031	0.0008
4Y	0.5454	0.4393	0.3375	0.2943	0.2550	0.1930	0.1470	0.0925	0.0630	0.0456	0.0274	0.0129	0.0039
5Y	0.6753	0.5710	0.4730	0.4268	0.3818	0.3118	0.2545	0.1709	0.1202	0.0868	0.0495	0.0214	0.0053
6Y	0.8182	0.7148	0.6153	0.5681	0.5265	0.4429	0.3739	0.2695	0.1935	0.1421	0.0810	0.0313	0.0059
7Y	0.9610	0.8552	0.7547	0.7096	0.6556	0.5726	0.4991	0.3726	0.2810	0.2125	0.1266	0.0521	0.0112
8Y	1.0774	0.9724	0.8670	0.8211	0.7754	0.6885	0.6094	0.4722	0.3630	0.2771	0.1653	0.0715	0.0144
9Y	1.1813	1.0726	0.9728	0.9271	0.8814	0.7818	0.6975	0.5569	0.4319	0.3386	0.2078	0.0814	0.0137
10Y	1.2483	1.1464	1.0506	0.9970	0.9421	0.8574	0.7813	0.6230	0.4967	0.3929	0.2416	0.1001	0.0148
12Y	1.3060	1.2079	1.1093	1.0648	1.0206	0.9333	0.8436	0.6891	0.5520	0.4445	0.2727	0.1031	0.0110
15Y	1.3191	1.2274	1.1340	1.0984	1.0510	0.9601	0.8793	0.7362	0.6071	0.4865	0.3195	0.1295	0.0207
20Y	1.1912	1.1077	1.0304	0.9899	0.9532	0.8850	0.8142	0.6797	0.5634	0.4703	0.3163	0.1451	0.0274

Table 7.1: *Caplet market prices.*

Summarizing, in absolute errors terms, every model is quite accurate when fitting caplet market prices, although this accuracy worsen within the strike. However, in relative errors terms, shifted SABR and FB-SABR models tend to perform better in every considered in-sample test, with slight preference for the shifted SABR. Regarding maturity in-sample analysis, for the shortest maturities both are the unique admissible models, and for the longest maturities they can be considered the most accurate ones. On the other hand, in terms of strike in-sample analysis, shifted SABR and FB-SABR account for the best models as well. Models as normal SABR, Vasicek and Hull-White perform reasonably well in the low-strike range, but they all fail in the high-strike range, while shifted Black and Bachelier models tend to perform unsatisfactory in both strike and

maturity in-sample analysis.

7.1.4 Strike out-of-sample analysis

Now is tested the *strike out-of-sample* accuracy of every model under consideration when recovering caplet prices, i.e., models pricing accuracy when interpolating prices for strikes not included in the calibration (excluded from the sample).

Figure (7.9) presents an aggregate of several caplet prices term structures in comparison with caplet market prices when out-of-sampling some representative strikes.

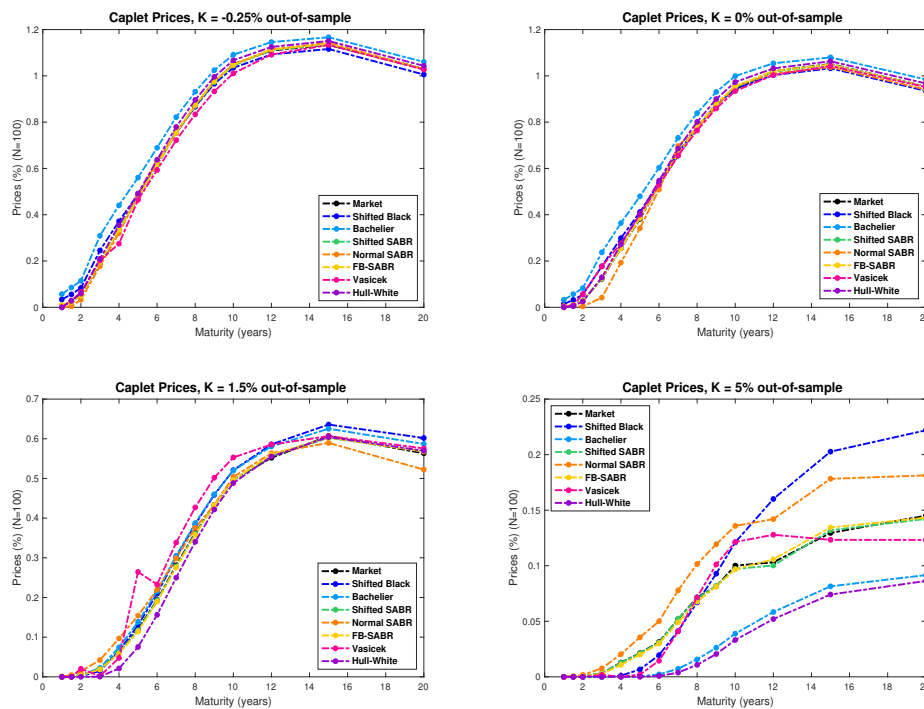


Figure 7.9: *Models' pricing strike out-of-sample accuracy within the market benchmark for some representative strikes.*

Just like in the in-sample analysis⁶⁸, in this figure can be clearly observed that the adjustment accuracy of the models depends, in general, on the strike range. Within the negative and low-positive strikes prices term structures present a similar behaviour, while for high strikes, as is the case of $K = 5\%$, all models, except shifted SABR and FB-SABR, fail in pricing accurately.

In Figure (7.10) is tested the strike out-of-sample pricing accuracy of each model outstanding in terms of absolute and relative errors for the previously considered strikes. First and second columns of the figure present the absolute and relative pricing errors, respectively, of every model. Third column of the figure zooms the relative performance of the models with, at a first sight, smallest relative pricing errors. Finally, since shifted SABR and FB-SABR are the models that best reproduce market prices behaviour, the fourth column is devoted to their relative pricing errors.

⁶⁸Compare Figure (7.7) and Figure (7.9).

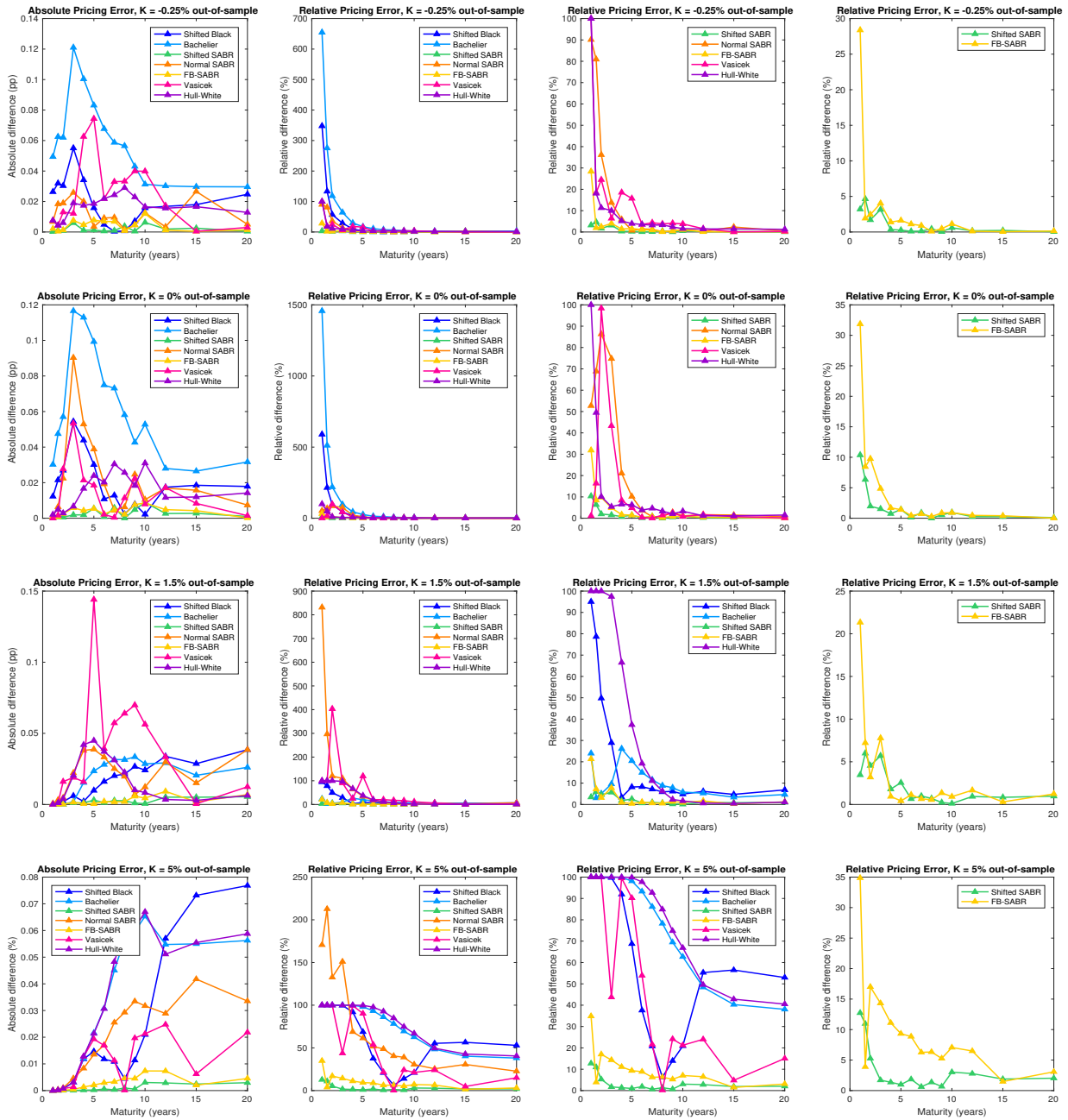


Figure 7.10: *Strike out-of-sample comparison of the different models in terms of absolute and relative pricing errors for some representative strikes.*

As it can be observed in the first column of the Figure (7.10), no huge absolute errors are made, as occurred in the in-sample analysis. Again, for every maturity and strike considered, shifted SABR and FB-SABR account for the most accurate models in terms of absolute pricing errors. The highest (in this scale) absolute error values are observed throughout the low-strike range and for the shortest maturities, highlighting Bachelier's and Vasicek's errors.

Second and third columns of the figure under examination exhibit, once again, that, with exception of shifted SABR and FB-SABR, every model fails in terms of relative pricing errors for the shortest maturities for at least one of the out-of-sampled strikes.

Finally, shifted SABR and FB-SABR relative pricing errors are compared through the fourth column of Figure (7.10). The high-grade performance of the shifted SABR model is clearly observed through these subfigures. Although FB-SABR relative errors are generally small, they increase considerably for both the lowest maturities and the highest strikes, and therefore this model performance is clearly poorer than the shifted SABR one.

Summarizing, when out-of-sampling in strike (interpolating prices for strikes not included in the calibration), the behaviour of the models in terms of pricing accuracy is very similar to the observed through the in-sample analysis. Shifted SABR and FB-SABR account as the best models under the strike out-of-sample analysis, with slight preference for the first one based on its general superiority in absolute and relative terms.

7.1.5 Maturity out-of-sample analysis

At last, the *maturity out-of-sample* accuracy of every model under consideration when recovering caplet prices, i.e., models pricing accuracy when interpolating prices for maturities not included in the calibration (excluded from the sample) is tested.

Figure (7.11) presents an aggregate of several caplet prices term structures in comparison with caplet market prices when out-of-sampling some representative maturities.

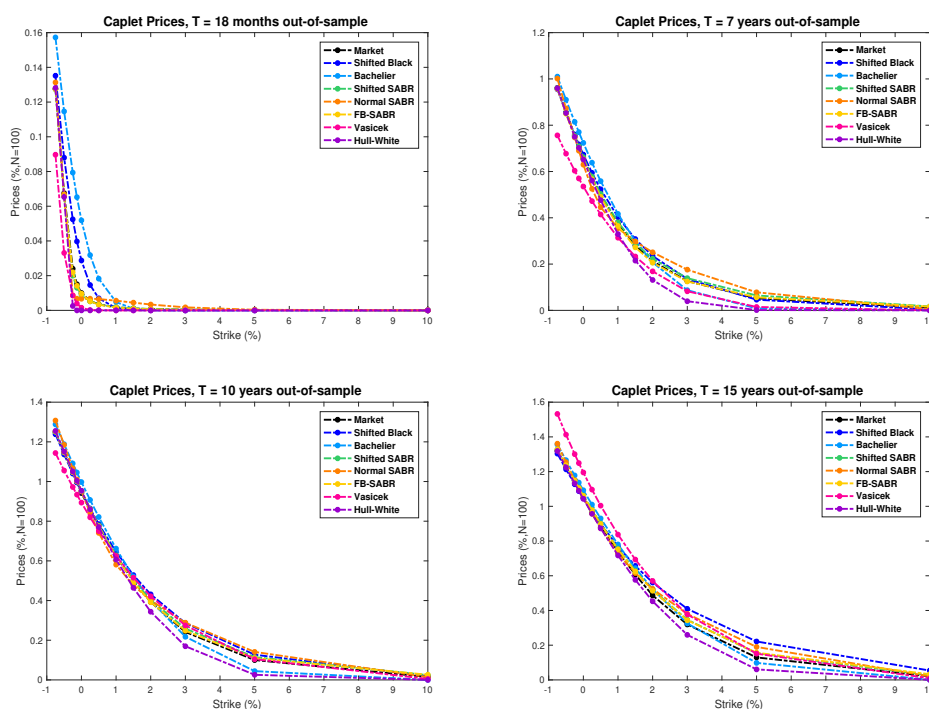


Figure 7.11: *Models' pricing maturity out-of-sample accuracy within the market benchmark for some representative maturities.*

As it can be observed, roughly speaking, it seems that every model fits market prices quite precisely, although the adjustment accuracy worsens as time to maturity increases. Moreover, caplet prices tend to rise as time to maturity grows for every strike under con-

sideration, in consonance with the results presented in Figure (7.6).

In Figure (7.12) is tested the maturity out-of-sample pricing accuracy of each model in terms of absolute and relative errors for the same representative maturities. First and second columns of the figure present the absolute and relative pricing errors, respectively, of every model. Third column of the figure is devoted to the shifted SABR and FB-SABR relative pricing errors, since those are the models that best reproduce market prices behaviour.

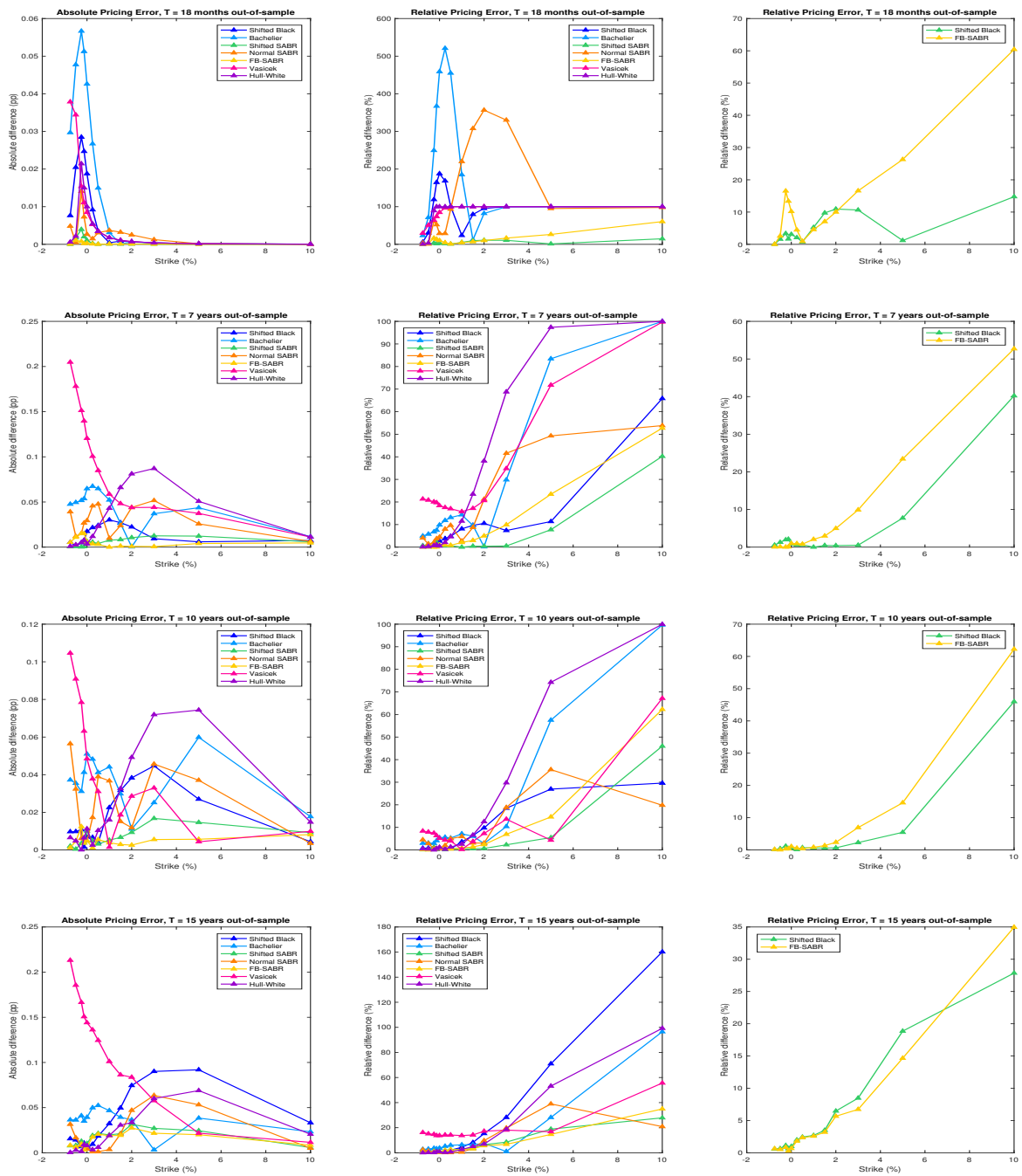


Figure 7.12: Maturity out-of-sample comparison of the different models in terms of absolute and relative pricing errors for some representative maturities.

The absolute errors observed in the first column above are, in average, higher than the ones observed in the in-sample and strike out-of-sample analysis presented in Figures (7.10) and (7.8), at least for maturities $T = 7, 15$ and Vasicek model. Moreover, it can be seen that absolute errors in the low-strike range (from -0.75% to $4 - 5\%$), especially for the shortest maturities, are higher than the ones in the high-strike range (from $5 - 6\%$ to 10%), where they tend to decrease with the strike for every model. Again, shifted SABR and FB-SABR account as the best models in terms of absolute errors, while the rest of models are, in general, quite unsatisfactory.

Regarding second column of the figure, it is clear that models relative accuracy when predicting caplet prices for maturities removed from the calibration procedures is essentially challenged for the low-strike range in the shortest maturities and for the high-strike range in the longest maturities. The area resulting from the combination (high strikes, long maturities) is the most startling in terms of relative errors. Indeed, notice that in that area errors tend to increase with the strike almost uncontrollable for every model under consideration. Furthermore, for some particular strikes and maturities belonging to this zone, FB-SABR model is being outperformed in relative terms by several competitors as shifted Black and Vasicek models. On the other hand, Bachelier, normal SABR and Hull-White are still the worst candidates in relative errors terms.

These outcomes can result surprising, since in previous analysis the behaviour of the relative pricing errors, especially for the shifted SABR and FB-SABR models, was smoother than the observed ones in Figure (7.12). However, notice that these models are focused on advanced accuracy in smile-fitting process, while interpolation in maturity is conducted through piecewise constant hypothesis, which attends for less precision. Furthermore, when a maturity is removed for out-of-sampling purposes, a full model is being eliminated from the calibration, since a different model for each maturity is calibrated, and the made assumption is that previous-maturity implied volatility applies for the maturity outstanding. Therefore, this argument supports maturity out-of-sample obtained results.

Finally, fourth column of Figure (7.12) shows the relative pricing errors made by shifted SABR and FB-SABR models, since, although they perform worse in the maturity out-of-sample analysis, they are still the models that best fit the prices, in average terms. As it can be seen, in the low-strike range both models perform quite accurately, with slight preference for the shifted SABR, while for the high-strike range both of them fail systematically because of their pronounced relative errors.

Summarizing, when out-of-sampling in maturity (interpolating prices for maturities not included in the calibration), the pricing accuracy of the models suffers a reduction, in relative terms, due to its nature and the method of interpolation in maturity used. However, again, shifted SABR and FB-SABR account as the best models under the maturity out-of-sample analysis, with slight preference for the first one based on its general superiority in absolute and relative terms.

7.2 Greeks and parameters sensitivities

This Section is devoted to the empirical analysis of the different caplet prices sensitivities under the shifted SABR model since it accounts as the best model in terms of accuracy in pricing caplets.

7.2.1 Delta and Vega

Figure (7.13) shows delta⁶⁹ (sensitivity of the caplet price with respect to infinitesimal changes in *today's* forward rate value, which accounts for the underlying of the caplet) with respect to the underlying forward values for each strike outstanding. Additionally, Table (7.2) shows the value of each underlying forward rate with its corresponding maturity, i.e., the maturity of its corresponding caplet. Since the underlying forward rate and the corresponding caplet maturity are directly related, the behaviour of the Δ -curve will be analysed equivalently either in terms of forward rates or in terms of maturities.

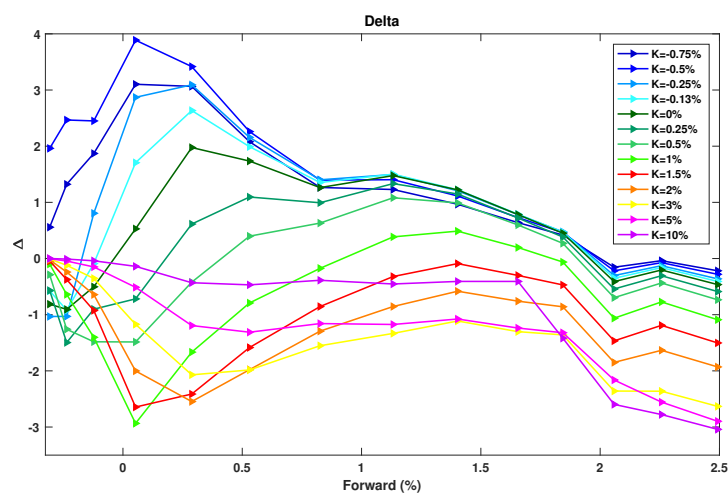


Figure 7.13: *Delta with respect to the underlying forward rate for each strike under consideration.*

T (years)	1	1.5	2	3	4	5	6	7	8	9	10	12	15	20
f (%)	-0.31	-0.24	-0.12	0.05	0.29	0.53	0.83	1.13	1.41	1.65	1.84	2.06	2.26	2.49

Table 7.2: *Forward rates with their corresponding maturities.*

For the shortest maturities, where the underlying forward rate is negative or zero, a clear difference between delta for low strikes, $K = -0.75, -0.25, -0.13, 0, 1(\%)$ (cold colours) and delta for middle-high strikes, $K = 1.5, 2, 3, 5, 10(\%)$ (warm colours) can be observed. While the curve is increasing for the lowest strikes, it is decreasing for the

⁶⁹Actually, this delta is referred to the Bartlett's delta, since Bartlett's correction provides more stable and robust hedges, as it was explained in Section 4.1. The same argument applies for vega, which is in fact Bartlett's vega.

highest ones. For middle maturities ($T = 4 - 7$ years approximately), this Δ -behaviour is opposite, and for largest maturities the evolving of the curves is similar for every strike, indeed, the values of delta converge to a given (negative) long-term value with time to maturity.

The sign of delta depends to a large degree on the shape of the volatility smiles/skews, at least for some maturities. In order to compare Δ -curves behaviour with respect to the volatility curves, Figure (7.14) presents the shifted SABR implied volatilities through every strike under consideration and for some representative maturities. For each maturity, the vertical line crosses the point of the curve which corresponds to the at-the-money strike volatility, and it is used as a *delimiter* between two clearly differentiated areas. Indeed, in the first area, which corresponds to the strikes below the ATM's one, the volatility curve is decreasing. The second area corresponds to the strikes above the ATM's one and there the volatility curve is increasing. Notice that for the longest maturities ($T = 15$, in this case) the volatility smile is decreasing irrespective of the ATM-strike area, although it smoothly increases for the highest strikes.

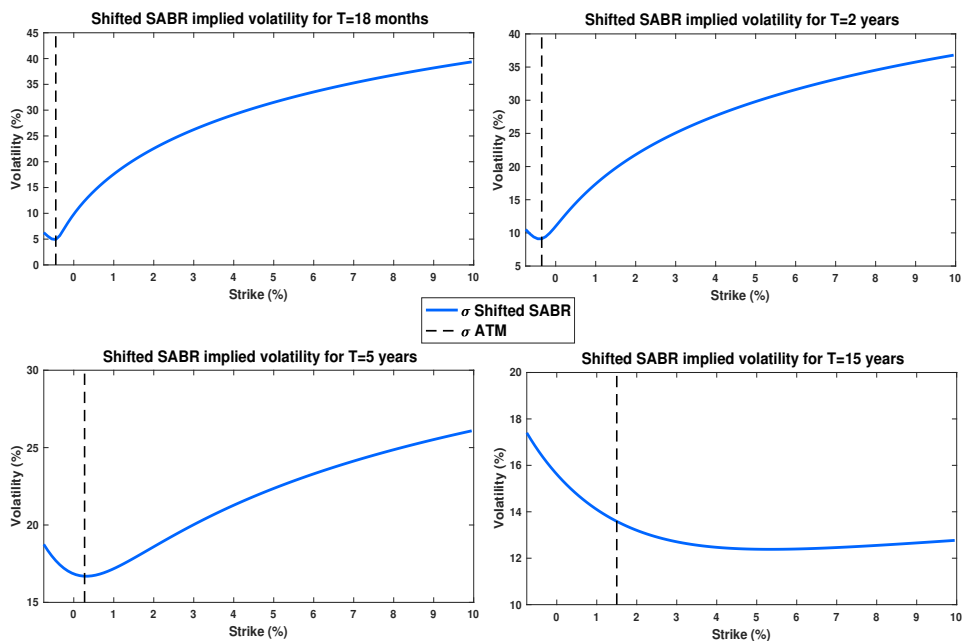


Figure 7.14: *Shifted SABR implied volatilities through every strike under consideration and for some representative maturities.*

Before analysing the figures, it is crucial to take into account some important issues about the relationship between caplet price V_{caplet} , implied volatility σ , strike K , and *today's* forward rate f .⁷⁰ Firstly, notice that an increase in the *today's* forward rate f can be seen as equivalent to a decrease in the strike K . Indeed, if the value of f goes up *today*, the corresponding caplet will have an smaller strike K , since the payoff of a caplet is $\max(0, f - K)$.⁷¹ Secondly, when the implied volatility σ goes up/down, the cor-

⁷⁰Since this Section is devoted to the sensitivity analysis under the shifted SABR model exclusively, subscripts and superscripts in the notation result redundant, and therefore they are omitted.

⁷¹This is a simplified version of the right payoff-formula (1.7).

responding caplet price goes down/up, since vega is positive for all strikes and maturities under consideration, as it will be observed in Figure (7.15).

Regarding the volatility curves in Figure (7.14), for maturities $T = 1.5, 2, 5$ in the left part (below K^{ATM}) the volatility goes down when the strike increases, and in the right part (above K^{ATM}) the volatility goes up with the strike. For $T = 15$, volatility goes down for almost every strike (note that for $K = 7, 8, 9, 10\%$ the curve increases smoothly). Then, as illustrated in Figure (7.13), the behaviour of Δ is as follows.

- Short-middle maturities ($T = 1, 1.5, 2, 3, 4, 5, 6, 7, 8, 9, 10$)⁷²:
 - If $K < K^{ATM}$ (the volatility curve decreases), then $\uparrow f(\equiv \downarrow K) \Rightarrow \uparrow \sigma \Rightarrow \uparrow \mathbf{V}_{\text{caplet}} \Rightarrow \Delta > \mathbf{0}$.
 - If $K > K^{ATM}$ (the volatility curve increases), then $\uparrow f(\equiv \downarrow K) \Rightarrow \downarrow \sigma \Rightarrow \downarrow \mathbf{V}_{\text{caplet}} \Rightarrow \Delta < \mathbf{0}$.
- Long maturities ($T = 12, 15, 20$): $\Delta < \mathbf{0} \forall \mathbf{K}$ (irrespective of the ATM-strike area).

This Δ -behaviour depending on the dynamic evolution of the volatility curve is clear in the short-middle maturity range, however for long maturities the argument does not apply. Indeed, since in these cases the volatility curve is decreasing in almost all strikes, delta *should be* positive, but it is clearly negative. This fact could be a result of an unsuitable performance of the shifted SABR model in calibrating products with large maturities, as it was commented Section 3.1.

In what follows, the vega (sensitivity of the caplet price with respect to infinitesimal changes in the volatility of the underlying forward rate) is analysed. As it was previously discussed⁷³, there are two different ways of computing the vega, with respect to α (*today's* forward rate volatility) or with respect to σ_B (implied shifted SABR volatility). In order to clarify the differences between them, Figure (7.15) presents *both types* of vega for every strike and maturity under consideration.

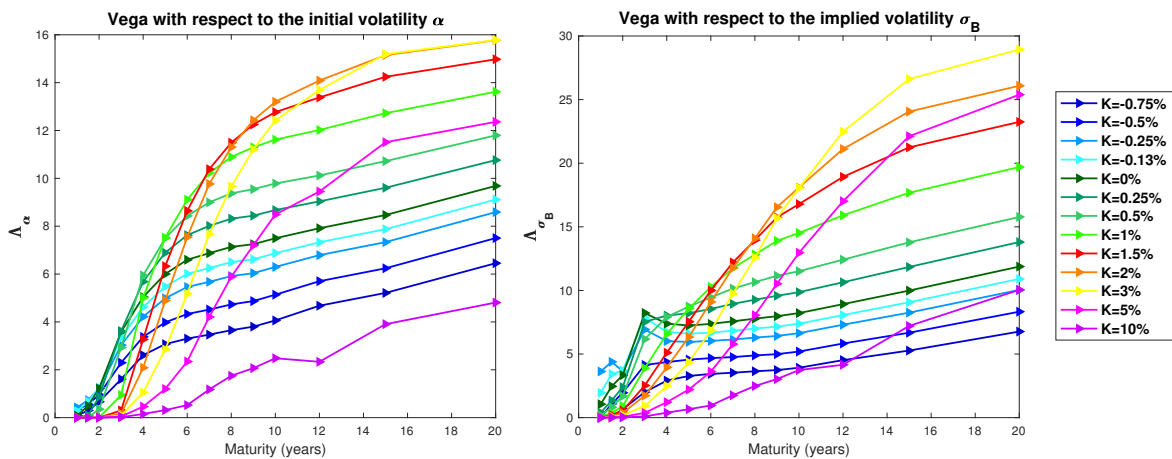


Figure 7.15: Vega with respect to the volatility parameter α (left) and with respect to the implied volatility σ_B (right) for each strike and maturity under consideration.

⁷²See the shape of the corresponding smiles in Figure (7.5).

⁷³See Section 4.1.

As it can be seen in Figure (7.15), the shape of the sensitivity curves are very similar in both cases, being the vega-curves with respect to α smoother (notice that vega with respect to σ_B presents some peaks corresponding to the negative and lowest positive strikes at maturity $T = 3$). Furthermore, the values of the vega with respect to the implied volatility σ_B are quite higher than the ones achieved by the vega with respect to the parameter α (notice the scale in both subfigures) and this indicates that the caplet prices are more sensitive to the changes in σ_B than to the changes in α . The most important issue is that vega, irrespective of the volatility considered for its computation, is always positive. That means that when the volatility grows, the caplet price grows too, and this is the typical market behaviour, since more uncertainty usually makes prices go up.

7.2.2 Gamma, Dual-delta, Vanna and Volga

This Subsection is devoted to other Greeks also important for the hedging analysis.

Figure (7.16) shows the Greek gamma (sensitivity of delta with respect to infinitesimal changes in *today's* forward rate value) with respect to the underlying forward values for each strike outstanding.

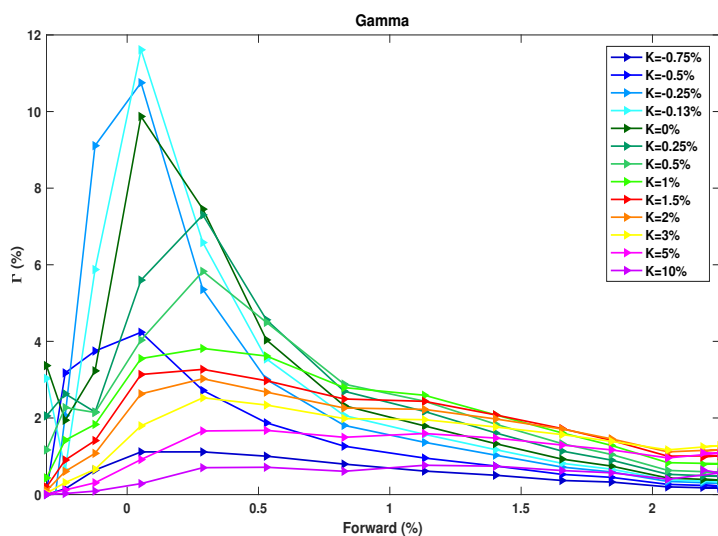


Figure 7.16: *Gamma with respect to the underlying forward rate for each strike under consideration.*

As it can be observed, for strikes around zero, particularly $K = -0.25, -0.13, 0, 0.5, 1\%$, gamma curves form a pronounced peak (high positive value) around the maturity $T = 3$, corresponding to the forward rate $f = 0.05\%$ (see Table (7.2)), contrary to their behaviour for the rest of strikes, which is quite smooth through the values of the underlying forward rate. However, these peaks disappear as time to maturity increases, leading to monotonous decreasing gamma-curves that converge to a given long-term value with the time to maturity for every strike.⁷⁴

⁷⁴Notice that these gamma curves resemble classical Black-Scholes gammas.

Regarding the sign of this Greek, gamma is positive for all strikes and maturities under consideration. At first sight this fact would result natural, since under the classical Black-Scholes model call-gammas are positive and they have a similar shape as the observed in Figure (7.16). However, these results are *not mathematically consistent* with the delta-curves presented in Figure (7.13). Indeed, delta-curves are increasing and decreasing, depending on the maturity range under consideration, then since gamma is the derivative of delta with respect f , gamma should be positive and negative, depending on the maturity range under consideration. The analysis of this inconsistency is not obvious and it is left for further research.

Figure (7.17) presents the Greek dual-delta (sensitivity of the caplet price with respect to infinitesimal changes in the strike rate) with respect to the strike for every maturity outstanding.

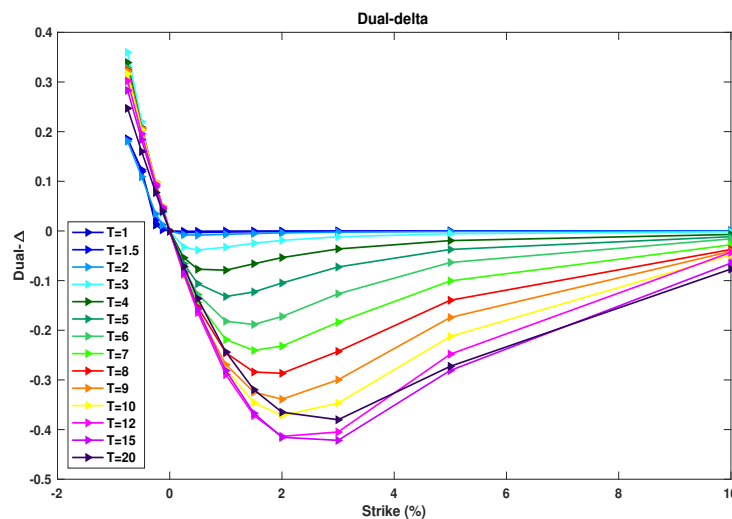


Figure 7.17: *Dual-delta with respect to the strike for each maturity.*

As it can be seen in this figure, for all maturities under consideration, the sign of this Greek is always opposite to the sign of the strike, the parameter with respect to which this caplet price sensitivity is computed. Indeed, for negative strikes the dual-delta is positive, for strike zero its value is zero, and for positive strikes it becomes negative, with independence of the considered maturity. Furthermore, the behaviour of the different dual-delta curves is completely symmetric, since the curves for each maturity have the same shape through the strikes, being clearly more negative the curves corresponding to the long maturities. Additionally, notice that all of them converge to the same value (zero) with the strike.

Finally, Figure (7.18), shows the Greeks vanna and volga (sensitivities of delta and vega, respectively, with respect to infinitesimal changes in the volatility of the underlying forward rate α).

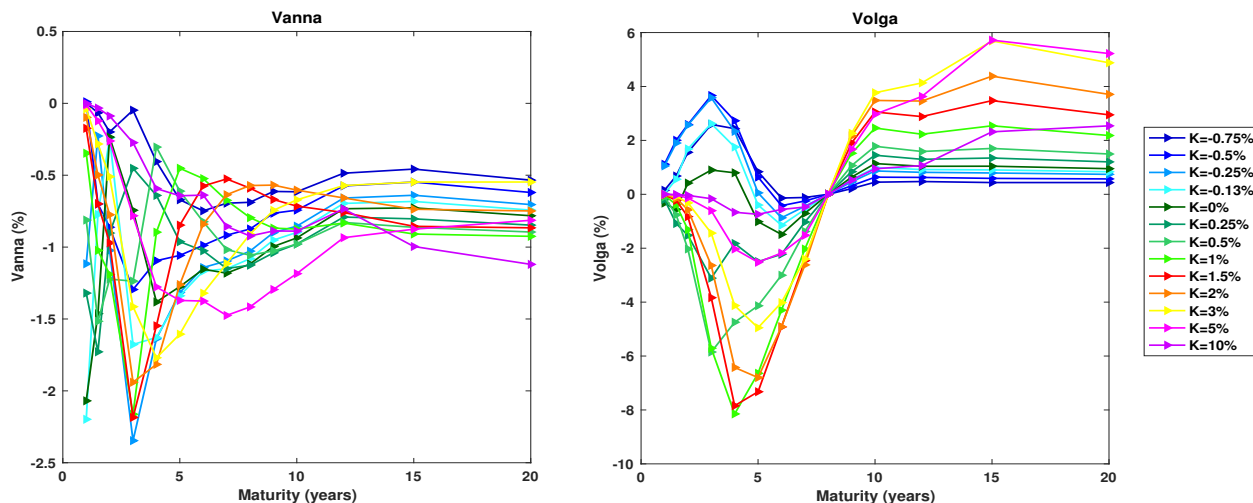


Figure 7.18: *Vanna* (left) and *volga* (right) with respect to the maturity for each strike under consideration.

Firstly, vanna (left graph) is analysed. The behaviour of the vanna-curves is quite unstable, since they present many (negative) peaks for the shortest maturities for almost all strikes irrespective of their sign. Furthermore, this Greek takes negative values for all strikes and maturities under consideration, and converges to a long-term (negative) value.

Secondly, volga (right graph) is analysed. Again, the difference in these curves is observed between negative and positive strikes, at least in the shortest maturities. Indeed, in the maturity range $T = [1, 5]$, for the negative strikes volga curves are positive, and for the positive strikes they are negative. For maturities $T = 8, 9$ volga curves are negative for all strikes, and for $T = [10, 20]$ they are all positive, converging to a given (positive) long-term value. However, these results are *not mathematically consistent* with the ones obtained for the vega in Figure (7.15). Indeed, vega-curves (with respect α) are increasing in maturity for all strikes outstanding, then since volga is the derivative of vega with respect α , volga-curves should be all positive. As in the gamma case, the analysis of this inconsistency is left for further research.

7.2.3 Parameters sensitivities

As stated in (Deloitte, 2016) [12], in some practices, the daily risk-management goes even further by managing the sensitivities associated to the SABR parameters. Therefore, these sensitivities are empirically analysed now.

Figure (7.19) shows the sensitivities of the caplet prices calibrated with the shifted SABR model with respect to its parameters: β (the power parameter), ρ (the correlation between the Brownian Motions of F_t and σ_t), ν (the volatility-of-volatility, i.e., the volatility of σ_t), and the shift parameter s .

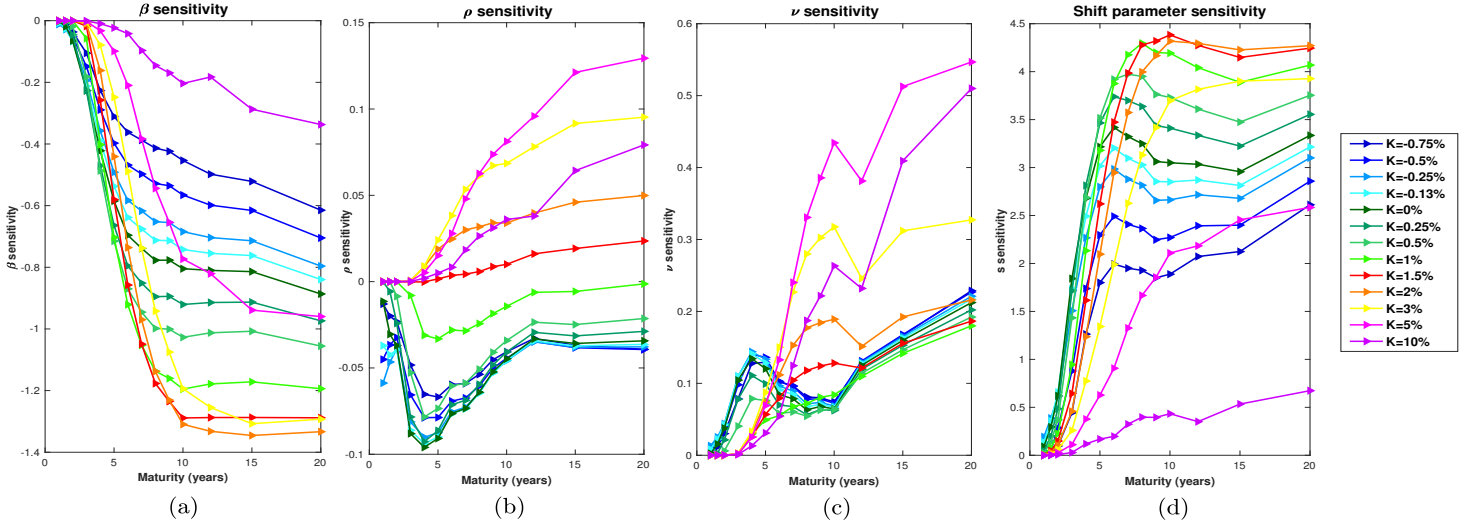


Figure 7.19: Shifted SABR parameters sensitivities.

The main conclusions of the analysis of Figure (7.19) are the following.

- β sensitivity ($\mathcal{S}^{(\beta)}$) (subfigure (a)). $\mathcal{S}^{(\beta)}$ is negative for all strikes and for all maturities under consideration. The dependence of the caplet prices with respect to the parameter β decreases drastically with time to maturity until 5 – 7 years, and then becomes smoother for all strikes under consideration. Furthermore, the smallest values of $\mathcal{S}^{(\beta)}$ are observed for the strikes around zero.
- ρ sensitivity ($\mathcal{S}^{(\rho)}$) (subfigure (b)). $\mathcal{S}^{(\rho)}$ is positive for the highest strikes ($K = 3, 5, 10\%, \forall T$), and negative for the rest (negative and low positive strikes, $\forall T$).
- ν sensitivity ($\mathcal{S}^{(\nu)}$) (subfigure (c)). $\mathcal{S}^{(\nu)}$ is positive for all strikes and for all maturities under consideration. The sensitivity of the caplet prices with respect to ν increases drastically in the maturity range $[1, 5] \cup [10, 20]$ for the negative and low positive strikes, while for the highest strikes it increases through all maturities, reaching its major values for $K = 5, 10\%$ and $T = 15, 20$ years.
- s sensitivity ($\mathcal{S}^{(s)}$) (subfigure (d)). $\mathcal{S}^{(s)}$ is positive for all strikes and for all maturities under consideration. The dependence of the caplet prices with respect to the shift parameter s increases drastically with time to maturity until 5 – 7 years, and then becomes smoother for all strikes under consideration. Furthermore, the major values of $\mathcal{S}^{(s)}$ are observed for the strikes around zero.

As it can be observed, the behaviour of the β and s sensitivities is *inversely proportional*, since the shape of both set of curves seems to be the same but inverted, *as the axis of the strike were a mirror*, although β -sensitivity curves accomplish smaller negative values (the scale is from 0 to -1.4) than the positive ones accomplished by the s -sensitivity curves (the scale is from 0 to 4.5).⁷⁵ This means that there might exist an inverse relation between β and s , when one increase the other decreases, and vice versa.

⁷⁵Compare subfigures (a) and (d) of Figure (7.19).

Furthermore, all parameters sensitivities seem to converge to a long-term value (obviously, different in each case), although each of them in a different way. However, in every case it can be seen that the curves for the highest strikes ($K = 5, 10\%$) are the ones that present a different behaviour in convergence terms, with respect to the sensitivity curves for other strikes (negative and low positive).

Conclusion

The current negative rates environment has led to difficulties in using standard models for pricing and hedging fixed income derivatives. On the other hand, the assumption of constant volatility in traditional simplistic models is inconsistent with existent smile/skew effect in the volatility curves observed within markets.

During this MSc Thesis several models able to cope with negative rates have been calibrated and compared in terms of accuracy when recovering caplet prices term structures, testing both their in-sample fit and out-of-sample forecast. Empirical results have shown that each model under consideration fits market prices fairly well, however in terms of absolute and relative pricing errors, not all models have been appropriate. Shifted SABR and Free-Boundary SABR definitely outperformed the remaining models, with explicit preference for the former. This result supports Shifted SABR's general acceptance in the industry.

Since the utility of the Shifted SABR model as a pricing tool has been empirically shown, in the second part of the practical approach, its ability to produce reliable risk measures has been tested. Greeks and parameters sensitivities of significant practical importance have been analysed, and the reached outcomes have resulted consistent with the markets behaviour, highlighting delta risk which strongly depends on the shape of the volatility curve.

Although the results seem satisfying, there are several areas that might be considered in a further research in order to improve the quality of the empirical analysis.

Piecewise constant hypothesis used in the research does not seem precise enough, since pricing accuracy of the Shifted SABR model, particularly, worsens when maturity out-of-sample analysis is considered. Therefore, the influence of the functional form in maturity of the caplet implied volatility in the stripping process should be tested in order to select the most appropriate one.

The setting of the parameter β at 0.5 in the Shifted SABR model, based on the general agreement among academics and practitioners, should be tested (either fixing it at other values or calibrating it directly) in order to check the influence of this parameter on the subsequent results.

The use of single discount curve for both computing the forward rates and the discount factors is a simplification of today's standard market practice, where *multi-curve framework* is used. Therefore, this *new* approach should be adopted in order to deal with the *possible* inconsistencies resulting from the single-curve method.

Hull-White model was calibrated through its analytical pricing formula. However, the standard calibration method for this model is numerical, based on tree approaches. Therefore, this short-rate model should be calibrated numerically, in consonance with the common practice, in order to test the influence of the used method (analytical or numerical) on the subsequent comparative results.

Hedging analysis has been performed only for the Shifted SABR model, since it has accounted as the preferred one in terms of pricing accuracy. In order to justify empirically its superiority in producing reliable risk metrics, hedging analysis for the rest of models should be fulfilled.

Since caps are the instruments that actually are quoted within markets, a conversion of both caplet pricing and hedging analysis should be performed for caps. That would result in higher interest for the industry. Furthermore, a parallel analysis should be done for floors, what would not imply an additional difficulty, and for swaptions, for instance, what would require a completely different methodology given the nature of this product.

Bibliography

- [1] AGARWAL N. AND MCWILLIAMS G., *Evolution of volatility surface under SABR model*, Courant Institute of Mathematical Sciences, NYU, 2010. 25
- [2] ANTONOV A., KONIKOV M., AND SPECTOR M., *The free boundary SABR: natural extension to negative rates*, January 2015. 22
- [3] BACHELIER L., *Théorie de la spéculation*, Annales scientifiques de l'É.N.S. 3(17), pp. 21–86, 1900. 9
- [4] BARTLETT B., *Hedging under SABR model*, Wilmott Magazine, pp. 2–4, July 2006. 25
- [5] BIANCHETTI M., *Two curves, one price: pricing & hedging interest rate derivatives decoupling forwarding and discounting yield curves*, Risk Magazine, August 2004. 6
- [6] BLACK F., *The pricing of commodity contracts*, Journal of Financial Economics 3, pp. 167–179, 1976. 10
- [7] BURDEN R. AND FAIRES J., *Numerical analysis*, Brooks/Cole, 2011. 74
- [8] BRIGO D. AND MERCURIO F., *Interest rate models - theory and practice with smile, inflation and credit*, Springer, 2006. 4, 13, 14
- [9] COX J., *Notes on option pricing I: constant elasticity of diffusions*, Unpublished draft, Stanford University, 1975. 70
- [10] SKANTZOS N., VAN DOOREN K., AND GARSTON G. (DELOITTE), *Calibration and pricing using the free SABR model*, October 2016. 22
- [11] SKANTZOS N., CASTELEIN N., VAN DOOREN K., AND GARSTON G. (DELOITTE), *Interest rate derivatives in the negative-rate environment. Pricing with a shift*, February 2016. 22, 37, 38
- [12] SKANTZOS N., VAN DOOREN K., AND GARSTON G. (DELOITTE), *Risk management under the SABR model*, October 2016. 26, 62
- [13] DERMAN E. AND KANI I., *Riding on a smile*, Risk 7, pp. 32-39, February 1994. 16, 71
- [14] DERMAN E. AND KANI I., *The volatility smile and its implied tree*, Goldman Sachs, January 1994. 16, 71

- [15] DERMAN E., KANI I., AND ZOU J., *The local volatility surface: unlocking the information in index options pricing*, Financial Analysts Journal 52(4), pp. 25-36, July 1996. 71
- [16] DUPIRE B., *Pricing with a smile*, Risk 7(1), pp. 18-20, January 1994. 16, 71
- [17] ELTON E., GRUBER M., AND MICHAELY R., *The structure of spot rates and immunization*, Journal of Finance, June 1990. 40
- [18] FRANKENA L., *Pricing and hedging options in a negative interest rate environment*, Master's thesis, February 2016. 22, 70
- [19] HAGAN P. AND KONIKOV M., *Interest rate volatility cube: construction and use*, July 2004. 37
- [20] HAGAN P. AND LESNIEWSKI A., *Bartlett's delta in the SABR model*, April 2017. 25, 27
- [21] HAGAN P., KUMAR D., LESNIEWSKI A., AND WOODWARD D., *Arbitrage free SABR*, Willmott Magazine, January 2014. 25
- [22] HAGAN P., KUMAR D., LESNIEWSKI A., AND WOODWARD D., *Managing smile risk*, Willmott Magazine, September 2002. 2, 16, 17, 18, 20, 25, 29, 71
- [23] HANSEN S., *The SABR model – theory and application*, Master's thesis, April 2011. 27
- [24] HEATH D., JARROW R., AND MORTON A., *Bond pricing and the term structure of interest rates: a new methodology for contingent claims valuation*, Econometrica 60, pp. 77-105, 1992. 12
- [25] HESTON S., *A closed-form solution for options with stochastic volatility with applications to bond and currency Options*, Review of Financial Studies 6(2), pp. 327–343, 1993. 17
- [26] HULL J. AND WHITE A., *LIBOR vs. OIS: the derivatives discounting dilemma*, Journal of Investment Management 11(3), pp. 14–27, March 2012. 6
- [27] HULL J. AND WHITE A., *Optimal delta hedging for options*, Journal of Banking and Finance, May 2017. 25
- [28] HULL J. AND WHITE A., *Pricing interest-rate-derivative securities*, Review of Financial Studies 3(4), pp. 573–592, 1990. 13
- [29] KOOIMAN T., *Negative rates in financial derivatives*, Master's thesis, December 2015. 15
- [30] KOPECKY K., *Root-finding methods*, Lecture Notes, 2007. 35, 37
- [31] LABORDÉRE H., *Analysis, geometry, and modelling in finance: advanced methods in option pricing*, CRC Press, 2008. 70
- [32] LESNIEWSKI A., *The volatility cube*, New York University, February 2008. 33

-
- [33] McDONALD, R., *Derivatives markets*, Pearson, 2006. 27
- [34] OBLÓJ J., *Fine-tune your smile: correction to Hagan et al.*, Imperial College London, March 2008. 18
- [35] REBONATO R., MCKAY K., AND WHITE R., *The SABR/LIBOR market model*, WILEY, June 2009. 19, 20, 21, 26, 29, 39
- [36] ROUAH F., *The SABR model*, Lecture notes, 2007. 21
- [37] ROUAH F., *T-forward measure*, Lecture notes, 2007. 4, 8
- [38] SÅMARK U. AND JÖNSSON M., *Negative rates in a multi curve framework: cap pricing and volatility transformation*, Master's thesis, 2016. 37
- [39] SEBASTIAN A. AND WOLFF-SIEMSEN T., *Low strike extrapolation for SABR*, Wilmott Magazine 10, 2014. 21
- [40] SYDSÆTER K., *Matematisk analyse*, Gyldendal, 2005. 25
- [41] VASICEK O., *Equilibrium and term structure*, Journal of Financial Economics 5, pp. 177–188, 1977. 13
- [42] WEST G., *Calibration of the SABR model in illiquid markets*, Applied Mathematical Finance 12(4), pp. 371–385, 2004. 20
- [43] ZHANG J. AND WU Z., *Bloomberg volatility cube*, May 2016. 38

Appendix A

Constant Elasticity of Variance Model (1975)

The Constant Elasticity of Variance (CEV) model was developed by (Cox,1975) [9]. In this model the forward rate F_t follows the following stochastic differential equation

$$dF_t = \sigma \cdot F_t^\beta \cdot dW_t, \quad (\text{A.1})$$

where σ is the constant volatility and W_t is a Brownian Motion under the T -forward measure. The parameter β is the CEV-exponent and in interest rate markets, it usually holds $0 \leq \beta \leq 1$. Note that if $\beta = 1$ there is the Black model and if $\beta = 0$, the Bachelier model is obtained.

One of the main features of the CEV process (A.1), which concerns most analysts, is its *transition probability density function* $\mathbb{P}(F_t = f|f)$. (Frankena,2016) [18] shows that this function can be of two forms for $0 < \beta < 1$ depending on a boundary condition at $F_t = 0$.

- For $0 < \beta < \frac{1}{2}$ with an absorbing boundary condition at $F_t = 0$ and for $\frac{1}{2} \leq \beta < 1$ without the need of applying a boundary condition.
- For $0 < \beta < \frac{1}{2}$ with a reflecting boundary condition at $F_t = 0$.

The CEV process with an absorbing boundary condition is a martingale, while the CEV process with a reflecting boundary is not, as shows (Labordère,2008) [31]. Furthermore, paths $\{F_t\}_{t \geq 0}$ that hit zero, stay in zero *forever* with the absorbing boundary condition, but reflect to positive values with the reflecting boundary condition. The SABR model uses an absorbing boundary condition, since this allows the underlying process to be a martingale. Therefore, the transition probability density function of the CEV process with an absorbing condition gives insights on the probability density of the SABR model.

The main drawbacks of the CEV model are that it cannot deal with negative rates (unless it is shifted, in which case a restricted version of the shifted SABR model with constant volatility is obtained), and that it cannot reproduce the volatility smile/skew observed in the markets.

Appendix B

Local Volatility Models (1994)

As it was already described the implied volatility is not constant in practice. Dupire, Derman and Kani, see (Dupire,1994) [16], (Derman and Kani,1994) [14], (Derman and Kani,1994) [13] and (Derman et al.,1996) [15], found an apparent solution for this problem by introducing *local volatility*. They extended the Black model by replacing the constant volatility σ by the so-called local volatility function $\sigma_{LV}(t, F_t)$ that is dependent on time t and the underlying forward rate F_t . The stochastic differential equation that describes the dynamics of the forward rate F_t under the local volatility model is given by

$$dF_t = \sigma_{LV}(t, F_t) \cdot F_t \cdot dW_t, \quad (\text{B.1})$$

where W_t is a Brownian Motion under the T -forward measure \mathbb{F}^T .

(Dupire,1994) [16] argued that instead of theorizing about the unknown local volatility function $\sigma_{LV}(t, F_t)$, one should obtain it directly from the marketplace by *calibrating* the local volatility model to market prices of liquid options, i.e., by using the market prices of options to find an effective specification of the underlying process, so that the local implied volatilities match the market implied volatilities. Then, under the local volatility model, the value of a cap/floor, for instance, is obtained by Black's formula (2.10) by introducing the corresponding estimated volatility.

However, there is a major problem with the local volatility model. Although the smile calibration that provides is really accurate for any given maturity, it predicts that the market smile/skew moves in the opposite direction as the price of the underlying asset, i.e., it predicts that the smile/skew will shift to lower prices after an increase of the underlying. This is contrary to the typical market behaviour, in which smiles and skews move in the same direction as the underlying. In other words, it predicts the wrong dynamics of the volatility smile/skew. Due to this contradiction, as it is clearly explained and exemplified in (Hagan et al.,2002) [22], delta and vega risk metrics under the local volatility model may perform worse than the risk metrics of the naive Black model.⁷⁶

In conclusion, the local volatility model is suited for pricing purposes, but not for proper risk management, and, for this reason, the model has been discarded over the industry during recent years.

⁷⁶Full argument is omitted here because it lies beyond the objectives of the research, but interested readers can attend (Hagan et al.,2002) [22] for further details.

Appendix C

Vasicek and Hull-White calibrations. Numerical issues

During the Vasicek and Hull-White models calibrations through the caplet pricing formulae (2.13a) and (2.16a), several numerical difficulties have been found. Indeed, some different combinations of the parameters resulted in similar values of the considered objective function, and the algorithm struggled to optimize it in the parametric space.

One possible reason for these numerical obstacles might be the classical optimization problem of *getting stuck in a local critical point*. In order to test this possibility, models restrictions and initial values was subtly varied, and, in view of optimization process stopping criteria details, it seems that this is not the problem.

Another habitual cause that can aggravate the optimization results is the *discontinuity of the pricing function*. In Figure (C.1) is presented the dependence on the parameter θ of the Vasicek caplet pricing formula (2.13a) fixing k and σ to their values for $T = 3Y$ and $K = 0\%$, as a representative example.⁷⁷

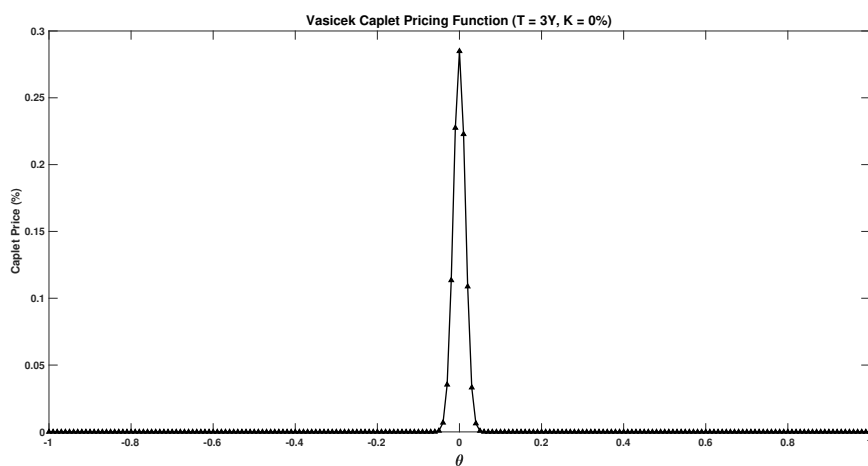


Figure C.1: *Vasicek caplet pricing formula as a function of the long term value θ .*

⁷⁷Since formulae (2.13a) and (2.16a) have a similar structure, the pricing problems are stated in both of them, and therefore the discussions made during the appendix applies for both of them.

As it can be seen the pricing function is notably discontinuous, and therefore the calibration algorithm cannot fit properly any price between two given points of the parametric space for θ . Indeed, since every considered point of the parametric space for θ gives a different price of the market price, the step-size tolerance is not enough to guarantee a proper fit for small caplet prices, where the relative pricing error increases highly as soon as the market price is not attained with proper accuracy.

Then, it seems that the problems during the optimization are due to the nature of the caplets pricing function, and not to the optimization procedure itself.

Appendix D

Numerical differentiation

This appendix summarizes the most commonly used *finite difference methods* when computing numerically first and second order (partial) derivatives.⁷⁸

Given the function $f(x, y, \mathbf{z}) \in \mathbb{R}^n$, $n \in \mathbb{N}$, the **first order partial derivative** of this function with respect the variable x (without loss of generality) can be approximated by the following equations.

- Forward Difference Method

$$\frac{\partial f}{\partial x}(x_0, y_0, \mathbf{z}_0) \approx \frac{f(x_0 + \Delta x_0, y_0, \mathbf{z}_0) - f(x_0, y_0, \mathbf{z}_0)}{\Delta x_0}. \quad (\text{D.1})$$

- Central Difference Method

$$\frac{\partial f}{\partial x}(x_0, y_0, \mathbf{z}_0) \approx \frac{f(x_0 + \Delta x_0, y_0, \mathbf{z}_0) - f(x_0 - \Delta x_0, y_0, \mathbf{z}_0)}{2\Delta x_0}. \quad (\text{D.2})$$

- Secant Method

$$\frac{\partial f}{\partial x}(x_0, y_0, \mathbf{z}_0) \approx \frac{f(x_0(1 + \Delta x_0), y_0, \mathbf{z}_0) - f(x_0(1 - \Delta x_0), y_0, \mathbf{z}_0)}{2x_0\Delta x_0}. \quad (\text{D.3})$$

The **second order partial derivative** of the function with respect to the variable x (without loss of generality) can be approximated by

$$\frac{\partial^2 f}{\partial x^2}(x_0, y_0, \mathbf{z}_0) \approx \frac{f(x_0 + \Delta x_0, y_0, \mathbf{z}_0) - 2f(x_0, y_0, \mathbf{z}_0) + f(x_0 - \Delta x_0, y_0, \mathbf{z}_0)}{\Delta x_0^2}, \quad (\text{D.4})$$

and the **second order cross partial derivative** with respect to x and y (without loss of generality) is given by

$$\frac{\partial^2 f}{\partial x \partial y}(x_0, y_0, \mathbf{z}_0) \approx \frac{f_{(1,1)} + f_{(-1,-1)} - f_{(1,-1)} - f_{(-1,1)}}{4\Delta x_0 \Delta y_0}, \quad (\text{D.5})$$

where $f_{(1,1)} = f(x_0 + \Delta x_0, y_0 + \Delta y_0, \mathbf{z}_0)$, $f_{(-1,-1)} = f(x_0 - \Delta x_0, y_0 - \Delta y_0, \mathbf{z}_0)$, $f_{(1,-1)} = f(x_0 + \Delta x_0, y_0 - \Delta y_0, \mathbf{z}_0)$, and $f_{(-1,1)} = f(x_0 - \Delta x_0, y_0 + \Delta y_0, \mathbf{z}_0)$.

⁷⁸For further details about the topic see (Burden and Faires, 2011) [7], for instance.

Appendix E

Market data

	STK	ATM	-0.75	-0.50	-0.25	-0.13	0.00	0.25	0.5	1.00	1.50	2.00	3.00	5.00	10.00
1Y	-0.20	5.57	2.70	4.30	5.80	7.40	9.00	11.60	13.80	17.40	20.40	22.80	26.80	32.60	41.00
18M	-0.20	6.88	6.90	6.40	6.90	8.30	9.70	12.00	14.00	17.30	20.00	22.30	25.90	31.10	38.60
2Y	-0.20	8.70	9.80	8.40	8.20	9.40	10.50	12.50	14.30	17.20	19.60	21.70	24.90	29.60	36.40
3Y	0.02	11.55	13.00	11.50	10.40	10.80	11.40	12.70	14.00	16.10	18.00	19.60	22.20	25.90	31.30
4Y	0.14	13.68	15.30	13.70	12.40	12.60	13.10	14.10	15.00	16.70	18.20	19.50	21.70	24.80	29.30
5Y	0.27	15.15	16.70	15.20	14.00	14.00	14.30	15.10	15.80	17.00	18.10	19.00	20.50	22.80	26.20
6Y	0.40	16.05	17.40	16.10	15.00	14.90	15.20	15.70	16.20	17.10	17.80	18.40	19.40	20.90	23.30
7Y	0.52	16.46	17.80	16.60	15.60	15.50	15.60	16.00	16.40	17.00	17.50	17.90	18.60	19.70	21.70
8Y	0.65	16.61	18.00	16.90	15.90	15.80	15.90	16.20	16.50	16.90	17.20	17.40	17.80	18.70	20.30
9Y	0.77	16.58	18.10	17.00	16.10	16.00	16.10	16.20	16.40	16.70	16.80	16.90	17.10	17.60	18.80
10Y	0.88	16.45	18.10	17.10	16.30	16.10	16.10	16.20	16.40	16.50	16.50	16.50	16.50	16.80	17.60
12Y	1.06	16.06	18.10	17.20	16.40	16.20	16.20	16.20	16.20	16.10	15.90	15.80	15.50	15.40	15.70
15Y	1.26	15.42	17.90	17.10	16.30	16.20	16.10	15.90	15.80	15.60	15.30	15.00	14.60	14.20	14.30
20Y	1.42	14.66	17.60	16.80	16.10	15.90	15.80	15.60	15.40	15.00	14.60	14.30	13.80	13.30	13.20

Table E.1: *Implied Shifted Black EUR volatilities (%) at 23-May-2017.*

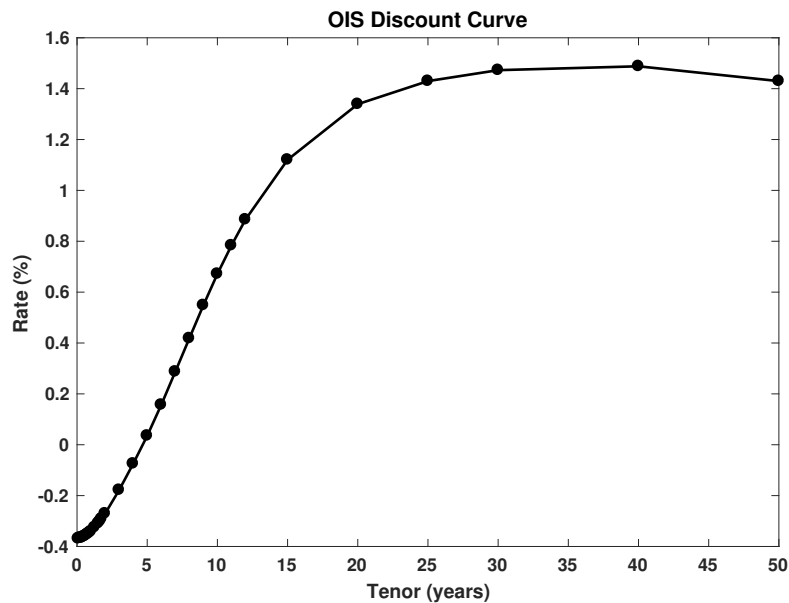


Figure E.1: *EUR OIS discount curve at 23-May-2017 with tenors from 1 day to 50 years.*